Norges miljø- og biovitenskapelige universitet

**Master's Thesis 2018 60 ECTS**

Department of Medical Genetics, Oslo University Hospital Ullevål
Main Supervisor Mari Tinholt

# The role of Coagulation Factor V in Breast Cancer

Marianne Staff Fredhjem
Chemistry and Biotechnology
Faculty of Chemistry, Biotechnology and Food Sciences

# Acknowledgements

The work presented in this thesis was performed between August 2017 and May 2018 at the Department of Medical Genetics, Oslo University Hospital Ullevål. This thesis was a part of the Master program in Chemistry and Biotechnology, at the Faculty of Chemistry, Biotechnology and Food Sciences (KBM) at the Norwegian University of Life Sciences (NMBU).

First of all, I wish to express my sincere gratitude to my main supervisor Dr. philos Mari Tinholt at the Department of Medical Genetics. The door to your office was always open, whenever I ran into difficulties or had questions about my research or writing. Your advices and constructive feedback have been a great motivational support. I also want to thank my supervisor Dr. philos Nina Iversen, for giving me the opportunity to be a part of the research group, and all your valuable guidance and support through this project. I owe a gratitude to the Department Engineer Marit Sletten, your knowledge and expertise in the laboratory has been an inspiration. I appreciate all the patience, guidance and practical assistance you have given me. I would also like to thank my internal supervisor at NMBU, Professor Harald Carlsen.

I would like to thank my fellow students, Cathrine McCoig and Anne Rydland, for sharing times of both happiness and frustrations at Ullevål. It would not have been the same without you. Finally, I must express my gratitude to my family and friends, in particular to my parents, for providing me with your endless patience, help, and support through the process of researching and writing this thesis. A special thank to Aksel Pettersen, for your encouragement and for always believing in me.

Ås, May 2017

Marianne Staff Fredhjem

## Sammendrag

Pasienter med kreftsykdommer har en økt risiko for thromboemboliske sykdommer, og det er også etablert en sammenheng mellom koagulasjons faktorer og økt risiko for tumor progresjon. En bedre forståelse av de underliggende molekylære mekanismene bak sammenhengen mellom kreft og trombose kan føre til en mer individualisert terapi for pasienter med kreft eller kreft-relatert trombose. Koagulasjons faktor V (FV) sin rolle i kreft er ukjent, men det er funnet assossiasjoner mellom SNPs i *F5* genet og økt risiko for brystkreft. I denne avhandlingen var målet å karakterisere koagulasjons faktor V sin rolle i kreftutvikling, ved å studere effekten og reguleringen av *F5* genet i funksjonelle studier i brystkreft cellekulturer.

To FV overekspresjons modeller ble konstruert for å studere reguleringen av *F5* i cellelinjer. Effekten av overtrykket av FV ble studert *in vitro* på genekspresjons og protein nivå, ved kvantitativ RT-qPCR og ELISA/Western blotting, i MDA-MB-231 og MCF-7 brystkreft cellelinjer. Videre ble den funksjonelle effekten av FV overekspresjon eller eksogen tilsetning av human factor V testet *in vitro* for programmert celledød, celle vekst, migrasjon, og celle signalering i de to brystkreft cellelinjene.

Den konstruerte FV overekspresjonsmodellen pcDNA5/FRT-V viste seg å ikke være optimal da den førte til et høyt uttrykk av F5 mRNA, men lave nivåer av FV protein sammenliknet med pMT2-V ekspresjons vektoren. Overkspresjonen av FV i brystkreft cellelinjene viste liten effekt på celledød og cellevekst, men en redusert celle migrasjon. Overutrykk av FV førte til opp- (hypoxia, Myc/Max, og celle syklus) eller nedregulering (notch og p53) av flere celle-signalerings mekanismer. Eksogen tilsetning av hFV hadde liten effekt på cellevekst i MDA-MB-231, men ved høy konsentrasjon av eksogen hFV økte celleveksten i MCF-7. Likt som for overutrykk av FV, så viste eksogen hFV en redusert celle migrasjon. Kun nedregulering av transkripsjonsfaktor aktiviteten for Wnt celle reaksjonsveien i MCF-7 viste seg å være påvirket av eksogen hFV.

For å oppsummere, tyder resultatene i denne avhandlingen på at FV har en redusert effekt på celle migrasjon, og kan derfor mulig være involvert i brystkreft angiogenese. I tillegg, så fører overutrykk av FV til aktiverering/nedregulering av flere viktige transkripsjonsfaktorer involvert i blant annet celleproliferasjon og tumorutvikling.

# Abstract

The risk of thrombotic diseases is increased in cancer patients, and there is also established a correlation between coagulation and cancer progression for coagulation factors and thromboembolic patients. A better understanding of the relationship between cancer progression and blood coagulation is desirable in order to achieve an improved individualized treatment for both cancer and cancer-related thrombosis. The role of coagulation factor V (FV) in cancer remains undiscovered. However, SNPs in the *F5* gene have been discovered to be associated with breast cancer, and a higher expression of *F5* is found in breast cancer tumours compared to normal tissue. The main aim of this thesis was to receive a better understanding of the role of coagulation FV in breast cancer progression.

Two plasmid-based vector systems for FV overexpression were constructed to study the regulation of *F5* in cell lines. The *in vitro* effect of FV overexpression was studied in MDA-MB-231 and MCF-7 breast cancer cells, and analysed at the gene expression and the protein level with RT-qPCR or ELISA and western blotting. Moreover, the functional effects of FV overexpression or exogenously added human FV on apoptosis, cell growth, cell migration, and cell-signalling pathways were studied *in vitro* in the breast cancer cell lines.

The constructed pcDNA5/FRT-V FV overexpression vector showed an increased expression of *F5* mRNA in MDA-MB-231 and MCF-7, but low levels and secretion of FV protein in comparison to the pMT2-V vector. FV overexpression resulted in an unaffected apoptotic effect and cell growth, but an interestingly reduced effect on cell migration. Several cancer-signalling pathways were either upregulated (hypoxia, Myc/Max, and cell cycle) or downregulated (notch and p53) in the breast cancer cell lines, due to overexpression of FV. Exogenous human FV displayed small effects on cell growth in MDA-MB-231, but increased the growth of MCF-7 cells at high doses of hFV. Moreover, exogenous human FV also reduced cell migration. None of the cancer-signalling pathways were affected by hFV in MDA-MB-231, and only downregulation of the Wnt pathway was existent in MCF-7.

In conclusion, the effects of FV on cell migration propose that FV may have a role in breast cancer angiogenesis. FV overexpression activates or downregulates several important transcription factors involved in cell proliferation, tumour development, and prevention of the cell to enter the cell cycle.

# Abbreviations

| | |
|---|---|
| A | Adenine |
| APC | Activated protein C |
| Arg | Arginine |
| AT | Anti-thrombin |
| BCA | Bicinchinonic acid |
| Bp | Base pair |
| BSA | Bovine Serum Albumin |
| cDNA | Complementary DNA |
| C | Cytosine |
| CRISPR | Clustered Regurlarly Interspaced Short Palindromic Repeats |
| Ct | Threshold cycle |
| ddNTP | dideoxyribonucleotide |
| DMEM | Dulbecco's Modified Eagle Medium |
| DNA | Deoxyribonucleic acid |
| dNTP | deoxyribonucleotide |
| DPBS | Dulbecco's Phosphate Buffered Saline |
| *E.coli* | *Escherichia coli* |
| ELISA | Enzyme-linked immunoabsorbent assay |
| EPCR | Endothelial protein C receptor |
| ER | Estrogen receptor |
| FBS | Fetal Bovine Serum |
| FRT | Flp recombination target |
| F | Factor |
| *F5* | Coagulation factor V gene |
| FV | Coagulation factor V protein |
| FVa | Activated factor V protein |
| FVII | Coagulation factor VII |
| FVIII | Coagulation factor VIII |
| FIX | Coagulation factor IX |
| FX | Coagulation factor X |
| G | Guanine |
| Gly | Glycine |

| | |
|---|---|
| HER2 | Human epidermal growth factor receptor 2 |
| hFV | exogenous Human Factor V protein |
| His | Histidine |
| HR | Hormone receptor |
| HRP | Horse-radish-peroxidase |
| IHC | Immunohistochemistry |
| IL | Interleukin |
| ISH | In situ hybridization |
| LN | Lymph node |
| Lys | Lysine |
| LB | Luria Broth |
| MP | Micro particle |
| mRNA | messenger ribonucleic acid |
| NTC | Non template control |
| p53 | Tumour protein 53 |
| PAR | Protease activation receptor |
| PCR | Polymerase Chain Reaction |
| PMM1 | Phosphomannomutase 1 |
| PR | Progesterone receptor |
| PS | Phosphatidylserine |
| pRB | Retinoblastoma protein |
| RIPA | Radioimmunoprecipitation assay buffer |
| RNA | Ribonucleic acid |
| RT-qPCR | Real-time Quantitative PCR |
| RQ | Relative quantity |
| SD | Standard deviation |
| SDS-PAGE | Sodium dodecyl sulfate polyacrylamide gel |
| SNP | Single nucleotide polymorphism |
| S.O.C | Super Optimal broth with Catabolite repression medium |
| SRPI | Solid phase reversible immobilization |
| T | Thymine |
| TF | Tissue factor |
| TFPI | Tissue factor pathway inhibitor |
| TM | Thrombomodulin |

| | |
|---|---|
| TMB | Tetramethylbenzidine |
| TNF-α | Tumour necrosis factor alpha |
| TRE | Transcriptional regulatory element |
| UV | Ultraviolet |
| VEGF | Vascular endothelial growth factor |
| VT | Venous thrombosis |
| wt | Wild type |

# Table of contents

# 1 Introduction

## 1.1 Cancer and blood coagulation

### 1.1.1 Cancer

Cancer is a complex and heterogeneous disease, where an increasing number of abnormal cells divide within an organism. Normal cell division is strictly controlled by cell signalling and takes place as the demand of new cells occurs in the human body. When a cell is exposed to injury (mutation) in its genome and normal cell signalling control results in neither mutational repair nor cell destruction, a cascade of mutations in several genes takes place. This may lead to uncontrolled and abnormal cell growth and the formation of a cancer cell. Gene alterations responsible for cancer cell formation are divided into proto-oncogenes, tumour suppressor genes, or DNA maintenance genes. A proto-oncogene functions in cell signalling of cell division or regulates induced cell death (apoptosis). When a proto-oncogene is altered for mutation, also called an oncogene, it can cause cancer cell development (Weinstein & Joe 2006). A tumour suppressor gene is responsible for induction of apoptosis and reduction of cell growth. A mutation in a tumour suppressor gene results in a loss of function, and cause cancer cell development. Alterations in DNA maintenance genes involved in DNA repair pathways are closely linked to the development of abnormal cell growth and malignancies (Chae et al. 2016). However, about only 5-10% of cancer cases are caused by genetic defects, while the remaining 95% of cancer incidents are results of environmental factors and lifestyle (Anand et al. 2008). There are established several environmental factors that increase the risk of cancer, such as tobacco use, reproductive and menstrual traits, exogenous hormone treatment, obesity and sun exposure (Kolonel et al. 2004). Today, cancer is one of the leading causes of death worldwide.

### 1.1.2 Breast cancer

Breast cancer represents the second most frequent diagnosed cancer after lung cancer, and had 1.7 million reported incidents in 2012 (Ferlay et al. 2015). Despite the steady increase of reported incidents, the mortality rate over the past years has decreased as a result of good screening programs and improved treatment of breast cancer, ranking breast cancer as the 5$^{th}$ worldwide for highest incidents of death due to cancer. Breast cancer is still the primary cause of death amongst women globally (Ferlay et al. 2015). Environmental risk factors known to

cause breast cancer are age, genetic heritage, early menstruation, late pregnancy, late menopause, hormone replacement treatment, obesity, and use of tobacco and alcohol (Kolonel et al. 2004). The genetic inheritance of breast cancer is considered to be 5-10%, mainly caused by mutations in the tumour suppressor genes *BRCA1* and *BRCA2* (Larsen et al. 2014).

Breast cancer is a heterogeneous disease, which has a broad variation in both clinical and molecular characteristics. Physical characteristics, such as tumour size, lymph node (LN) status and the histological grade (low, medium and high), have laid the foundation of several subgroups. Moreover, on the molecular level different hormone receptor markers are also used to classify the subgroups of breast cancer. The hormonal levels of estrogen receptors (ER) and progesterone receptors (PR) are determined with immunohistochemistry (IHC), while the overexpression of the human epidermal receptor 2 (HER2) protein is determined by either IHC or in situ hybridization (ISH) (Anderson et al. 2014). The presence of these predictive hormone markers is used to identify patient's prognosis as well as their ability to respond to hormonal treatment. According to gene expression patterns, breast cancer tumours are divided into four main intrinsic molecular subtypes, including basal-like, luminal A, luminal B, and HER2-enriched tumours. Whereas the basal-like tumours are defined as triple negative for the three hormone receptors (absence of ER, PR and HER2 overexpression), the luminal tumour subtypes are typical ER positive. Hormone receptor positive tumours represent the majority of breast tumours, and are likely to have an effective response to endocrine (hormonal) targeted treatment. The HER2 overexpressing and triple negative tumours are characterized clinically to have a more aggressive tumour growth and a poor prognosis (Anderson et al. 2014; Vuong et al. 2014). Tumours that are HER2 enriched often lack response to or develop resistant to HER2-targeted therapies, due to control mechanisms such as pre-existing or emerging alternative signalling pathways (i.e. ER, deregulated downstream pathways, or the immune microenvironment of the tumour). Recent studies have shown some benefit from anti-HER2 treatment combined with a single chemotherapy agent (Veeraraghavan et al. 2017), however, there is an increasing need for advances in patient stratification to accelerate development of new strategies in HER2-targeted treatment. When it comes to triple negative tumours the biological classification has been insufficient to create a unified model for molecular diagnosis, and specific therapies have not been available. Recently acquired knowledge about molecular alterations in triple negative breast cancer has lead to possible clinical approaches, such as DNA damage response targeting, anti-androgens, and immune checkpoint inhibitors, and is currently being evaluated (Denkert et al. 2017).

### 1.1.3 Cancer and tumour progression

A cancer cell has the ability of not being regulated and controlled of normal cell signals for cell division and maturation in the body, and the division of cancer cells leads to tumour formation. Abnormal cell growth in an early stage typically forms benign tumours, which is limited within the boundaries of normal tissues and does not have the ability to invade and destroy other organs in the body. Highly unstable and abnormal cell growth that leads to malignant tumour formation is more likely to lead to metastasis, the process of invasion and destruction of nearby tissues. Malignant tumours also have the ability to spread throughout the body, through the blood or lymph system, causing new tumours distant from the origin of the cancerous tumour.

Six biological hallmarks of cancer have been proposed to understand the underlying molecular mechanisms of cancer tumorigenesis, in addition to two emerging hallmarks involved in cancer pathogenesis (Figure 1) (Hanahan & Weinberg 2000; Hanahan & Weinberg 2011).

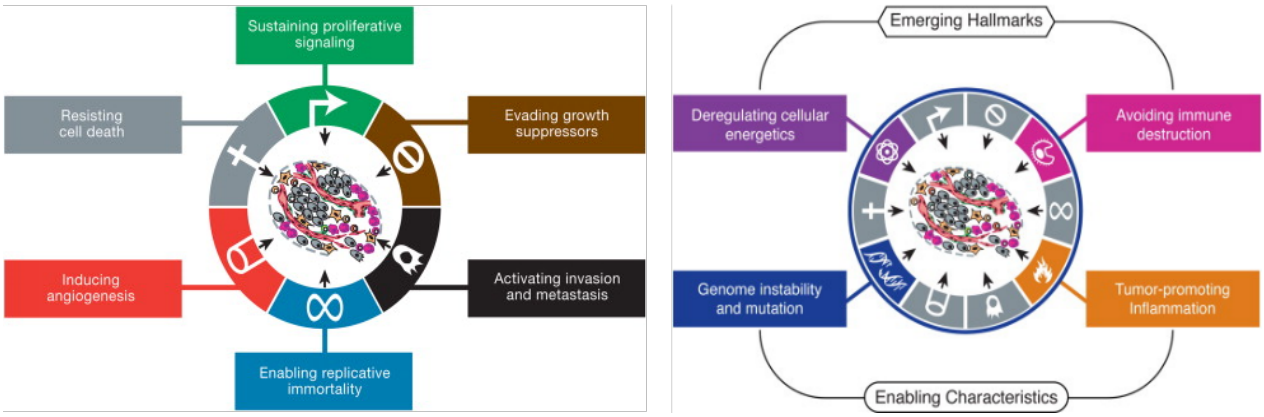


**Figure 1. The hallmarks of cancer.** Illustration of the six critical biological hallmarks of acquired cancer capabilities (left), and the two emerging biological alterations and enabling characteristics (right) (Hanahan & Weinberg 2011).

The six proposed biological hallmarks of cancer consist of (Figure 1, left):

I. **Sustaining proliferative signalling.** Cancer tumours are able to produce and control their own cell growth pathways, and are therefore not affected by exogenous cell signalling.

II. **Evading cell growth suppressors.** Alterations in tumour suppressor genes such as the *P53* gene makes the tumour cells resistant to normal cell cycle prevention of

cell growth and division. Whereas loss-of-function mutations in the retinoblastoma protein (pRb) enable the tumour cells to enter the cell cycle.

III. **Enabling replicative immortality.** Cancer cells express a specialized DNA polymerase called *telomerase*, which prevents shortening of the preserved telomere region of DNA. Following a potential of continuous elongation of cancer chromosomes and evasion of induced cell death.

IV. **Inducing angiogenesis.** Initiation of pro-angiogenic factors in cancer tumours stimulates migration of endothelial cells for blood vessel development, supporting increased blood flow to the tumour.

V. **Resisting cell death.** The cancer tumours possibility to increase expression of anti-apoptotic regulators in combination with down regulation of pro-apoptotic factors and loss of p53 activity prevents the cancer cell to undergo programmed cell death (apoptosis).

VI. **Activating invasion and metastasis.** The cancer cell's gain and loss of cell-to-cell and extracellular matrix adhesion molecules facilitate the intravasation of blood or lymphatic vessels. Through a multistep process, the tumours enhance metastasis. Altered expression of integrins and extracellular proteases assist in colonizing of the invaded tissue.

The recently proposed emerging hallmarks of cancer (Figure 1, left) involve regulation of cellular genetics and avoidance of immune destruction (Hanahan & Weinberg 2011). In addition, the two enabling characteristics: genome instability and tumour-promoting inflammation facilitates the hallmarks of cancer (Figure 1, left) (Hanahan & Weinberg 2011).

Recent technological advances including sequencing of cancer subtypes have revealed information about genetic and epigenetic alterations associated with these specific hallmarks of cancer. The emergence of genome editing technologies, in particular the system of Clustered Regurlarly Interspaced Short Palindromic Repeats (CRISPR), has the ability to advance cancer research in the near future (Moses et al. 2018).

### 1.1.4 Cancer and thrombosis

The association between cancer and thrombosis was first described in the 19th century by Bouillard and Trousseau, but the fact that hypercoagulability is a regular occurrence in cancer has been well established since then (Elaymany et al. 2014). Venous thrombosis (VT), arterial occlusion with stroke, and angina symptoms have been commonly reported incidents in cancer patients and suggested to be related to genetic predisposition (Khorana 2012). Development of VT in cancer patients are related to cancer treatment and cancer itself, dependent on the tumour type, the stage of cancer, and treatments with antineoplastic agents (Brose & Lee 2008; Elaymany et al. 2014). Cancer patients are exposed to a 4-20% risk of evolving VT, and cancer-associated VT represents the second leading cause of death in cancer patients after the cancer itself (Hisada & Mackman 2017; Khorana et al. 2007). The rates of VT are discovered to vary according to cancer types, leaving pancreatic, ovarian, brain, stomach, gynaecologic, and hematologic cancers with the highest incidents of VT. Breast cancer is reported as one of the cancer types with lowest risk of VT. However, there is a 3 to 4-fold increased risk of evolving VT in women with breast cancer, compared with women of an equivalent age without cancer (Hisada & Mackman 2017; Walker et al. 2016). Moreover, dysfunctions in specific proteins that contribute to haemostasis are also discovered to be involved in cancer progression, indicating a bidirectional link of thrombosis and the risk of cancer development (Falanga et al. 2013; Jain et al. 2010).

### 1.1.5 Cancer progression linked to coagulation

Cancer patients are predisposed to thrombosis or haemorrhage due to an imbalance in the haemostatic system. The pathogenesis of cancer-associated thrombosis is multifactorial and influenced by both clinical and biological factors. Most important are the tumour-specific properties that have the ability to activate the host haemostatic system, which are driven by the same oncogenes responsible for the cellular neoplastic transformation (Falanga et al. 2017). Tumour cells can activate coagulation through expression of coagulation proteins, exposure of pro-coagulant lipids, through direct adhesion and activation of host vascular cells (i.e. platelets, endothelial cells and leucocytes), and by release of inflammatory cytokines (i.e. TNF-α and IL-1β) and micro particles (MPs) (Falanga et al. 2013). These tumour-specific pro-thrombotic properties (Figure 2) can be divided into coagulation dependent and coagulation independent properties.

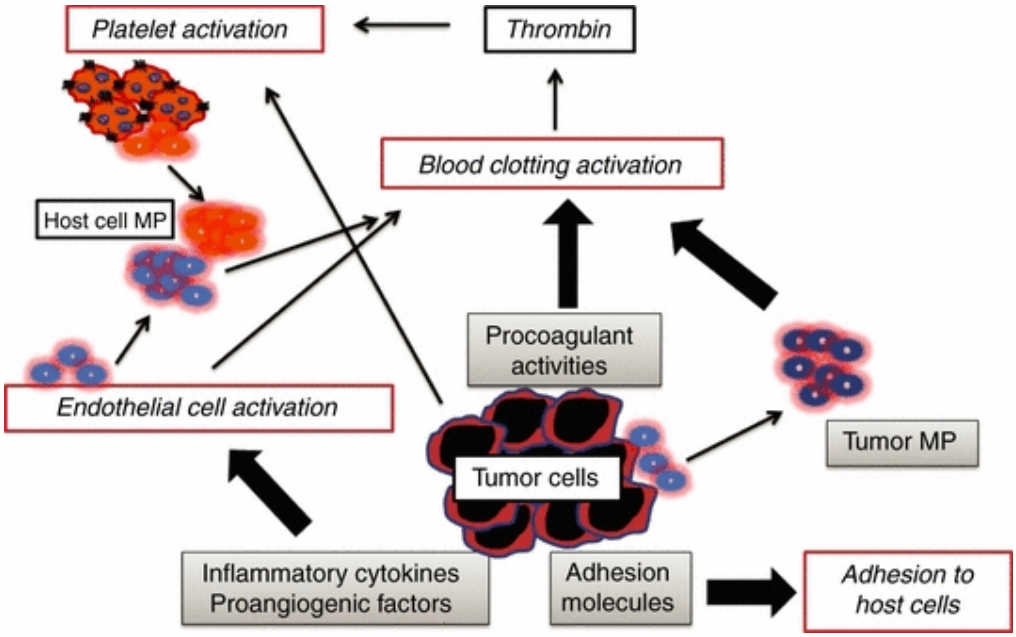


**Figure 2. Tumour-haemostatic system interactions.** Tumour cells can activate the haemostatic system in multiple ways. Release of procoagulant proteins and MPs activates the coagulation cascade. Cancer cells may also activate the host haemostatic cells (endothelial cells and platelets), by the release of soluble factors or direct adhesive contact (Falanga et al. 2013).

The coagulation dependent properties of the tumour progression include deposition of fibrin on the tumour cell surface. Fibrin participates in increasing the metastatic potential in cancer cells by providing a structural surface for tumour settlement and neovascularization. In addition, the fibrin provides protection of growth and angiogenic factors from degradation. Furthermore, physical interaction between platelets and tumour cells protects the tumour cell surface from immunological recognition (Falanga et al. 2017).

Cancer progression is also enhanced by mechanisms including haemostatic proteins independent of direct coagulation activity. The tissue factor (TF) plays an important role inducing vascular endothelial growth factor (VEGF) expression and promoting tumour neovascularisation. TF and thrombin function in the activation of protease activation receptors (PARs). Tumour cells expressing activated PARs facilitate cell survival, adhesion, angiogenesis, and cell migration. Finally, locally generated inflammatory mediators (i.e. TNF-α) activate neutrophils in the tumour microenvironment. This leads to tumour adhesion and protection, and assist tumour cell migration across endothelial barriers (Falanga et al. 2013).

## 1.2 Coagulation factor V

### 1.2.1 Haemostasis

Haemostasis is an important physiological process in the body. After a vessel injury the haemostatic system control the initiation of vascular spasms, formation of platelet plugs/fibrin clots at the disrupted site and eventually restoration of the vascular integrity. Multiple mechanisms and factors play a central role in maintaining a balanced haemostatic system. A well-controlled haemostatic process relies on pro-coagulant and anti-coagulant factors as well as cellular components and plasma proteins. Activation and inhibition of coagulation factors are important to maintain blood in a fluid state, while fibrinolytic factors dissolve any generated blood clots. Insufficient control of the haemostatic mechanisms may lead to fatal consequences, such as excessive bleeding (haemorrhage) after injury or the opposite: generation of unwanted blood clots.

### 1.2.2 Blood coagulation and regulation

The coagulation process is one of the most important haemostasis mechanisms at bigger injury incidents. The coagulation process includes a number of factors, which are triggered at injury (Versteeg et al. 2013). This leads to a cascade of coagulation factor activation until fibrin is formed, briefly described in the figure below (Figure 3).

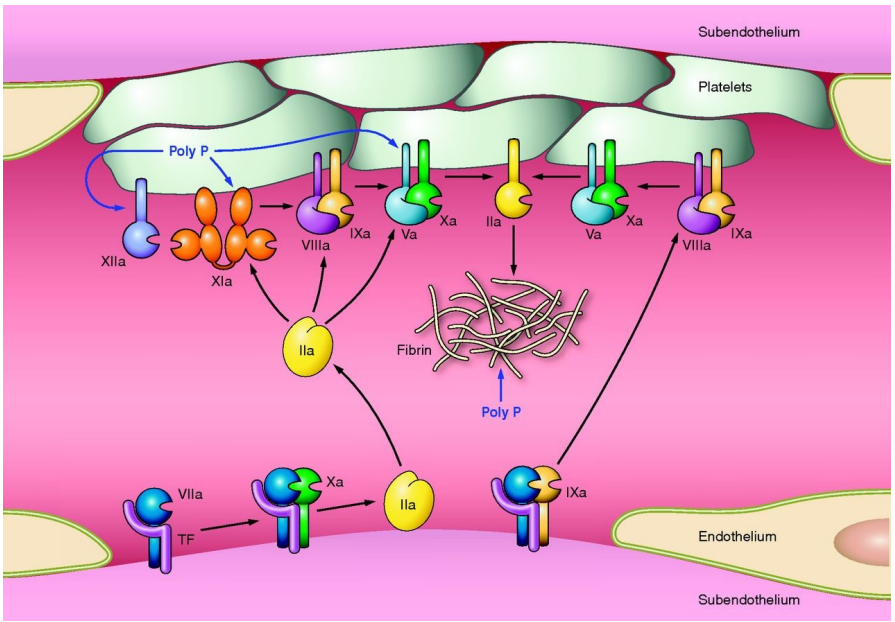


**Figure 3. Cell based model of the coagulation process.** Upon injury of endothelial lining, tissue factor (TF) bearing cells are exposed to blood and binds factor VII. Further, the activated TF:VIIa complex leads to activation of factor X and prothrombin (II), and small amounts of thrombin (IIa) stimulates activation of platelets, FV, FVIII and FXI. The coagulation factors assemble on the platelet surface, and the tenase complex (FIXa-FVIIIa) activates FX to FXa. Subsequently, the prothrombinase complex (FXa-FVa) alters prothrombin to thrombin, resulting in increased thrombin formation necessary for generation of a platelet-fibrin clot that plugs the injury (Versteeg et al. 2013).

When platelets are activated during the coagulation process (Figure 3), negatively charged phospholipids such as phosphatidylserine (PS) are translocated to the outer platelet membrane. Resulting in development of a pro-coagulant surface, onto which coagulation factors can assemble, mediated by $Ca^{2+}$ ion bridges (Krishnaswamy 2013; Smith 2009). Resting endothelial cells under healthy conditions lack PS on their outer membrane, and do not support coagulation activity. Thrombin generation is therefore only located to the site of injury, where cells are triggered to express pro-coagulant surfaces. Nevertheless, to avoid an excessive and potentially harmful coagulation, the coagulation process is well regulated by anti-coagulant pathways. There are several important coagulation inhibitors that contributes to a normal haemostatic system, such as anti-thrombin (AT), tissue factor pathway inhibitor (TFPI), and protein C, which targets specific coagulation factors (Figure 4) (Smith 2009).

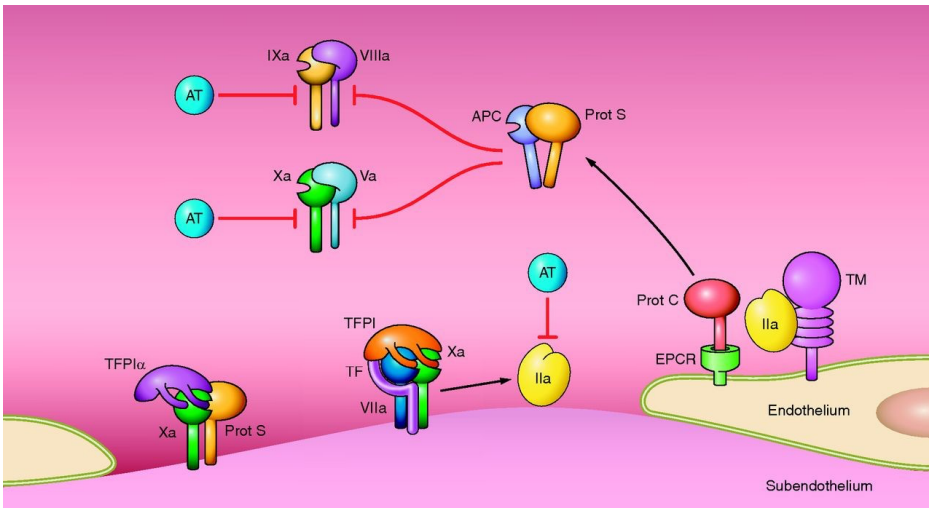


**Figure 4. Negative regulation of the coagulation process.** TFPI obstructs TF initiated coagulation by inhibition of FXa (enhanced by protein S) or the TF-FVIIa-FXa complex. Anti-thrombin inhibits FIXa, FXa and thrombin. TM bound thrombin is presented to protein C in complex with EPCR. The activated APC complex and its co-factor protein S thereafter inactivates FVa and FVIIa (Versteeg et al. 2013).

The tissue factor pathway inhibitor (TFPI) is a protease inhibitor of the TF initiated coagulation, resulting in less generated thrombin. TFPI inhibits free FXa as well as the TF-FVIIa complex, and is enhanced by the binding of protein S (Smith 2009). Anti-thrombin (AT) is a serine protease inhibitor, which inhibits several activated coagulation factors, including thrombin, FXa, and FIXa (Smith 2009; Versteeg et al. 2013). Further the protein C pathway is an important anti-coagulant mechanism. Thrombin bound to thrombomodulin (TM) on the endothelial cell surface activates protein C, complexed with the endothelial protein C receptor (EPCR). Activated protein C (APC) binds its cofactor protein S and cause inactivation of FVIIIa and FVa, respectively suppressing the activity of the tenase and the

prothrombinase complexes. In addition, the presence of protein S and intact functionality of FV, acts as an additional cofactor to the APC-mediated cleavage of FVa and FVIIIa (Versteeg et al. 2013).

### 1.2.3 Structure and function of coagulation factor V

Coagulation factor V (FV) is a cofactor in the coagulation process, and was first discovered in 1943 by the Norwegian haematologist Paul Owren, whom depicted FV as a fifth component required in formation of fibrin (Asselta et al. 2006; Mann & Kalafatis 2003; Owren 1947). The discovery of FV also identified its pro-cofactor properties, as the need of FV for prothrombin activation and generation of thrombin.

The human *F5* gene was first isolated in 1992 (Cripe et al. 1992; Duga et al. 2004), it spans about 80 kb of chromosome 1, and comprises 25 exons (Figure 5A). Following transcription, the 6.9 kb long *F5* mRNA sequence encodes the FV protein consisting of 2224 amino acids. The pre-procofactor V includes a 28-residue signal peptide, which is removed after translocation to the endoplasmic reticulum (Mann & Kalafatis 2003), resulting in the A1-A1-B-A3-C1-C2 domain structure of inactive cofactor V (Figure 5B). The B domain keeps FV in a procofactor form and is proteolytically cleaved in the presence of a pro-coagulant membrane surface, leading to activated FV (FVa). The cleaved FVa consist of a heavy (A1 and A2) and a light chain (A3, C1, and C2), held together by hydrophobic interactions and a $Ca^{2+}$ ion (Figure 5C).

The single-chain FV protein (330 kDA) circulates in blood in its inactive form, whereas 80% of FV circulates in plasma at a concentration of approximately 20 nM (7.0 µg/mL) (Asselta et al. 2006; Duga et al. 2004). The remaining 20% of FV present in whole blood is contained in platelet α-granules. The platelet storage of FV is associated with the Multimerin protein, and the proteins are released upon platelet activation (Mann & Kalafatis 2003). Synthesis of plasma-derived FV is performed by hepatocytes in the human liver (Dashty et al. 2012), while the platelet fraction of FV is partly synthesized by megakaryocytes and partly absorbed from plasma via endocytosis (Duga et al. 2004). Factor V has the possibility to express both pro-coagulant and anti-coagulant cofactor properties (Figure 5B), and a deficiency in the *F5* gene might cause misbalance in the pro-coagulant and anti-coagulant activities, leading to thrombosis or haemorrhage.

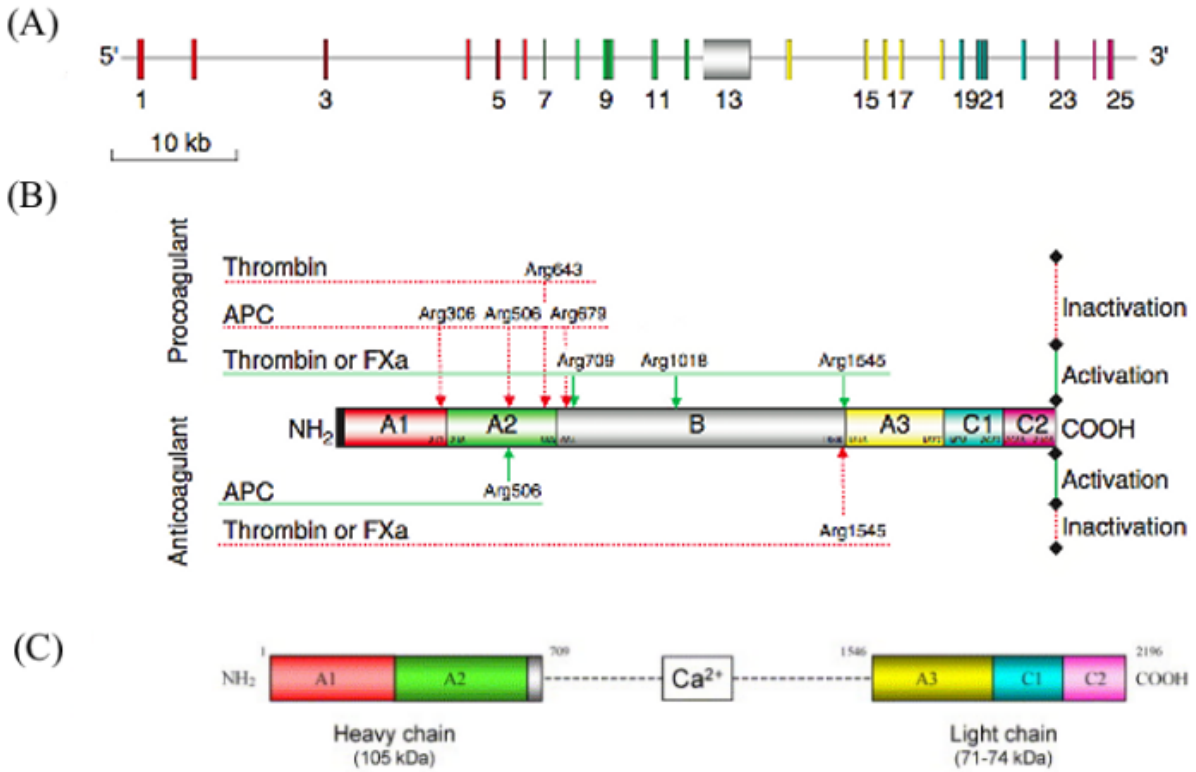


**Figure 5. Schematic structure of the *F5* gene and the FV protein.** (A) Representation of the 6.9 kb long *F5* gene and its exon-intron structure. The exons are presented as coloured boxes according to the encoded domain. (B) Schematic overview of the single-chain 330 kDA FV domain. The six domains (A1, A2, B, A3, C1, and C2) are indicated with different colours. Numbers within each box indicates the N- and C-terminal residues of each domain. The black box at the N-terminus represents the 28-residue signal peptide. Positions of proteolytic cleavage sites responsible for activation and inactivation of the pro- and anti-coagulant properties of FV are illustrated in the domain with arrows (Asselta et al. 2006). (C) Schematic overview of the activated FVa domain structure. After activation by thrombin or FXa, the FVa domain is composed of a heavy (A1 and A2) and light chain (A3, C1, and C2) detained by a single calcium ion (Duga et al. 2004).

### 1.2.4 Pro-coagulant factor V

#### *Activation of FV to pro-coagulant FVa*

Factor V is activated to cofactor FVa by thrombin, FXa, or plasmin. Thrombin is the main activator of FV, and cleaves FV at three sites chronologically in an early stage of the blood coagulation process, respectively the Arg709, Arg1018, and Arg1545 sites (Figure 5B, and Figure 6A) (Dahlback 2016; Mann & Kalafatis 2003). Upon cleavage, the B domain is removed and the heavy and light chain of FVa is noncovalently linked with a calcium ion (Figure 5C), whereas FVa exposes a high-affinity binding-site to FXa. The Arg709 and Arg1018 sites in the B domain are kinetically favoured for cleavage, but results in a partially FV cofactor activity to FXa. Hence, the completely generated cofactor activity to FXa is only

gained when the Arg1545 site is cleaved and the whole B domain is released (B. 2017; Dahlback 2016).

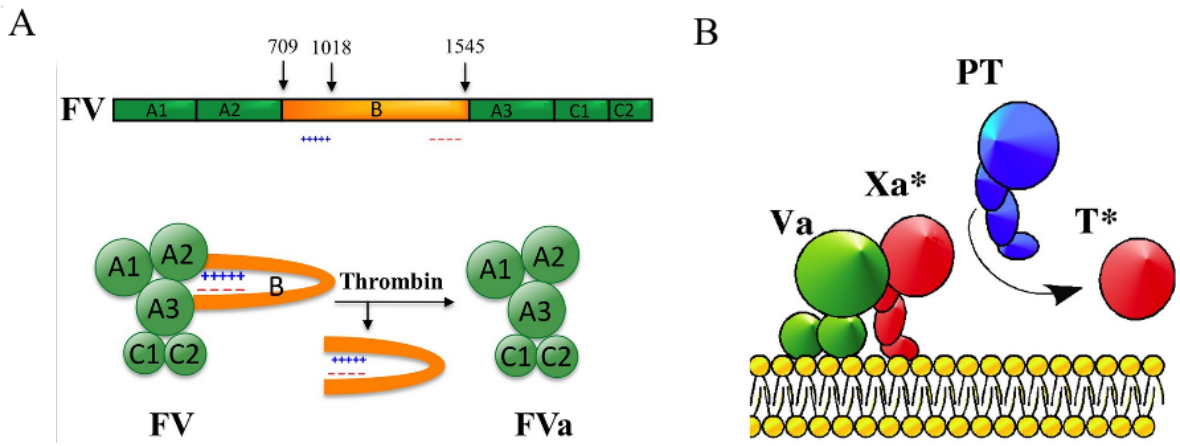


**Figure 6. Thrombin activation of the pro-coagulant FV, and formation of the prothrombinase complex.** (A) FV is cleaved by thrombin at Arg709, Arg1018, and Arg1545, releasing the B domain. The A1 and A2 domains are linked to the A3, C1, and C2 domains with a calcium ion and hydrophilic interactions, resulting in FVa. (B) The activated FVa binds to FXa and assembles on a PS surface, forming the prothrombinase complex. The complex is an efficient activator of prothrombin to thrombin. Modified from (Dahlback 2016).

The binding of cofactor FVa and FXa on a negatively charged phospholipid surface (i.e. activated platelets) creates the prothrombinase complex (Figure 6B). Further, this complex is essential for activation of prothrombin to thrombin. The binding of FVa enhances the FXa enzyme affinity to phospholipid membrane binding and the FXa activity. Thus, increasing the conversion of prothrombin to thrombin by 5-fold, compared to FXa catalysing the reaction alone (Lee & Mann 1989; Mann & Kalafatis 2003; Zeibdawi & Pryzdial 2001).

The FXa enzyme cleaves and activates FV at the same sites as thrombin, but the FXa concentrations present in the initiation phase of coagulation are unsatisfactory to explain the levels of activated of FV (Mann & Kalafatis 2003). The serine protease plasmin is a catalyst of fibrinolysis, and has the ability to initiate both the active and inactive form of FV (Mann & Kalafatis 2003), providing an impact on the pathology of thrombosis. Plasmin activation of FV has an efficiency of 20-30% compared to thrombin and FXa activation of FV. However, the plasmin inactivation of FVa is favoured over FV activation when FV/FVa is bound to a membrane surface (Lee & Mann 1989).

### *Inactivation of pro-coagulant FVa*

The proteolytic inactivation of pro-coagulant FVa by APC, thrombin, and plasmin are important for regulation of the coagulation process (Cramer & Gale 2012) (Lee & Mann 1989). Activated protein C binds and attacks FVa at several peptide bonds sensitive for proteolytical cleavage, including Arg306, Arg506, and Arg679 (Figure 5B), resulting in the loss of FVa pro-coagulant activity (Figure 7) (Dahlback 2016). The most efficient cleavage site by APC is the Arg506, decreasing the FVa activity due to reduced affinity to FXa (Dahlback 2016). Conversely, this site has low accessibility when FVa is assembled with FXa in the prothrombinase complex. The following cleavage of Arg306 completes the inhibition of FVa. Single cleavage of the Arg306 site requires the presence of protein S, which serves as a cofactor to the APC (Figure 7), while cleavage of Arg679 is suggested to be less important (Asselta et al. 2006; B. 2017; Duga et al. 2004).

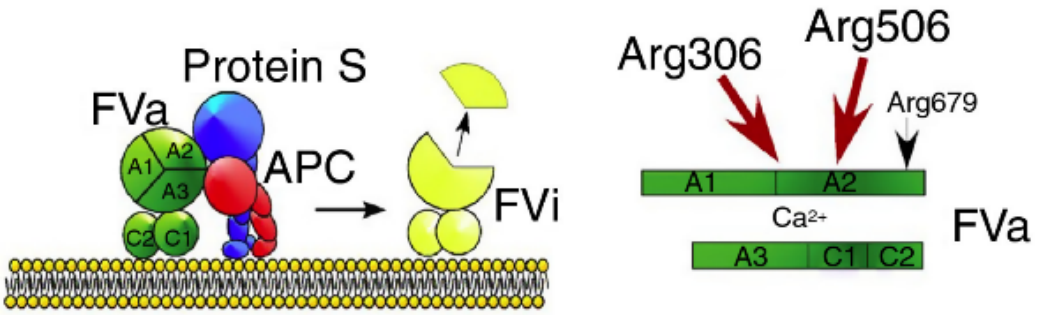


**Figure 7. Inactivation of pro-coagulant FVa by the APC-protein S complex.** FVa bound to a phospholipid surface is sensitive to cleavage in the heavy chain by APC. In the absence of FXa the APC cleaves FVa at Arg506, resulting in a partially loss of FVa function. APC in complex with protein S is able to cleave FVa at Arg306 and Arg506, causing complete inactivation of FVa (FVai) (B. 2017).

Thrombin inactivation of FVa occurs in the presence of endothelial cells, whereas FVa is proteolytically cleaved at Arg643 and gains a reduced affinity between the heavy and light chain of FV (Figure 5B) (Asselta et al. 2006). Inactivation of FVa by plasmin involves cleavage at Lys309, Lys310, Arg313, and Arg348, and is dependent on the FVa bound to a membrane surface (Lee & Mann 1989; Mann & Kalafatis 2003).

### 1.2.5 Anti-coagulant properties of factor V

Factor V serves as cofactor in the APC/protein S inactivation of factor VIIIa (Figure 8). APC cleavage of FV at Arg506 (Figure 5B), before thrombin or FXa has activated the pro-coagulant FVa, generates the anti-coagulant properties of FV (Cramer & Gale 2012; Mann & Kalafatis 2003). Hence, the APC cleavage of FV is dependent on the C-terminal end of the B-

domain. In addition, the presence of protein S as a cofactor to APC is essential of the cofactor activity of FV towards APC inhibition of the tenase complex (FIXa-FVIIa) (Figure 8) (B. 2017). Membrane bound cofactor activity of FV and FVa with an intact B domain accelerate the inactivation of FVIIIa by the APC-protein S complex by 2-fold (Mann & Kalafatis 2003).

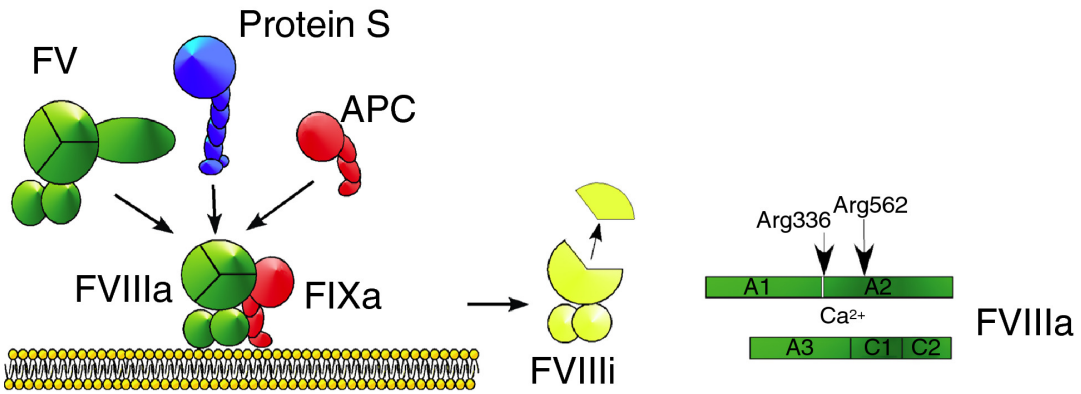


**Figure 8. The anti-coagulant FV as a cofactor to the APC-protein S inactivation of FVIIIa.** The tenase complex (FIXa-FVIIIa) is bound to a negative PS surface. FV acts as a cofactor to APC cleavage of FVIIIa, in the presence of protein S. Modified from (B. 2017).

The anti-coagulant FV may be inactivated and disabled to a semi pro-coagulant molecule by thrombin or FXa cleavage at Arg709, Arg1018, and Arg 1545 (Asselta et al. 2006). The cofactor activity of FV to APC is only lost when the Arg1545 site is proteolytically cleaved, leading to detachment of the B domain from A3.

### 1.2.6 Other non-coagulant properties of factor V

Inflammation is proposed as one of the enabling characteristics of cancer (section 1.1.3). Several evidences suggest that the tumour microenvironment consists of inflammatory cells, which participate in the neoplastic process by promoting tumour initiation, cell proliferation, survival, and migration (Coussens & Werb 2002; Eiró & Vizoso 2012; L. 2017). Tumour cells have adopted signal molecules of the innate immune system, including selectins and chemokines. Moreover, coagulation factors such as TF, thrombin and fibrinogen are linked with inflammation diseases (Davalos & Akassoglou 2012). Anti-coagulant FV is associated with anti-inflammatory response due to its cofactor function of aPC. The TF-FVIIa-FXa complex is destabilized by aPC in the presence of PS, protein S, and cofactor FV, leading to inhibition of EPCR activation of the inflammatory PAR2 signalling (Sun 2015).

Mutations in the *F5* gene have been associated with cancer. The prothrombotic factor V Leiden (rs6025) polymorphism in homozygous carriers is shown to increase the risk for colorectal cancer with 5.8-fold, compared to non-carriers (Vossen et al. 2011). Klee *et al*. discovered high expression levels of *F5* mRNA in prostate cancer tissues, and a high storage of thrombin, suggesting that FV may be an important biomarker for prostate cancer (Klee et al. 2012). Previous findings in our research group also proposed an association of *F5* and breast cancer, but to be independent of FV Leiden carrier status (Tinholt et al. 2014).

### 1.2.7 The role of factor V in breast cancer

Single nucleotide polymorphisms (SNPs) in *F5* have been associated with breast cancer patients. Recently studies in our research group discovered higher expression of *F5* in breast tumours compared to normal tissue (Tinholt et al. 2018). Breast cancer patients with elevated *F5* expression levels had tumour characteristics of aggressive nature (hormone receptor negative-, triple negative-, HER2 overexpressing-, and basal-like tumours). Furthermore, breast cancer patients with basal-like tumours were also suggested to have a greater survival rate when expressing high levels of *F5* (Tinholt et al. 2018). However, the specific biological role of FV remains undiscovered, but high expression of FV may be used as a possible clinical marker of aggressive breast cancer. This underlines the importance of developing new therapeutic strategies targeting the coagulation processes in cancer.

## 1.3 *In vitro* cell models

*In vitro* experiments are performed with microorganisms, cells, or biological molecules outside their normal biological environment. The complexity of a living organism makes it difficult to study and identify interactions between components at a detailed level. A poor overlap between species when using animal models before introducing the systems in humans has been a challenge especially in the pharmaceutical industry, when introducing new drugs into the market (Waring et al. 2015). *In vitro* cell models are widely used to study the biological responses and mechanisms related to human health and disease. Cell models can be used for overexpression in cell lines or more complex systems in specialized cells, tissues, or organs. *In vitro* experiments enable a more detailed and specified study by removing the cell from its original context. It arises advantages of simplifying the biological functions, analysis, and sample size, in addition to enabling pharmacological manipulations and genetic modifications. Results obtained from *in vitro* experiments can be used further to predict the

effect *in vivo* (in the living organism), but it includes making a consistent and reliable extrapolation procedure in the transition to an *in vivo* experiment.

### 1.3.1 FV overexpression plasmid systems

Recombinant DNA technology has made it possible to clone a gene of interest into an expression vector, which can be introduced further into cultured eukaryotic cells to study the gene regulation and the protein biosynthesis. Plasmids are double-stranded, circular DNA molecules (Lodish et al. 2000), and are commonly used as expression vectors for *in vitro* experiments. Cloning of a gene of interest can be done with restriction enzymes, which recognize specific restriction sites in DNA, preparing the gene for insert in a vector through 3'→5' phosphodiester linkage. Further, the vector is introduced to a host cell, and then reproduced through replication along with the host cell's DNA. The most commonly used host cells for DNA cloning are *Escherichia coli (E. coli)* and the bacteriophage lambda (λ) vector (Lodish et al. 2000). Plasmids often contain other functions than what are necessary for DNA replication, such as a drug-resistance gene (i.e. antibiotic resistance), providing a selective growth of transformants.

The constructed expression vector can be transfected to a cell model to study the *in vitro* effects of the gene or the protein function, either through transient- or stable transfection of cells. In transient transfection, the gene of interest is introduced to the cell nucleus but is not incorporated to the host cells genome (Kim & Eberwine 2010). The overexpression plasmid often contains an eukaryotic promoter, resulting in high gene and protein expression. But, due to cell division, the expression is time limited and dependent of cell type. In contrast, stable transfection enables the genetic material to be integrated into the host cells genome, controlling the host cell to express the gene of interest when it replicates (Kim & Eberwine 2010). In addition, an eucaryotic marker gene for antibiotic resistance in the plasmid is used for selection of transfected cells, whereas only cells with the integrated plasmid will survive a longer period of incubation with the appropriate antibiotic.

In this thesis two plasmid-based expression vector systems were used to study the *in vitro* effects of FV overexpression in breast cancer cell lines. We possessed a commercial expression vector containing the *F5* gene: pMT2-V (ATCC®). However, as the pMT2-V plasmid lacks an eukaryotic selection marker, the *F5* sequence was subcloned from the

pMT2-V vector into the pcDNA5/FRT mammalian expression vector. Unlike the pMT2 vector, the pcDNA5/FRT contains a mammalian antibiotic resistance gene (*Hygromycin*), which enables selection of cell lines with stable overexpression of the desired gene (in this case *F5*).

# 2 Aims of the study

The risk of thrombotic diseases is increased in breast cancer patients, and a correlation between coagulation and cancer progression for coagulation factors such as tissue factor, tissue factor pathway inhibitors, and factor VII, have been identified. A better understanding of the relationship between cancer progression and blood coagulation is desirable in order to achieve an improved individualized treatment for both cancer and cancer-related thrombosis. Previous results from the research group showed that single nucleotide polymorphisms (SNPs) in *F5* (encoding for the coagulation factor V protein) were associated with breast cancer. They also found a higher expression of *F5* in breast cancer tumours compared to normal tissue, and that *F5* expression is increased in aggressive breast tumours. *F5* expression may therefore be a possible marker of aggressive breast cancer. Breast cancer patients with basal-like tumours have a better survival rate when expressing high levels of *F5* (Tinholt et al. 2018). However, the functional role of coagulation factor V (FV) in cancer remains undiscovered. The main objective of this thesis was to characterize the role of coagulation factor V in breast cancer progression. FV overexpression models and exogenous FV were used to study the *in vitro* functional effects of FV in breast cancer cell lines.

The specific objects of this study were:

I. *In vitro* effects of factor V overexpression in breast cancer cells:
   - Create plasmid-based vector systems for FV overexpression in cell lines.
   - Test the efficiency of the FV expression plasmids at the gene and protein level in breast cancer cells.
   - Study the functional effects of FV overexpression on apoptosis (programmed cell death), cell growth, migration, and cell signalling.

II. *In vitro* effects of exogenous FV in breast cancer cells:
   - Study the functional effects of exogenously added FV on cell growth, migration and cell signalling.

# 3 Materials and methods

Material outline for reagents, chemicals, solutions, kits, instruments, software, antibodies, primers, vectors and cells used in this thesis is presented in Appendix A.1-A.9.

## 3.1 Creation of plasmid-based expression vectors for FV overexpression

Two plasmid-based expression vector systems were created in order to study *in vitro* effects of FV overexpression in breast cancer cells. We possessed a commercial expression vector containing the *F5* gene: pMT2-V (ATCC®). However, as no empty pMT2 vector was available, therefore we created an empty version of the pMT2-V vector to be used as vector control in cell experiments. With limited knowledge about the features of the plasmid, and a lack of eukaryotic selection markers, the *F5* sequence was subcloned from the pMT2-V vector into the pcDNA5/FRT mammalian expression vector. Unlike the pMT2 vector, the pcDNA5/FRT contains a mammalian antibiotic resistance gene (*Hygromycin*), which enables selection of cell lines with stable overexpression of the desired gene (in this case *F5*). The pcDNA5/FRT vector is also constructed with an Flp-In™ System from the manufacturer, which engages introduction of an Flp Recombination Target (FRT) site into the genome of the mammalian cell line. The site-specific recombinase technology is based on the *Flp* recombinase binding to the FRT site of the vector, and enables integration and expression of the desired gene at a specific genomic location in the mammalian cell line of choice (Craig 1988; Sauer 1994). All vectors used in this thesis are presented in Appendix 6.

### 3.1.1 Creation of an empty pMT2 control vector

#### *Restriction enzyme digestion of the pMT2-V plasmid*

We possessed an overexpression vector containing the entire *F5* cDNA sequence: the pMT2-V (ATCC®) plasmid. To create an empty vector for overexpression studies of FV in breast cancer cell lines, the plasmid was digested with the restriction enzyme *SalI,* which recognition sites was flanking both sides of the *F5* cDNA insert (Figure 9). The Thermo Scientific's FastDigest Kit was used and the manufacturer's protocol for plasmid DNA was followed. In short, the reaction mixture (Table 1) was incubated at 37°C in a heat block for 15 minutes. To control the function of the restriction enzyme, one additional reaction with undigested pMT2-V was included. To verify the digestion, a 0.7% agarose gel was run (described in 3.3.1).

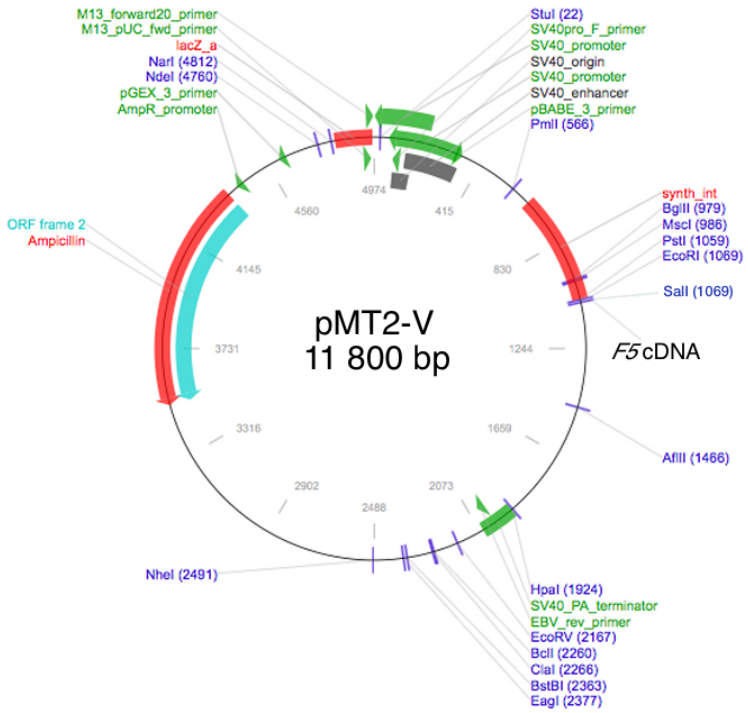


**Figure 9. Map overview of the pMT2-V plasmid.** The total size of the circular plasmid is 11 800 bp, and the 6 900 bp long *F5* cDNA insert is located at the *SalI* restriction site (modified from https://www.addgene.org/vector-database/3650/). The figure illustrates different enzyme restrictions sites and functions of the vector, with an ampicillin resistance gene located 3500-4350 bp downstream the vector.

**Table 1. Reagents and volumes used for the digestion of pMT2-V.**

| **Reagents** | **Volume for digestion of plasmid (1x reaction)** | **Volume for undigested plasmid (1x reaction)** |
|---|---|---|
| Water, nuclease-free | 36.7 µL | 15.0 µL |
| 10X FastDigest Green Buffer | 5.0 µL | 2.0 µL |
| pMT2-V (5.0µg) | 3.3 µL | 2.0 µL |
| FastDigest *SalI* enzyme | 5.0 µL | - |
| Total volume | 50.0 µL | 20.0 µL |

The linearized pMT2 vector was isolated from the gel and purified using the Wizard® SV Gel and PCR Clean-Up System Kit, by following the manufacturer's protocol for DNA purification. The DNA yield was determined using the NanoDrop® ND-1000 spectrophotometer as described in section 3.3.4.

### *Re-ligation of the pMT2 plasmid*

The linearized and purified pMT2 fragment was recircularized using Thermo Scientific's Rapid DNA Ligation Kit. The *T4 DNA ligase* catalyses the formations of a phosphodiester bond between the cleaved ends of DNA. Reagents (Table 2) were combined and incubated at 22°C for 15 minutes.

**Table 2. Reagents and amounts used for one ligation reaction to recircularize the linear pMT2 fragment.**

| **Reagents** | **Sample volume (1x reaction)** |
|---|---|
| Linearized pMT2 vector (50 ng) | 6.5 µL |
| 5X Rapid Ligation Buffer | 10.0 µL |
| *T4 DNA Ligase*, 5 U/µL | 1.0 µL |
| Water, nuclease-free | 32.5 µL |
| Total volume | 50.0 µL |

5.0 µL of the ligation mixture was used for transformation of OneShot® TOP10 chemically competent *Escherichia coli* cells (described in 3.2.1). Plasmid DNA from *E. coli* cell culture was isolated and purified by the ZymoPURE™ Plasmid Maxiprep Kit (described in 3.3.2). Two control approaches were made to verify a successful relegation, and thereby the creation of an empty pMT2 vector. The newly made pMT2 vector was verified by:

1) Restriction enzyme cutting with *SalI*, followed by running an agarose gel.
2) PCR with *F5* specific primers (described in 3.3.6).

## 3.1.2 Subcloning of *F5* into the pcDNA5/FRT vector

### *Long range PCR of F5 cDNA*

The pMT2-V plasmid was used as a template for subcloning of the *F5* cDNA to an empty pcDNA5/FRT plasmid, for use in overexpression studies of FV in breast cancer cell lines. For amplification of the nearly 7 kb long *F5* sequence the Q5® High Fidelity long-range PCR Kit was used (section 3.3.6). To make the amplified *F5* cDNA compatible for restriction digestion and subcloning to the pcDNA5/FRT plasmid, *F5* specific primers tailed with *HindIII* and *NotI* overhangs (Table A.9.2, Appendix A.9) were used in the long-range PCR. The newly constructed empty pMT2 vector was used as a negative control. The long-range

PCR products were loaded on a 1.0% agarose gel for verification of a successful amplification, followed by purification with the Wizard® SV Gel and PCR Clean-Up kit.

### *Restriction enzyme digestion of F5 cDNA and destination vector*

To produce compatible ends before ligation, the amplified *F5* cDNA and the pcDNA5/FRT vector (Figure 10) were double digested with *HindIII* and *NotI* enzymes. Single-digested and undigested samples were included as controls for enzyme activity. Reactions were combined at room temperature (Table 3), and incubated at 37°C in a heat block for 30 minutes. The enzymes were inactivated at 80°C for 10 minutes. Samples were separated by agarose gel electrophoresis. The digested *F5* cDNA was cleaned directly by using the Wizard® SV Gel and PCR Clean-Up Kit to gain the highest possible yield, while the digested pcDNA5/FRT vector was isolated and purified from gel.

**Table 3. Reagents and volumes used for FastDigestion of pcDNA5/FRT and *F5* cDNA.**

| **Reagent** | **Digested w/ *HindIII* and *NotI*** | **Control, undigested** | **Control, digested w/*HindIII*** | **Control, digested with *NotI*** | **Digested *F5* PCR product** |
|---|---|---|---|---|---|
| pcDNA5/FRT plasmid (1.0 µL ) | 1.0 µL | 1.0 µL | 1.0 µL | 1.0 µL | - |
| *F5* cDNA (0.2 µL) | - | - | - | - | 1.54 µL |
| 10x FastDigest Green Buffer | 2.0 µL | 2.0 µL | 2.0 µL | 2.0 µL | 2.0 µL |
| Enzyme:<br>*HindIII*<br>*NotI* | <br>1.0 µL<br>0.9 µL | <br>-<br>- | <br>1.0 µL<br>- | <br>-<br>0.9 µL | <br>1.0 µL<br>0.9 µL |
| Nuclease free $H_2O$ | 15.1 µL | 17.0 µL | 16.0 µL | 16.1 µL | 24.56 µL |
| Total volume | 20.0 µL | 20.0 µL | 20.0 µL | 20.0 µL | 30.0 µL |

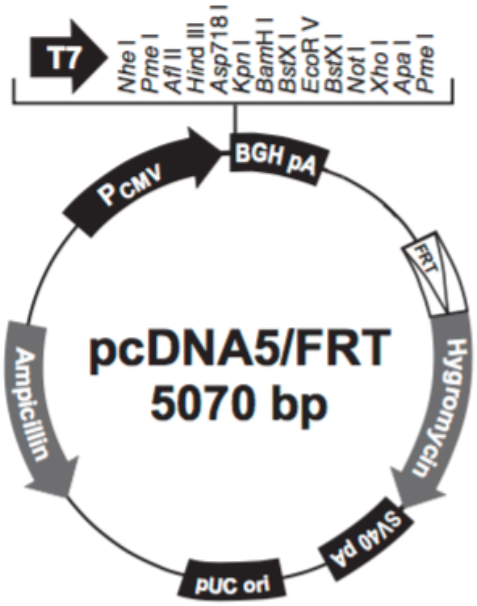


**Figure 10. Map overview of the pcDNA5/FRT vector.** The 5070 bp long pcDNA5/FRT vector contains different enzyme restriction sites, situated between the T7 and BGH promoter. The pcDNA5/FRT was digested with *HindIII* and *NotI*, for preparation of ligation with the *F5* cDNA insert. (Modified from https://www.thermofisher.com/order/catalog/product/V601020).

### *Ligation of F5 cDNA and destination vector*

After digestion and purification, the Thermo Scientific's Rapid Ligation kit was used for ligation of the digested and purified *F5* cDNA with the linearized pcDNA5/FRT vector (Table 4). Insert and vector were ligated in a 3:1 ratio. All reagents were assembled at room temperature and incubated at 22°C for 20 minutes.

**Table 4. Reagents and amounts used for ligation with *T4 DNA ligase*.**

| **Reagent** | ***F5* and pcDNA5/FRT digested w/ *HindIII* + *NotI*** |
|---|---|
| *F5* cDNA (62.48 ng) | 5.36 µL |
| Linearized vector pcDNA5/FRT (11.95 ng) | 1.0 µL |
| 5X Rapid Ligation Buffer | 4.0 µL |
| *T4 DNA Ligase*, 5 U/µL | 1.0 µL |
| Nuclease free $H_2O$ | 8.64 µL |
| Total volume | 20.0 µL |

After ligation, 5.0 µL of the ligation mixture was used for transformation of OneShot® TOP10 chemically competent *E. coli* cells (section 3.2.1), by following the manufacturer's protocol. The pMT2-V plasmid was used as a positive control, while untransformed cells served as a negative control. Plasmid DNA from *E. coli* cell culture was isolated and purified by the ZymoPURE™ Plasmid Maxiprep Kit (described in 3.3.2).

Further, different approaches were made to control the subcloning of *F5* to pcDNA5/FRT:

1) A PCR with *F5* specific primers (3.3.6) was performed directly on the bacteria cultures. The pMT2-V vector was used as a positive control in the amplification of *F5,* and the empty pcDNA5/FRT vector acted as a negative control.
2) To further confirm incorporation of *F5* cDNA to the pcDNA5/FRT vector and a successful ligation, both the newly created pcDNA5/FRT-V vector and the empty pcDNA5/FRT vector were restriction digested with *HindIII* and separated by gel electrophoresis.
3) Sanger sequencing was performed to confirm the correct sequence of *F5* cDNA after subcloning of *F5* to pcDNA5/FRT-V (section 3.3.7).

## 3.2 Microbiological techniques

### 3.2.1 Cloning and transformation of Escherichia coli

Within recombinant DNA technology, large numbers of DNA molecules can be prepared for insert in a vector, through 3'→5' phosphodiester linkage. The vector is introduced to a host cell where it is reproduced through replication along with the host cells DNA, also known as DNA cloning. The most commonly used host cells are *Escherichia coli (E. coli)* and the bacteriophage lambda (λ) vector (Lodish et al. 2000). In this thesis, constructed vectors (pMT2 and pcDNA5/FRT-V) were used in transformation of chemically competent *E. coli* cells. Transformation enables the *E. coli* cells to absorb and incorporate DNA from its surroundings, in this case circular plasmids. The chemically competent cells have been treated with calcium chloride ($CaCl_2$) that promotes DNA plasmid binding to the cell membrane. Heat shocking the cells allows plasmid DNA to enter the cell through opened membrane pores. Plasmids often contain other functions than what is necessary for the DNA replication, such as a drug-resistance gene, which can provide the host cell with antibiotic resistance (Lodish et al. 2000). Both of the constructed plasmids in this thesis (pMT2 and pcDNA5/FRT-V) contain an *ampicillin* resistance gene.

Briefly, *E. coli* cells mixed with plasmid(s) were heat shocked at 42°C and incubated in S.O.C. medium before the transformed cells were spread and cultivated overnight at 37°C on Luria Broth (LB) agar plates containing 0.1 µg/µL ampicillin for selection of transformants. Single colonies were picked and cultured in separate tubes of Luria Broth (LB) medium containing 0.1 µg/µL ampicillin, and incubated at 37°C and 200 rpm overnight for further isolation and purification of plasmid DNA (section 3.3.2).

## 3.3 Molecular techniques

### 3.3.1 Agarose gel electrophoresis

Agarose gel electrophoresis is the most common technique for separation of DNA fragments varying in size from 100 bp up to 25 kb (Lee et al. 2012). Agarose forms a network of pores during gelation, and the pore size depends on the percentage of agarose used in the gel solution. An electric field makes the negatively charged phosphate backbone of DNA migrate through the pores and towards the positively charged anode. DNA with smaller fragment sizes will migrate faster and longer through the agarose pores, and will be separated from the larger fragments. In this thesis, 1xTAE buffer and SeaKem® LE Agarose were used for running different concentrations of agarose gels (Appendix A.2). Visualization and determination of fragments were enabled with UV light (ImageQuant™) and compared to a loaded DNA Ladder Mix with known fragment size.

### 3.3.2 Purification and isolation of DNA

Plasmid DNA was isolated and purified from transformed *E. coli* cell cultures by using the Zyppy™ Plasmid Miniprep Kit or the ZymoPURE™ Plasmid Maxiprep Kit, depending on the desired yield of plasmid. Isolation and purification were performed according to the manufacturer's protocol. In short, the *E. coli* cell culture was lysed with alkaline conditions and neutralized to keep the DNA stabilized in its native form. The lysate was centrifuged to precipitate chromosomal DNA and proteins. The supernatant with plasmid DNA was transferred to a DNA binding column and contaminants were washed out before elution of pure plasmid. 3 mL of cell culture containing plasmid DNA was used for isolation and purification with the Zyppy™ Plasmid Miniprep Kit, while 150 mL of pre-cultured cells were required for the ZymoPURE™ Plasmid Maxiprep Kit procedure.

### 3.3.3 RNA isolation

Total RNA isolation was conducted using the RNAqeous® Kit according to the manufacturer's protocol. The kit is based on the ability of glass fibres to bind nucleic acids in a concentrated chaotropic salt solution. In short, 64% ethanol solution enabled binding of RNA to the glass fibres in the filter cartridge, before washing of any possible impurities. RNA was eluted in 90 µL pre-heated elution solution (70°C), and concentrations were measured (3.3.4). All samples were stored at -20°C, or at -80°C degrees for long time storage.

### 3.3.4 RNA and DNA quantity and purity

Absorbance-based determination of nucleic acids with UV-light was used for quantification of concentration and purity of both RNA and plasmid DNA samples in this thesis, using a NanoDrop® ND-1000 instrument. Nucleic acids, such as nucleotides, RNA, ssDNA and dsDNA absorb UV-light at 260 nm, while proteins absorb at 280 nm. The 260/280 ratios were used as an estimate for purity. A 260/280 ratio around 1.8 is considered pure for DNA and 2.0 is considered pure for RNA.

### 3.3.5 cDNA synthesis

For analysis of FV mRNA expression with RT-qPCR (3.3.6), the isolated RNA samples had to be reverse transcribed to complementary DNA (cDNA). A High-Capacity cDNA Reverse Transcription Kit was used for this procedure according to the manufacturer's protocol. An equal input (1120-6790 ng) in a total volume of 25 µL RNA was used within each run and mixed with the cDNA reverse transcription reaction (Table 5). Samples were prepared on ice, followed by running a thermo cycling program (Table 6) with a 2720 Thermal Cycler. Synthesized cDNA was stored at -20°C.

**Table 5. Volumes needed for a master mix for the cDNA reverse transcription reaction.**

| Component | Volumes (µL) / reaction (2.5x) |
|---|---|
| 10X RT Buffer | 5.0 µL |
| 25X dNTP Mix (100 mM) | 2.0 µL |
| 10X RT Random Primers | 5.0 µL |
| *MultiScribe™ Reverse Transcriptase* | 2.5 µL |
| Nuclease free $H_2O$ | 10.5 µL |
| Total volume | 25.0 µL |

**Table 6. High-Capacity cDNA Reverse Transcription thermo cycling program.**

| | Step 1 | Step 2 | Step 3 | Step 4 |
|---|---|---|---|---|
| Temperature (°C) | 25 | 37 | 85 | 4 |
| Time | 10 minutes | 120 minutes | 5 minutes | ∞ |

### 3.3.6 Polymerase Chain Reaction

Polymerase Chan Reaction (PCR) is a molecular technique used to amplify DNA. A *DNA polymerase* synthesizes a new strand of DNA complementary to the template strand of interest, by adding nucleotides to the 3'OH group of a primer annealed to the template DNA strand.

#### *Long-range PCR*

For amplification of DNA fragments bigger than 1000 bp, the efficiency and proofreading of a routine PCR with *Taq polymerase* is no longer optimal. The reason for why a long-range PCR is optimized for amplification of long DNA fragments (up to 30 kb). In this thesis, the Q5® High Fidelity long-range PCR Kit was used for amplification of the nearly 7 kb long *F5* sequence. *F5* specific primers tailed with *HindIII* and *NotI* overhangs (Table A.9.1, Appendix A.9) were used in the long-range PCR to make compatible restriction sites with the pcDNA5/FRT vector (section 3.1.2). The newly constructed empty pMT2 vector was used as a negative control. All reaction components (Table 7) were prepared on ice before addition of template DNA, and transferred to a preheated thermo cycler (Table 8).

**Table 7. Volumes and reagents needed for long-range PCR amplification of *F5*, with *Q5 DNA polymerase*.**

| Reagents | Volume per sample |
|---|---|
| 5X Q5 Reaction Buffer | 5.0 µL |
| dNTP mix (10 mM) | 0.5 µL |
| Primer *HindIII* overhang (10 µM) | 1.25 µL |
| Primer *NotI* overhang (10 µM) | 1.25 µL |
| pMT2-V (0.5 ng/µl) | 0.5 µL |
| *Q5 High-Fidelity DNA Polymerase* | 0.25 µL |
| 5x Q5 High GC Enhancer | 5.0 µL |
| Nuclease free $H_2O$ | 11.25 µL |
| Total volume | 25.0 µL |

**Table 8. Thermo cycling-conditions for long-range PCR with *Q5 High Fidelity Polymerase*.**

| Temperature | Time | Stage | Cycles |
|---|---|---|---|
| 98°C | 30 seconds | Initial denaturation | |
| 98°C<br>60°C<br>72°C | 5–10 seconds<br>10–30 seconds<br>20–30 seconds/kb →6.5 minutes extension | Denaturation<br>Annealing<br>Extension | 30 Cycles |
| 72°C | 6.5 minutes | Final extension | |
| 4–10°C | ∞ | | |

### *PCR with DNA polymerase AmpliTaq Gold*

In this thesis an AmpliTaq Gold 360 PCR Kit together with two *F5* specific primer pairs (Table A.9.1, Appendix 9) were used for validation purposes during creation of the two plasmid-based vector systems for FV overexpression (section 3.1). Briefly, all reagents for the PCR reaction (Table 9) were combined and a previously optimized PCR thermo cycling program was used with a Veriti 96 well Thermo Cycler (Table 10). The pMT2-V plasmid was used as a positive control and the empty pcDNA5/FRT vector as a negative control in the PCR reaction.

**Table 9. Reagents and volumes used in AmpliTaq Gold 360 PCR, with *F5* primer pairs, for control of *F5* sequence in vector constructs.**

| Reagents | Volume (1x reaction) |
|---|---|
| Nuclease free $H_2O$ | 10.1 µL |
| 360 GC Enhancer | 2.0 µL |
| 10X PCR Buffer | 2.0 µL |
| dNTP mix | 1.6 µL |
| $MgCl_2$ | 1.2 µL |
| Primer mix (*F5* forward and reverse), 10 µM | 2.0 µL |
| *Taq Gold 360 Polymerase* | 0.1 µL |
| DNA template ≈ 5 ng (plasmid) | 1.0 µL |
| Total volume | 20.0 µL |

**Table 10. Thermo Cycling conditions for the AmpliTaq Gold 360 PCR.**

| Temperature | Time | Stage | Cycles |
|---|---|---|---|
| 95°C | 10 minutes | Activation of hot start polymerase | |
| 95°C | 30 seconds | Denaturation | 25 |
| 60°C | 30 seconds | Annealing | |
| 72°C | 1 minute | Extension | |
| 72°C | 7 minutes | Final extension | |
| 4°C | ∞ | | |

### *Real time qPCR*

Real time quantitative polymerase chain reaction (RT-qPCR) enables to screen the progress of a PCR as it occurs. The quantification in real-time qPCR is based at the point of time during cycling when the amplification of a selected target is first detected. In this thesis, RT-qPCR was used to measure and compare the expression levels of gene targets. A two-step procedure of reverse transcription of RNA (3.3.5) followed by a PCR step with TaqMan® chemistry was used. The TaqMan® chemistry is based on the introduction of fluorogenic-labelled probes that use the 5' nuclease activity of a *Taq DNA polymerase* for extension (Figure 11). When the probe is cleaved, the reporter dye (5'end) and the quencher dye (3'end) are separated. This results in a higher level of energy transferred fluorescent light of the reporter,

than before the cleavage. The emitted fluorescent light is proportional to the amount of target present in the sample, which increases logarithmically during each cycle. After each PCR cycle, the fluorescent light is detected with a camera.

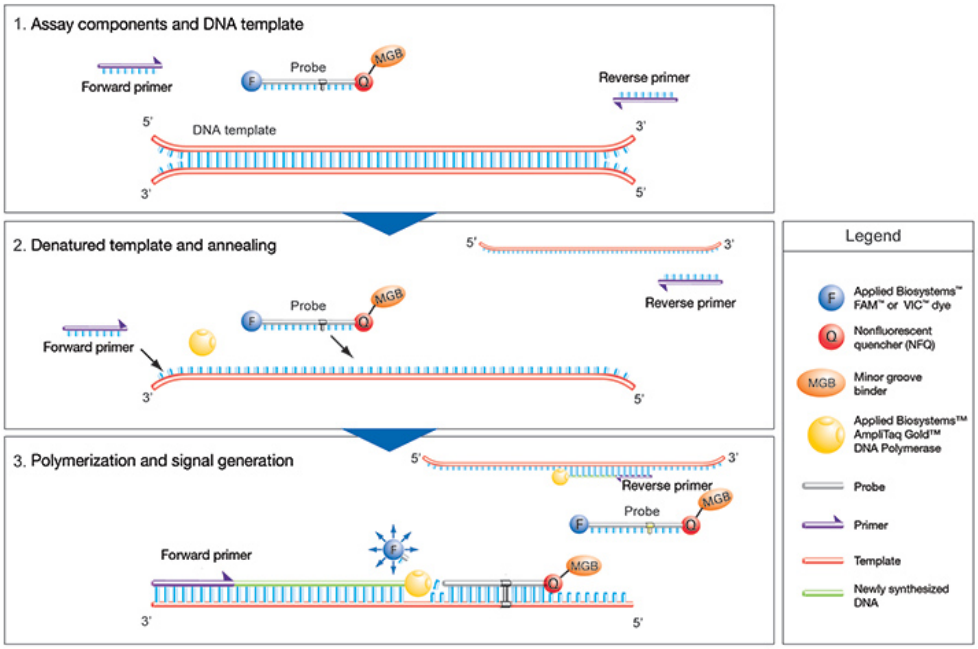


**Figure 11. Overview of the TaqMan chemistry gene expression assay process.** After denaturation of template DNA, primers and TaqMan probe is annealed to their specific target sequences. During extension the *Taq DNA polymerase* cleaves the TaqMan probe, resulting in fluorescent light emission by the reporter dye (modified from http://www.thermofisher.com/no/en/home/life-science/pcr/real-time-pcr/real-time-pcr-learning-center/real-time-pcr-basics/how-taqman-assays-work.html).

The amplification cycle can be divided into four phases (Figure 12):

1) A base line phase where the emitted fluorescent is too low for the identification limit of the detector.
2) An exponential phase of detected target present in the sample, and an increased emission of fluorescent light.
3) A linear phase where concentration reduction of one or more components of the PCR reaction is below a critical point, resulting in decreasing amplification.
4) In the plateau phase there is no increase in PCR product, hence no emission of fluorescent light.

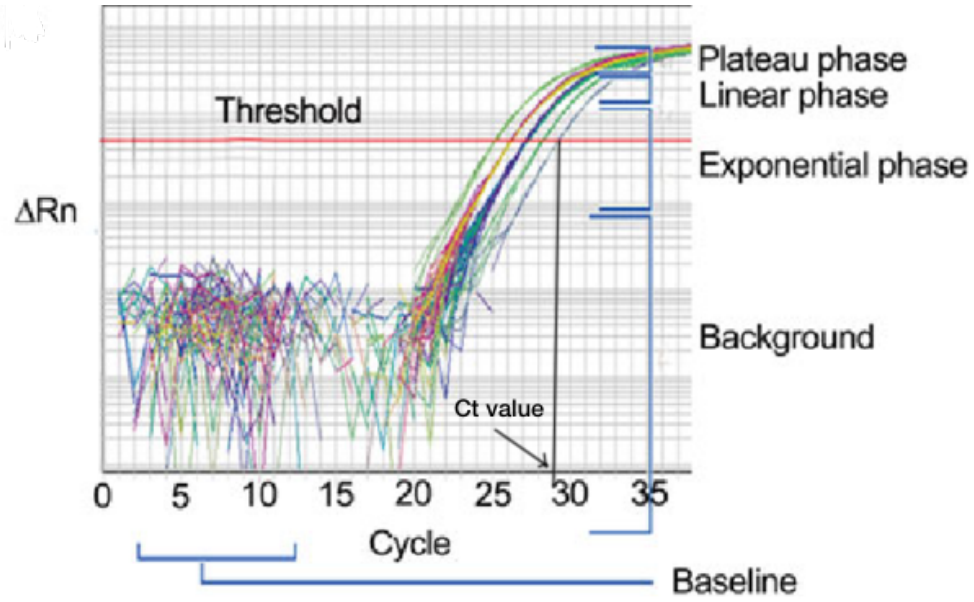


**Figure 12. RT-qPCR amplification plots illustration.** The amplification plot indicates the different phases of a RT-qPCR, a threshold line and the Ct value (modified from https://www.researchgate.net/Correct-and-incorrect-setting-of-baselines-and-thresholds-in-the-qPCR-amplifi-cations_fig6_264202734).

A threshold of the fluorescent light emission is reached after a number of cycles, determining Ct value of a sample (Figure 12), and is used further for calculation of the relative gene expression. The relative quantity (RQ) is calculated by using the comparative ΔCt method (equations I-III).

$$\text{(I)} \quad \Delta Ct = Ct_{\text{Target gene}} - Ct_{\text{Reference gene}}$$

$$\text{(II)} \quad \Delta\Delta Ct = \Delta Ct_{\text{Target sample}} - \Delta Ct_{\text{Reference sample}}$$

$$\text{(III)} \quad RQ = 2^{-\Delta\Delta Ct}$$

Quantification of relative FV mRNA expression in breast cancer cell lines was performed using RT-qPCR. The TaqMan® Gene Expression Master mix and assays (Appendix A.8) were used according to the protocol provided by the manufacturer (Table 11). The Phosphomannomutase 1 (PMM1) was used as a reference gene in the reaction as it is not affected by overexpression of *F5*. Briefly, triplicates (10 µL) of each sample reaction were transferred to a 384-plate including a negative control with nuclease free $H_2O$ for each assay (no template control, NTC), centrifuged at 1500 rpm, and run on the RT-qPCR cycling program (Table 12) with the Applied Biosystems QuantSTudio™ 12K Flex Real-Time System.

**Table 11. Composition of reagents and volumes used in the TaqMan® Gene Expression reaction mix, for real-time qPCR.**

| Reagent | Volume (µL) for 1x reaction |
|---|---|
| TaqMan® Gene Expression Master Mix | 5.0 µL |
| Assay (FV, PMM1) | 0.5 µL |
| cDNA ≈ 350 ng input<br>NTC (nuclease free $H_2O$) | 4.5 µL |
| Total volume | 10.0 µL |

**Table 12. RT-qPCR program run on the QuantSTudio™ 12K Flex Real-Time System.**

| | Step 1 | Step 2 | Step 3 (40 cycles) | |
|---|---|---|---|---|
| Cycle | - | - | Part 1 | Part 2 |
| Temperature | 50°C | 95°C | 95°C | 60°C |
| Time | 2 minutes | 10 minutes | 15 seconds | 1 minute |

### 3.3.7 Sanger DNA sequencing

DNA sequencing is the process of determining the sequence of nucleotides in a piece of DNA. Sanger sequencing is based on the incorporation of chain-terminating di-deoxynucleotidetriphosphates (ddNTPs) during amplification of a DNA template strand (Figure 13). This sequencing technique includes ddNTPs, ordinary deoxynucleotidetriphosphates (dNTPs), primers, DNA template, and a *DNA polymerase*. The ddNTPs lack a 3'-OH group, which is necessary in formation of phophodiester bonds between two dNTPs. When a modified ddNTP is randomly incorporated during DNA synthesis, *DNA polymerase* terminates the extension of the template DNA strand, resulting in DNA fragments of different lengths. Fluorescent labelling is used for detection of ddNTPs by capillary electrophoresis, whereas short fragments move quickly through the pores of the gel and longer fragments move more slowly.

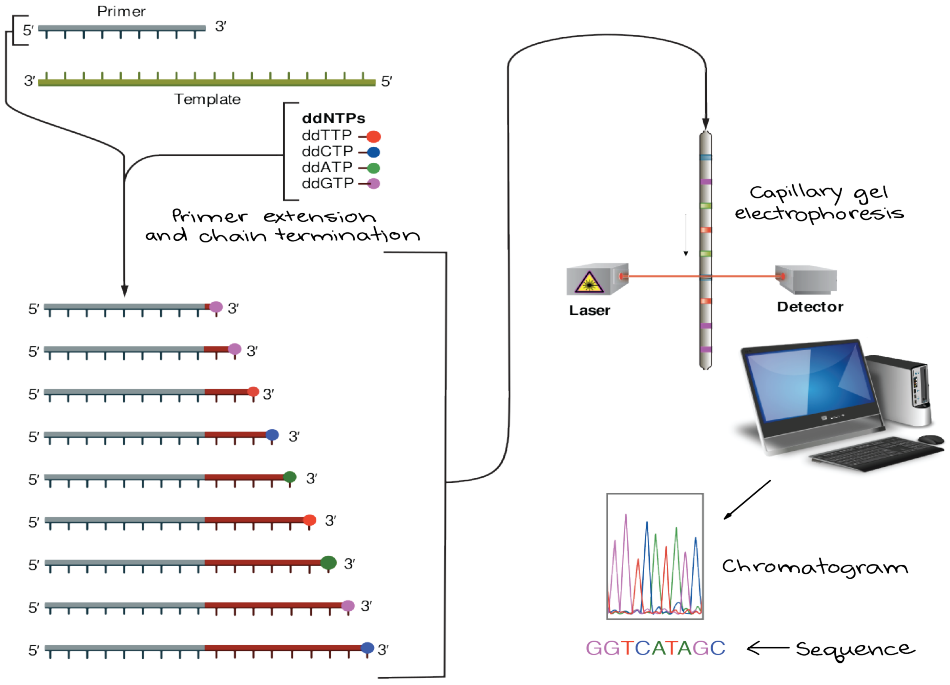


**Figure 13. Sanger DNA sequencing by capillary electrophoresis.** A lazer illuminates DNA fragments at the end of the capillary tube and the dye labelled ddNTPs will be detected. The four different ddNTPs emits light at different wavelengths. A detector reads the light emission, and data is recorded as a series of peaks in fluorescence intensity, shown in a chromatogram (Estevezj - Own work, CC BY-SA 3.0, https://commons.wikimedia.org/w/index.php?curid=23264166).

In this thesis, sequencing by the Sanger technique was performed to ensure that the created pcDNA5/FRT-V plasmid contained the correct *F5* cDNA sequence without any novel mutations compared to the initial template DNA. The sequencing reaction was performed using the BigDye™ Terminator v3.1 Cycle Sequencing Kit (Thermo Fischer Scientific) with *F5* specific primers covering the entire gene (Table A.9.3, Appendix 9). In short, all reagents were assembled on ice before addition of template DNA (Table 13), and placed in a Veriti 96 well Thermo cycler (Table 14).

**Table 13. Reagents and volumes used for the BigDye® sequencing reaction of *F5*.**

| **Reagents** | **Volume (1x reaction)** |
|---|---|
| MQ-$H_2O$ | 5.75 µL |
| DNA template: pcDNA5/FRT-V (100-200 ng) | 1.0 µL |
| 5x Sequencing Buffer | 2.0 µL |
| Primer (3.2 µM) | 1.0 µL |
| Big Dye Terminator v3.1 | 0.25 µL |
| Total volume | 10.0 µL |

**Table 14. The BigDye® Sequencing reaction cycling programme.**

| | Temperature | Time | Cycles |
|---|---|---|---|
| Initial activation | 96°C | 1 minute | |
| Denaturation | 96°C | 10 seconds | 25 cycles |
| Annealing | 50°C | 15 seconds | |
| Extension | 60°C | 4 minutes | |
| Final | 4°C | ∞ | ∞ |

The Agencourt® CleanSEQ Dye Removal kit was used to remove reagents and unused dNTPs and ddNTPs from the BigDye sequencing reaction. The procedure is based on Solid Phase Reversible Immobilization (SRPI) in several steps (Figure 14) and was carried out according to the manufacturer's protocol with a BioMek® FX robot. An ABI3730 sequencing analyser with capillary electrophoresis was used for determination of the *F5* sequence, and the data was analysed by sequence alignment to the *F5* reference sequence (NM_000130) using SecScape® software.

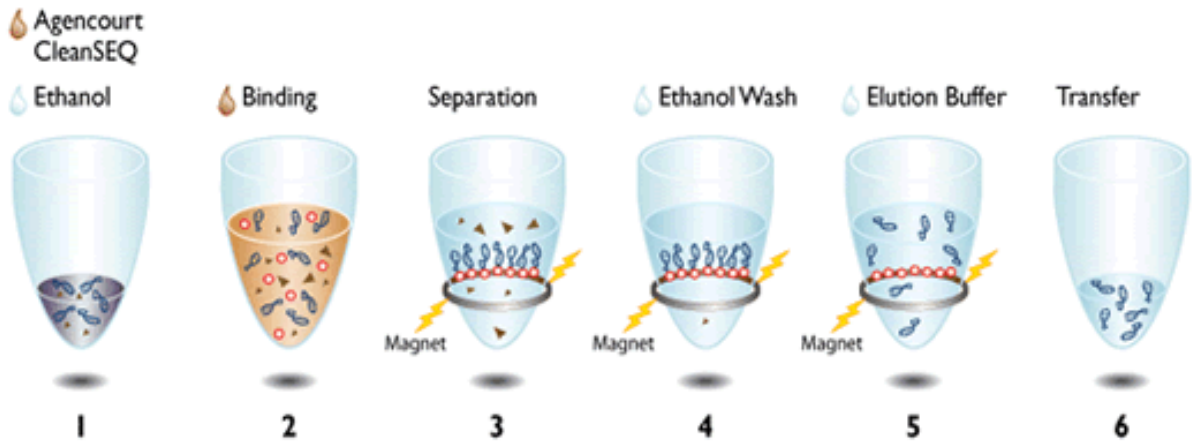


**Figure 14. Overview of the procedure steps of Agencourt® CleanSEQ.** 1) Agencourt® CleanSEQ and ethanol is added to the sequencing reaction. 2) Binding of sequencing products to magnetic beads. 3) Separation of sequencing product from contaminants by the use of a magnetic field. 4) Washing step with ethanol. 5) Elution of sequencing product from the magnetic beads. 6) Transfer of cleaned sequencing reaction from the magnetic beads (Modifed from the Agencourt® CleanSEQ® protocol).

## 3.4 Cell techniques

### 3.4.1 Breast cancer cell lines

In this thesis, the human breast adenocarcinoma cell lines MDA-MB-231 and MCF-7 were used for *in vitro* studies of FV overexpression and the effect of exogenous human Factor V. As previous established by the research group, both cell lines have a low endogenous expression of *F5* and were therefore considered a proper model for overexpression studies of FV. Both cell lines were originally derived from mammary gland by pleural effusion of Caucasian females with breast cancer. The cells represent two subtypes of breast cancer, with different characteristics (Table 15) (Kao et al. 2009).

#### *MDA-MB-231*

The basal like breast cancer cell line, MDA-MB-231 (Figure 15A), is considered to be triple negative for the overexpression of the ER, PR, and HER2 hormone receptors. The metastatic MDA-MB-231 cells are known to be mutant for the *TP53* gene, a *BRCA1* wt (Chavez et al. 2011) and resistant to treatment with the chemical drug doxorubicin (Smith et al. 2006).

#### *MCF-7*

The luminal breast cancer cell line, MCF-7 (Figure 15B), is hormone positive for the ER and PR receptors, and HER2 negative. The metastatic cell line is *TP53* wt (Welsh 2013). Characterization of the cell's sensitivity to treatment with doxorubicin was performed as described in section 3.7.

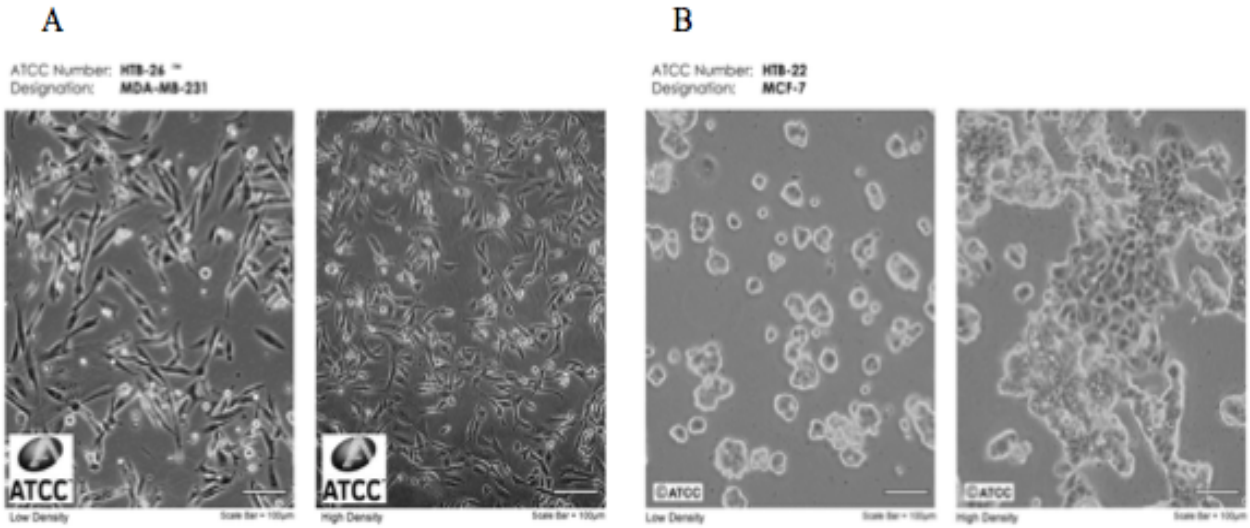


**Figure 15. Displaying the cell lines used for *in vitro* studies of the effect of FV.** Images represent (A) MDA-MB-231 and (B) MCF-7 cells during culturing, with differences between low and high confluence of cells (modified from ATCC).

**Table 15. Characteristics of the breast cancer cell lines used in this thesis**.

| Cell line | **MDA-MB-231** | **MCF-7** |
|---|---|---|
| Source | Pleural effusion | Pleural effusion |
| Tumour type | Metastatic adenocarcinoma | Metastatic adenocarcinoma |
| Subtype | Basal | Luminal |
| ER | - | + |
| PR | - | + |
| HER2 | - | - |
| *TP53* gene | Mutant | Wild type |
| Culture properties | Adherent | Adherent |
| Cell media | DMEM 10% FBS | DMEM 10% FBS |

### 3.4.2 Cell culture technique

Cells were handled with sterile techniques in a laminar flow hood. Cells were taken from long time storage in liquid nitrogen and transferred to a T-25cm$^2$ Nunc$^{TM}$ Cell Culture treated flask with fresh media. Both cell types were incubated at 37°C with 5% $CO_2$ and humidified in a Steri-Cycle $CO_2$ incubator. A Nikon Eclipse TE 300 microscope was used for visualization of morphology and confluence. Cell lines used in this thesis was regularly tested for Mycoplasma contamination with the MycoAlert™ Assay Control Set kit. All cells were approved for further studies and tested negative for mycoplasma infection.

Cells were split in a 1:3 or 1:6 ratio when reaching a confluence of 80-90%. The cell media was discarded and cells were washed with Dulbecco's Phosphate Buffered Saline (DPBS) to remove any traces of Trypsin EDTA inhibitors. Further the cells were detached using Trypsin EDTA and transferred to a new culture flask with fresh media.

### 3.4.3 Cell quantification

Quantification of cells was performed with the NucleCounter® System. In short, 100 µL cell suspension was lysed in 100 µL of Reagent A100 Lysis buffer and Reagent B Stabilizing buffer before loaded into a NucleoCasette™, which contains a fluorescent dye (propidium iodide) that stains the nuclei of cells. Total cell count (cells/mL) was determined using the NucleoCounter® System.

### 3.4.4 Transient transfection

Cell transfection enables the study of gene expression and functional effects of a gene of interest *in vivo*. In this thesis, chemically transient transfection was used to study the effects of overexpression of FV in MDA-MB-231 and MCF-7. The two plasmid-based vector systems (section 3.1) were transfected into the cells with the Lipofectamine™ 3000 Reagent. All plasmids were transfected in triplicates. In short, the procedure is based on transfer of nucleic acids (gene of interest) into a liposome, which is merged with the cell membrane. The Lipofectamine™ 3000 Reagent Protocol was followed for transfection of MDA-MB-231 and MCF-7. A 1.5 mL suspension of $3.0x10^5$ cells in DMEM 10% FBS was seeded in a 6-well, or a 0.6mL suspension of $1.5x10^5$ cells for a 12-well plate, and incubated overnight. The following day, plasmid DNA and Lipofectamine™ 3000 was combined (Table 16) at room temperature and incubated for 15 minutes, before 250 µL of the transfection mix was added to each well. After 4-6 hours of incubation, all cell media was replaced with fresh DMEM 10% FBS. The cells were harvested 48 or 72 hours after transfection (as described in 3.4.5).

**Table 16. Transfection mixes for MDA-MB-231 and MCF-7. Reagents and volumes are shown for one well (6-well plate).**

| | **MDA-MB-231** | | **MCF-7** | |
|---|---|---|---|---|
| **Reagents** | DNA mix | Lipofectamine mix | DNA mix | Lipofectamine mix |
| OptiMEM | 125.0 µL | 125.0 µL | 125.0 µL | 125.0 µL |
| Plasmid DNA | 2.5 µg | - | 2.5 µg | - |
| P3000 | 5.0 µL | - | 5.0 µL | - |
| Lipofectamine™ 3000 | - | 7.5 µL | - | 5.0 µL |

### 3.4.5 Harvest of cells and cell media

Cell media and cell lysates (RNA and protein lysates) were harvested from the transfected cells. Cell media was carefully discarded and transferred to eppendorf tubes and placed on ice. Samples were stored at -20°C until used for further analyses.

1) Cells harvested for protein analysis were washed 3x with cold DPBS, before lysed and scraped in 300 µL RIPA lysis buffer with 1X Halt™ Protease and Phosphatase inhibitor cocktail. Samples were stored at -20°C until used for further analyses.
2) Cells harvested for RNA analyses were washed 1x with cold DPBS and lysed in 600 µL RNA lysis buffer. Samples were stored at -20°C until used in RNA isolation.

## 3.5 Protein techniques

### 3.5.1 Total protein quantification

The Pierce™ BCA Protein Assay Kit was used for detection and quantification of total protein in cell lysate (harvested for protein as described in 3.4.5). This method is based on the reaction of bicinchinonic acid (BCA) with $Cu^{1+}$ ions, due to reduction of $Cu^{2+}$ to $Cu^{1+}$ after formation of protein-$Cu^{2+}$ complexes. The amount of BCA-$Cu^{1+}$ is proportional to the amount of protein in the samples. The total protein concentration in the samples were measured through UV light absorption at 570 nm and compared to a standard curve with known concentrations (Figure B1, Appendix B1). In short, all samples were spun down at 3500 rpm for five minutes to pellet cell debris. 5 µL of standard solutions and samples were combined with 200 µL of the BCA WR solution, mixed for 30 seconds at a Wallac DELFIA® Plate shaker, and incubated 37°C for 30 minutes. Absorbance was measured with a VersaMax™ microplate reader, and total protein concentrations were determined from the standard curve using the SoftMax Pro6.4 software.

### 3.5.2 Enzyme-Linked Immunosorbent Assay (ELISA)

Immunoassays are test-systems, which exploits the antigen-antibody interaction to determine the amount or concentration of a specific substance in biological fluid. Enzyme-Linked Immunosorbent Assay (ELISA) is a non-competitive immunoassay, where there is an excess of monoclonal antibodies in the reaction (Lea 2013). The ZYMUTEST Factor V ELISA Kit (Figure 16) was used to determine the concentration of Factor V antigen in cell media (harvested as described in 3.4.5) from cells transfected with FV overexpression plasmids. This is a "sandwich" ELISA where a microwell coated with a monoclonal FV specific antibody allows binding of immobilized FV proteins, present in the sample. Furthermore, adding a second FV specific antibody, coupled to horse-radish-peroxidase (HRP), creates a "sandwich" where the FV protein is captured between the two layers of antibodies. Finally, the peroxidase substrate tetramethylbenzidine (TMB) is introduced and a blue colour develops. The reaction was stopped with sulphuric acid, and absorbance was measured at 450 nm with a VersaMax™ microplate reader. The amount of colour developed is directly proportional to the concentration of FV in the sample solutions, which was calculated from a standard curve with known concentrations of human Factor V (Figure B2, Appendix B2), ranging from 0-200 ng/mL, using the SoftMax Pro6.4 software.

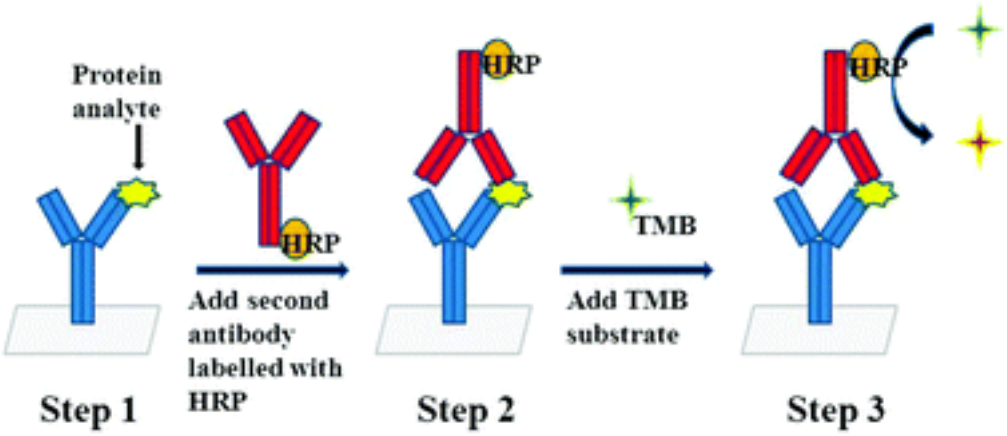


**Figure 16. Illustration of the principles of a sandwich (two-site) ELISA.** Step 1: the antibody attached to the microplate is introduced for target protein. Step 2: A secondary antibody labelled with HRP is added, and binds to the protein, making the "sandwich" reaction. Step 3: TMB substrate is added, resulting in interactions with HRP and a colour change occurs. Modified from (Zhang et al. 2014).

### 3.5.3 Western blot

Western blot is used for separation and detection of specific proteins in a sample (Mahmood & Yang 2012). The technique is divided into several steps:

1) Separation of proteins based on molecular weight with gel electrophoresis.
2) Blotting of separated proteins to a protein-binding membrane by using an electric field.
3) Blocking, antibody incubation, and washing. Blocking prevents binding of unspecific antibodies. The membrane is incubated with a primary antibody for specific binding to the target protein. The washing step is necessary to remove unbound antibody and minimize background.
4) Staining and detection of protein. A secondary antibody is added and incubated with the membrane, to recognize and stain the primary antibody with a chemiluminiscent agent. Finally, the target protein is visualized and detected through light emission.

Protein lysates, harvested (described in section 3.4.5) from MDA-MB-231 cells transfected with the two FV overexpression plasmid-based vector systems, were used for western blot analysis in this thesis, and tested for the presence of FV and PARP. Preparation of buffer and blocking solutions used in the western procedure are listed in the Appendix A.2. 10 µg protein sample, based on calculations from total protein levels in each lysate (3.5.1), was loaded to a 10% precast Mini-PROTEAN® TGX™ gel. The separated protein samples were blotted to a 0.2 µM Nitrocellulose membrane and blocked for one hour with 5.0% Bovine Serum

Albumine (BSA). Presence of FV in the transfected cells was tested by incubating the membrane with 10 µg/mL anti-human FV antibody overnight at 4°C. Additionally, the protein samples were screened for the effect of FV overexpression on apoptosis, by staining the membrane with the primary PARP antibody (1:1000 dilution). All antibodies used for western blot analysis is listed in Appendix A.7. Staining and detection of target proteins were performed with the Amersham™ ECL ™ Prime Western Blotting Detection Reagent Kit, and visualized with an ImageQuant™ LAS 4000 System for analysis with the ImageQuant™ TL 1D v8.1 software.

## 3.6 Functional assays

### 3.6.1 Cell growth

The cell proliferation agent Wst-1 was used for quantifying the cell viability, based on the reduction of tetrazolium salts by the presence of NADH and NADPH in the cell (Berridge et al. 1996). Higher amounts of the generated formazan dye indicate higher amounts of mitochondrial dehydrogenase activity and living cells. The breast cancer cell lines MDA-MB-231 and MCF-7 were used to study the effect of FV on cell growth. To test the effect of FV overexpression, the two plasmid-based vector systems (section 3.1) were used for reverse transfection of the cells. The effect of exogenous human Factor V (hFV) was tested by incubation with different concentrations (0.1 µg/mL, 7.0 µg/mL) of hFV 24 hours after seeding, and with and without starvation of the cells. In short, cells were seeded in a 96-well plate, and the cell viability was measured at 0, 24, 48 and 72 hours after transfection or at 48 and 72 hours incubation with hFV. After addition of Wst-1, the cells were incubated for 30 minutes at 37°C before absorbance measurements at 450-745 nm with a VersaMax™ microplate reader, and analysed using the SoftMax Pro6.4 software.

### 3.6.2 Cell death

The Cell Death Detection ELISA$^{PLUS}$ Kit (Sigma-Aldrich®) was used to test the effect of FV overexpression on apoptosis in breast cancer cells. This is a photometric enzyme-immunoassay procedure for determination of histone-associated-DNA-fragments after induced cell death, based on a sandwich-enzyme-immunoassay-principle (Figure 17). The procedure was carried out as described by the manufacturer, except from the sample preparation. Protein lysates were centrifuged at 1500 rpm for 10 minutes, and 5-fold diluted

before assayed. Absorbance at 405 nm was used for quantification of the histone-associated-DNA fragments present in the protein lysate with a VersaMax™ microplate reader.

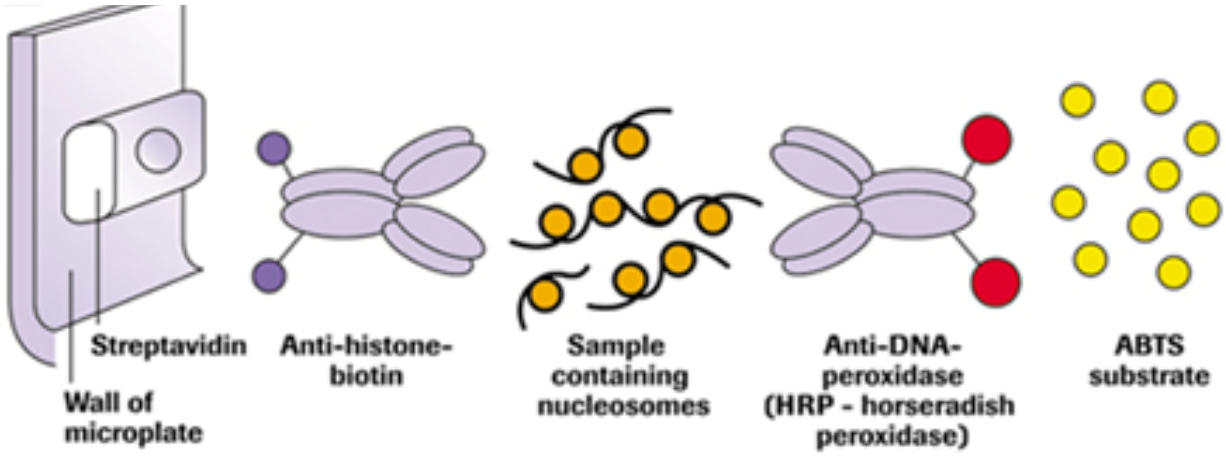


**Figure 17. Principle overview of the Cell Death Detection ELISA$^{PLUS}$.** Anti-histone-biotine antibodies bind histone-associated DNA fragments. A secondary antibody labelled with HRP is added, and binds the DNA fragments, making the "sandwich" reaction. ABTS substrate develops a colour complex with HRP and is used for absorbance measurement of the histone-assocaited-DNA fragments present in the sample. Modified from the manufacturer's protocol.

### 3.6.3 Migration

To study the effect of FV overexpression and addition of exogenous human FV (hFV) on cell migration in breast cancer cells, a wound-healing assay was performed. Cells were reverse transfected with the two FV plasmid-based vector systems (section 3.1) to study the effect of overexpression of FV. Transfected cells were seeded in migration chambers before incubation overnight. The migration chamber insert was removed when cells had reached 80-90% confluence, and fresh DMEM with 10% FBS was added. To study the effect of exogenous hFV a 96-well plate was used for seeding of cells, and a scratch-wound was made with a sterile pipette tip at 80-90% confluence. After making the scratch-wound, different concentrations of hFV diluted in DMEM 10% FBS were added, in addition to a buffer control solution. The effect of hFV on cell migration was also performed during starvation of cells for 24 hours, with dilution of hFV in DMEM 0.5% FBS. A Nikon Eclipse TE 300 microscope was used for capturing images of the wound healing, 0, 6, 17, and 24 hours after migration insert removal or making the scratch-wound.

### 3.6.4 Cell-signalling pathways

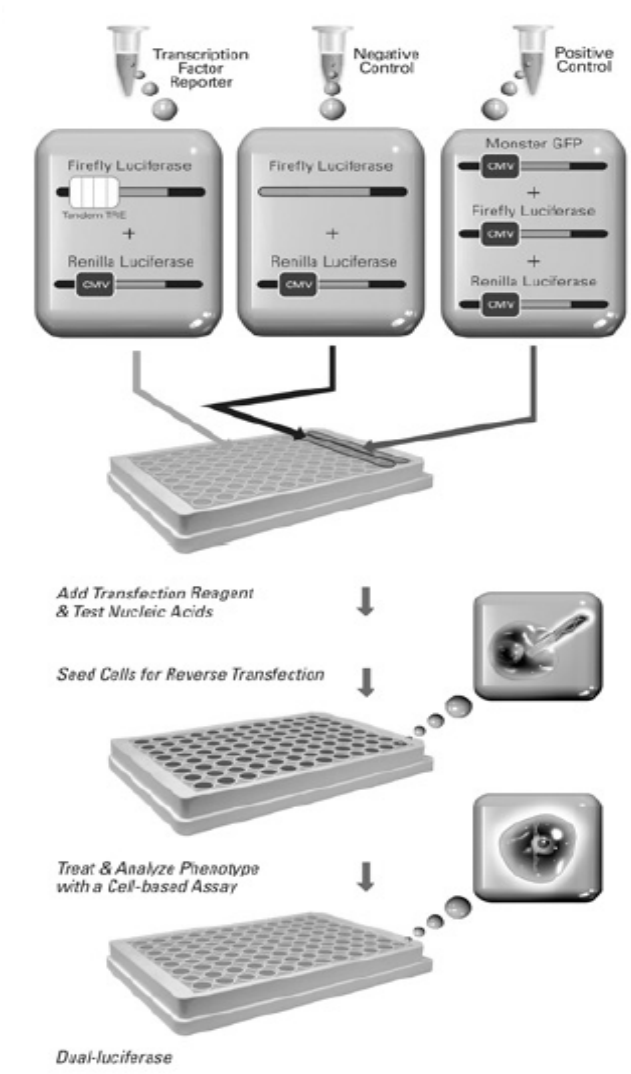


**Figure 18. Illustrates the Cignal Finder 10-Pathway Reporter array protocol.** Reporter constructs that encode a reporter gene under the control of a basal promoter element (TATA box) are joined to tandem repeats of specific transcriptional response elements (TRE). Specific TRE for the different signalling pathways are located upstream for the luciferase gene. The *Renilla* luciferase plasmid serves as a trasnfection control. Modified from the Cignal Finder Reporter Array Plate protocol handbook.

Cell signalling is an essential communication pathway, which control cell activity. A Cignal Finder Reporter Array was used for determination of cell-signalling pathways regulated by FV overexpression or exogenous human Factor V in breast cancer cells (Figure 18). The manufacturer's protocol for 10 cancer-signalling pathways (Table 17) was followed, based on a dual-luciferase assay. The two plasmid-based vector systems for FV overexpression (section 3.1) were used for reverse transfection of cells. To test the effect of hFV, cells were incubated with different concentrations of hFV 24 hours after seeding/transfection. To test for the effect of hFV with starvation, cells were starved for six hours and then incubated with different concentrations of hFV with starvation medium (DMEM 0.5% FBS) and incubated further for 24 hours. Cells were harvested after 48 hours after seeding/transfection for luciferase assay by washing the cells 1x with DPBS and lysis in 20 µL 1xPLB.

**Table 17. Cancer-signalling pathways investigated for the effect of FV on transcription factor activity.**

| Pathway | Transcriptional Regulatory Element (TRE) | Transcription factor |
|---|---|---|
| **Wnt** | TCF/LEF response element | TCF/LEF |
| **Notch** | RBK-Jκ binding element | RBK-Jκ |
| **p53/DNA Damage** | p53 response element | p53 |
| **TGFβ** | SMAD response element | SMAD2/SMAD3/SMAD4 |
| **Cell cycle/pRb-E2F** | E2F binding element | E2F/DP1 |
| **NFκβ** | NFκβ binding element | NFκβ |
| **Myc/Max** | E-box binding element | Myc/Max |
| **Hypoxia** | HIF response element | Hypoxia-inducible factor-1 (HIF-1) |
| **MAPK/ERK** | Serum response element (SRE) | Elk-1/SRF |
| **MAPK/JNK** | AP-1 binding element | AP-1 |

## 3.7 Chemical treatment of cells for characterization of MCF-7

Chemotherapy treatment prevents either cancer cells from growing, or it reduces the growth. Doxorubicin is a chemotherapy drug, used in extensive cancer treatment such as acute lymphoblastic leukaemia, breast carcinoma, and thyroid carcinoma amongst others (Drugbank 2005). *Topoisomerase II* is an enzyme that utilizes growth and cell division of cancer cells, and is blocked through stabilization by doxorubicin, which prevents catalyzation of the ligation-religation reaction (Drugbank 2005). In this thesis, the MCF-7 breast cancer cell line was tested for doxorubicin sensitivity. In short, 150 µL of cell suspension ($6.0x10^3$ cells/well) were seeded in a 96-well plate and exposed to different doxorubicin concentrations (0.0 µM, 1.0 µM, 2.0 µM, 5.0 µM, 10.0 µM and 50.0 µM), over a 24-hour period. The cell viability was measured with Wst-1 (as described in 3.6.1).

## 3.8 Statistics

The unpaired t-test for comparison of samples in two groups was used for statistical analysis in this thesis. Assuming the datasets was normally distributed and independent of each other. The difference between the tested groups was considered significant with a probability value $P \leq 0.05$. In this thesis, a significant p-value is marked with *.

# 4 Results

## 4.1 Creation of plasmid-based expression vectors for FV overexpression

Two plasmid-based expression vector systems were created in order to study *in vitro* effects of FV overexpression in breast cancer cells. We possessed a commercial expression vector containing the *F5* gene: pMT2-V (ATCC®). However, as no empty pMT2 vector was available, we needed to create an empty pMT2 vector to be used as vector control in cell experiments. In addition, the *F5* sequence was subcloned from the pMT2-V vector into the pcDNA5/FRT mammalian expression vector. Unlike the pMT2 vector, the pcDNA5/FRT contains a mammalian antibiotic resistance gene, which enables selection of cell lines with stable overexpression of the desired gene (in this case *F5*). The pcDNA5/FRT vector is also compatible with the Flp-In™ System that allows for integration and expression of the desired gene at a specific genomic location in the mammalian cell line.

### 4.1.1 Creation of an empty pMT2 vector

#### *Restriction enzyme digestion and religation of pMT2*

To create a proper control for the pMT2-V expression plasmid, an empty pMT2 vector was made by cutting out the *F5* cDNA sequence from the pMT2-V plasmid. Following restriction digestion with *SalI*, the linearized plasmid was separated from the *F5* cDNA with gel electrophoresis (Figure 19). The 4974 bp linearized pMT2 fragment was isolated and purified from the gel before religation with *T4 DNA ligase* (section 3.1.1). The empty pMT2 vector was transformed into *E. coli* cells, before further isolation and purification as described in section (3.2.2).

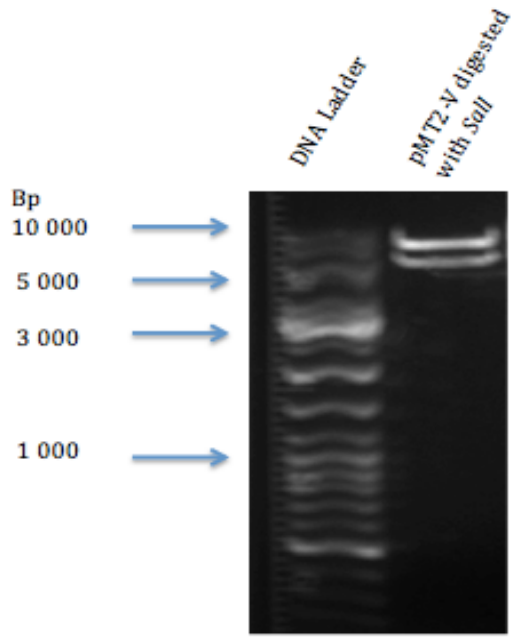


**Figure 19: Agarose gel electrophoresis of pMT2-V digested with *SalI*.** The pMT2-V vector was cut with *SalI*, and samples were run on a 0.7% agarose gel. The linear pMT2 vector fragment shows a band at 4.9 kb and the *F5* gene has a band at 6.9 kb.

### *Verification of an empty pMT2 vector*

To ensure a successful religation and thereby creation of an empty pMT2 vector, two control approaches were made;

1) Restriction enzyme cutting with *SalI* followed by running an agarose gel (Figure 20).
2) PCR with *F5* specific primers (described in 3.2.4) (Figure 21).

The control digestion of pMT2 was made with *SalI* and resulted in one band of the expected size of ~5000 bp after gel electrophoresis (Figure 20). Undigested pMT2 vector shows characteristics for supercoiled DNA, and a successful relegation of the constructed empty pMT2 vector was established due to differences in relaxed (linearized) and supercoiled (in red circle) vector (Figure 20).

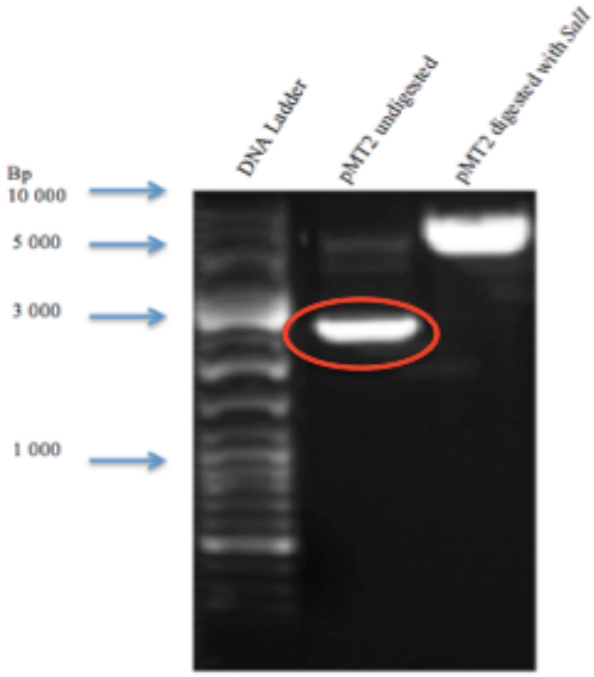


**Figure 20. Agarose gel electrophoresis of undigested (religated) and digested pMT2 vector.** The pMT2 vector was cut with *SalI* and run on a 1% agarose gel. Linearized vector shows a band with fragment size at ~5 kb.

To confirm the absence of a *F5* cDNA sequence, the newly constructed empty pMT2 vector was amplified with two *F5* specific primer pairs. The pMT2-V vector was used as a positive control, and showed the expected fragment sizes of 300 bp and 500 bp after amplification with the two primer pairs (Figure 21). The amplification of the empty pMT2 vector was negative for both primer pairs, hence confirming the construction of an empty pMT2 vector (Figure 21).

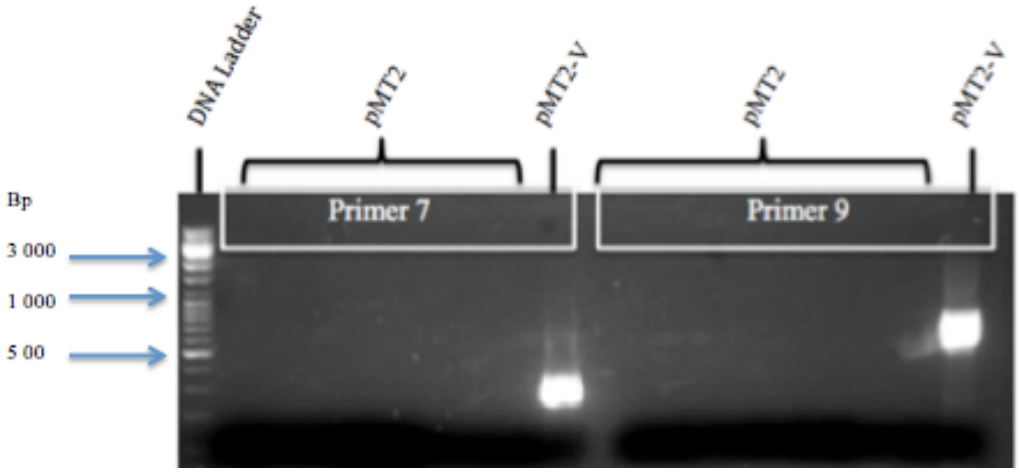


**Figure 21. Control PCR to confirm the construction of an empty pMT2 vector.** The control PCR was performed using two *F5* specific primer pairs to confirm the absence of *F5* cDNA in the pMT2 vector. The pMT2-V vector, containing the *F5* sequence, was used as a positive control in the amplification.

### 4.1.2 Creation of a FV overexpression plasmid

#### *Amplification and restriction enzyme digestion of F5 cDNA*

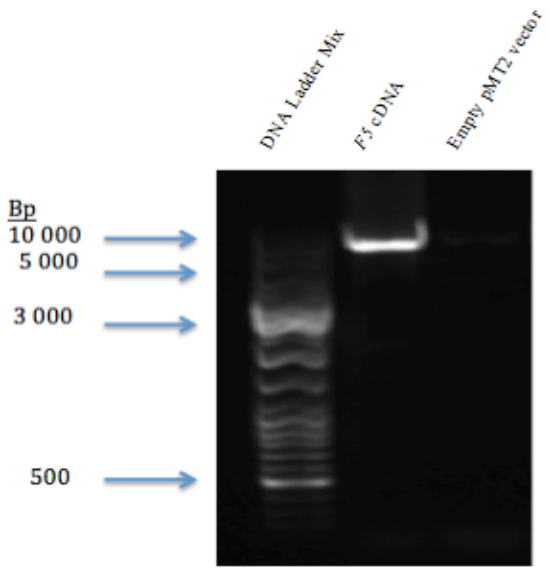


**Figure 22. Agarose gel electrophoresis of *F5* cDNA long-range PCR fragment.**
*F5* cDNA was amplified from pMT2-V, and the newly created empty pMT2 vector was used as a negative control in the amplification. Samples were run on a 1% agarose gel. The *F5* cDNA fragment is nearly 7000 bp long.

In order to create a new FV overexpression plasmid (containing a mammalian selection marker), the *F5* cDNA sequence needed to be isolated from pMT2-V before subcloning to the pcDNA5/FRT vector. As there were no compatible restriction sites for the pMT2-V vector and the pcDNA5/FRT destination vector, the *F5* cDNA was amplified with long-range PCR using *F5* specific primer pairs. The primers was based on the *F5* sequence (NM_000130) and designed with *HindIII* and *NotI* primer overhangs, in order to produce compatible ends for restriction digestion and ligation into the destination vector. Successful amplification of the expected ~7 kb *F5* cDNA sequence was confirmed with gel electrophoresis (Figure 22). *F5* cDNA was purified directly from the PCR reaction and cut with *HindIII* and *NotI* restriction enzymes to make compatible ends for ligation. To gain the

highest possible yield, the double digested *F5* cDNA was purified directly from the digestion reaction before ligation into the pcDNA5/FRT destination vector.

### *Preparation of the pcDNA5/FRT vector*

The pcDNA5/FRT vector was prepared for ligation by double digestion with *HindIII* and *NotI* enzymes, to generate compatible ends with the digested *F5* cDNA sequence. To control the avtivity of the enzymes the pcDNA5/FRT vector was also single digested with *HindIII* or *NotI*. Successful digestion of the vector was confirmed by gel electrophoresis (Figure 23). The double digested pcDNA5/FRT vector (in red circle) was isolated from the gel, and purified for further use.

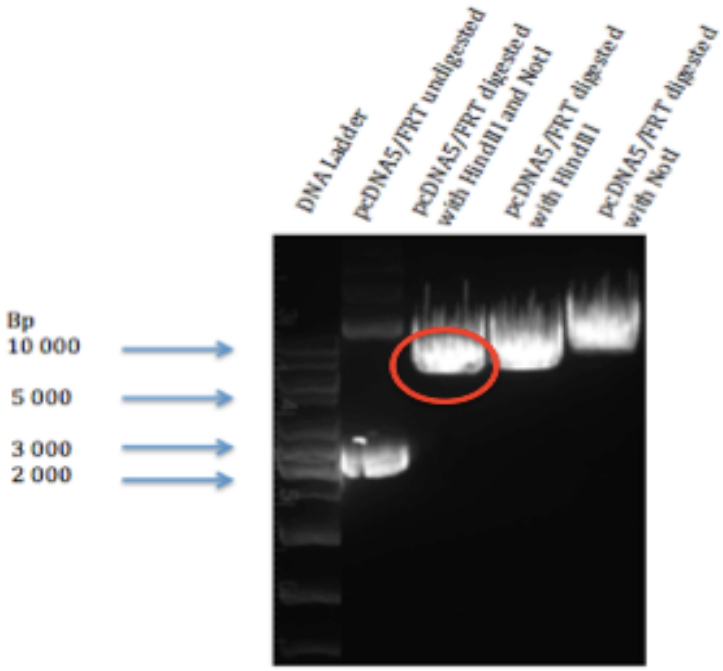


**Figure 23. Agarose gel electrophoresis of digested and undigested pcDNA5/FRT vector.** The linearized pcDNA5/FRT vector digested with *HindIII* and *NotI* enzymes, appearing close to the 5000 bp mark, was isolated from gel and purified. Undigested vector shows supercoiled features compared to the digested samples with *HindIII* or *NotI*. Samples were run on a 0.7% agarose gel.

### *Ligation of F5 cDNA and the pcDNA5/FRT vector*

Digested and purified *F5* cDNA and pcDNA5/FRT vector was ligated to form a new functional FV overexpression plasmid, hereafter named pcDNA5/FRT-V. The ligated plasmid was transformed into *E. coli* cells and cultured (as described in 3.1.3). Before isolation and purification of pcDNA5/FRT-V, the cultured colonies were tested for incorporation of the *F5* cDNA into the pcDNA5/FRT vector. A PCR with *F5* specific primers (3.2.4) was performed directly on the bacteria cultures, with the pMT2-V vector as a positive control, and the empty pcDNA5/FRT vector as a negative control (Figure 24). All tested colonies showed the expected band size of ~300 bp (primer 7), but with different intensity, and a slightly difference in size. Only colonies with the same intensity and fragment size (in red circles) as the positive control were purified and used in further conformational steps and sequencing of the constructed pcDNA5/FRT-V plasmid (Figure 24).

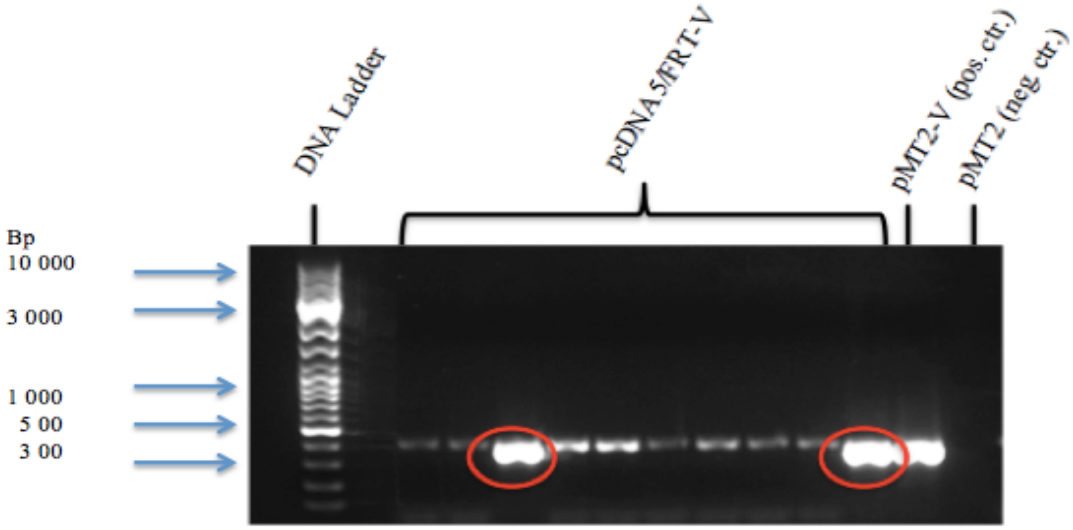


**Figure 24. Control PCR to confirm incorporation of *F5* cDNA to the pcDNA5/FRT vector.**
The control PCR was performed with a *F5* specific primer pair (primer 7), for amplification of *F5* fragments within the constructed pcDNA5/FRT-V vector, and run on a 1% agarose gel. Amplified *F5* fragments for pcDNA5/FRT-V and the positive control (pMT2-V) show bands at 300 bp. The empty pMT2 vector was used as a negative control.

As a final verification of successful ligation and incorporation of *F5* cDNA into the pcDNA5/FRT vector, the newly created pcDNA5/FRT-V vector and the empty pcDNA5/FRT vector were restriction digested with *HindIII* and separated by gel electrophoresis. The undigested pcDNA5/FRT-V plasmid indicated supercoiled features, confirming a successful ligation of the *F5* cDNA sequence and the destination vector (Figure 25). The expected fragment size of the linearized pcDNA5/FRT-V plasmid was confirmed to be 11 kb (in red circle), compared to the linearized empty pcDNA5/FRT vector with a fragment size of ~5 kb (Figure 26).

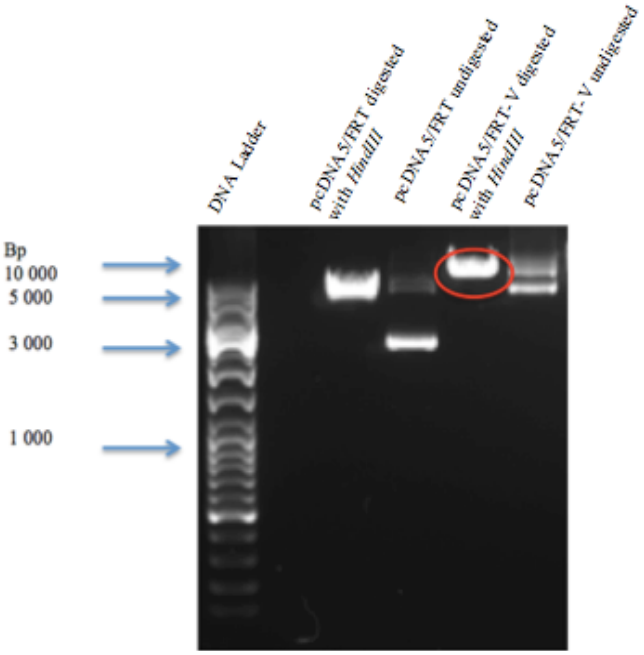


**Figure 25. Control digestion of pcDNA5/FRT-V vector.** pcDNA5/FRT-V and empty vector (pcDNA5/FRT) were digested with *HindIII* and separated by a 1% agarose gel. Size differences between both undigested and linearized pcDNA5/FRT-V and pcDNA5/FRT confirms the incorporation of *F5* cDNA and a successful subcloning.

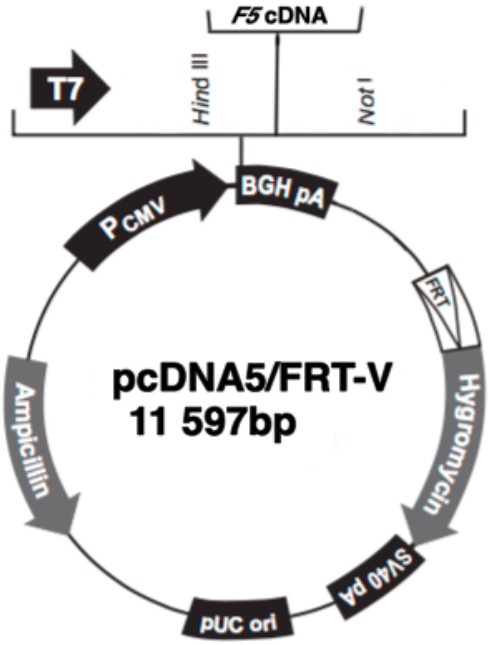


**Figure 26. Map overview of pcDNA5/FRT-V.** The *F5* cDNA sequence was subcloned between the *HindIII* and *NotI* restriction sites in the pcDNA5/FRT vector. The restriction sites of *HindIII* and *NotI* are flanking the *F5* cDNA insert. The size of the empty pcDNA5/FRT vector is 5070 bp, resulting in a total size of 11 597 bp for the newly constructed pcDNA5/FRT-V plasmid.

### *Sequencing of the pcDNA5/FRT-V plasmid*

Sanger sequencing was used to confirm the correct sequence of *F5* cDNA after subcloning of *F5* into pcDNA5/FRT-V. pcDNA5/FRT-V plasmids purified from several bacterial colonies were sequenced and aligned against the *F5* cDNA sequence in the pMT2-V donor vector to check for polymerase errors. A successful subcloning of the *F5* cDNA sequence to pcDNA5/FRT was established. Several SNPs in the *F5* cDNA sequence was revealed compared to the reference sequence (NM_000130.4) (Table 18). However, all SNPs revealed in the sequencing of pcDNA5/FRT-V were already present in the *F5* cDNA sequence template in the pMT2-V vector (Figure 27). Without any novel discovery of variations of the *F5* sequence, and a successful verification of the subcloning, the newly created pcDNA5/FRT-V plasmid was used further in overexpression studies of FV in this thesis.

**Table 18. Variations found in pcDNA5/FRT-V and pMT2-V compared to the reference sequence of *F5* (NM_000130.4).**

| SNP | Nucleotide change | Amino acid change | Exon number | Global Minor Allele Frequency |
|---|---|---|---|---|
| rs6016 | c.2208C>T | Synonymous | 13 | A = 0.2628/1316 |
| rs6017 | c.2235T>C | Synonymous | 13 | G = 0.2628/1316 |
| rs6021 | c.2301A>G | Synonymous | 13 | C = 0.2628/1316 |
| rs4524 | c.2573A>G | Lys>Arg | 13 | C = 0.2668/1336 |
| rs4525 | c.2594A>G | His>Arg | 13 | C = 0.2628/1316 |
| rs6032 | c.2773A>G | Lys>Glu | 13 | C = 0.2628/1316 |
| rs1800594 | c.3804T>C | Synonymous | 13 | G = 0.3095/1550 |
| rs9287090 | c.3948C>T | Synonymous | 13 | A = 0.2636/1320 |

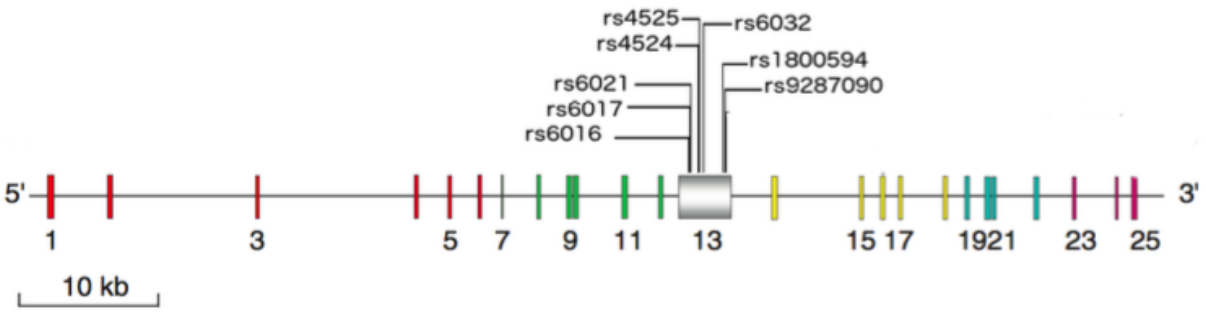


**Figure 27. The *F5* sequence and variations present in pcDNA5/FRT-V and pMT2-V.** The figure presents an illustration of the 25 exons that comprises the *F5* gene. Location of SNPs in exon 13 of the *F5* cDNA sequence compared to the reference sequence (NM_000130.4) is illustrated in the figure.

## 4.2 Transfection of the FV overexpression plasmids in breast cancer cell lines

After creation of the two plasmid-based expression vector systems, the pMT2-V and the pcDNA5/FRT-V expression plasmids were tested for their ability to overexpress FV in the MDA-MB-231 and MCF-7 breast cancer lines. The cells were transiently transfected and the expression of FV was analysed at both the mRNA and protein level.

### 4.2.1 Relative *F5* mRNA expression in MDA-MB-231 and MCF-7

48 hours after transfection, the *F5* mRNA expression in MDA-MB-231 was 25 000 and 26 000-fold higher for the pcDNA5/FRT-V and pMT2-V plasmids, respectively, compared to their corresponding empty vector controls (Figure 28A and B). After 72 hours, the relative *F5* mRNA expression of cells transfected with pcDNA5/FRT-V decreased to 18 000-fold compared to the empty vector control (Figure 28A). While, the cells transfected with the pMT2-V expression vector showed an increase in *F5* mRNA expression to 39 000-fold, compared to the empty pMT2 vector control (Figure 28B).

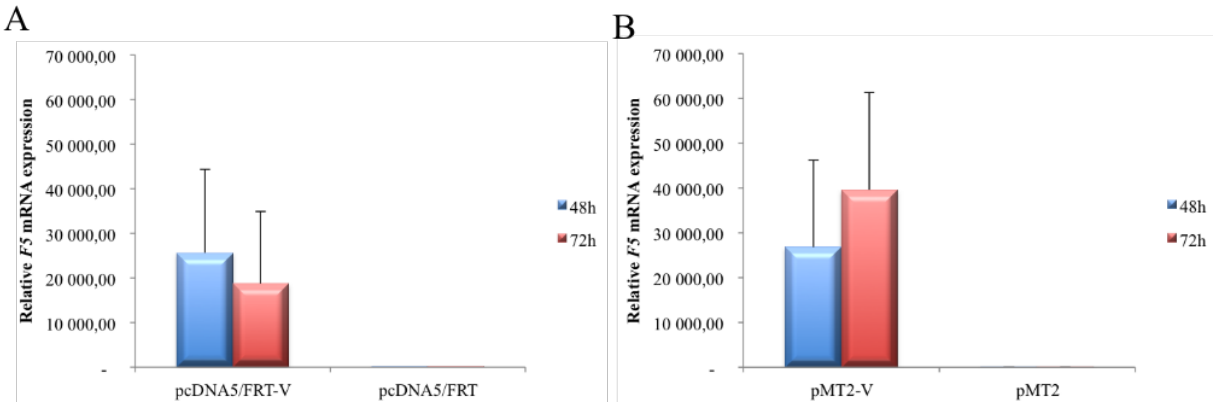


**Figure 28. Relative *F5* mRNA expression in MDA-MB-231 cells.** The cells were transfected with the pcDNA5/FRT-V (A) and the pMT2-V (B) FV expression plasmids, and their empty vectors as controls. *F5* mRNA expression is presented as mean RQ values, normalized against PMM1 as an endogenous control, and compared to the corresponding empty vector control. (A) Mean values + SD (n=8) at 48h and (n≥5) at 72h, and (B) mean values + SD (n≥7) at 48h and (n≥4) at 72h, from three independent experiments are shown.

In the MCF-7 cell line, the relative *F5* mRNA expression was higher than in MDA-MB-231 (Figure 29A and B). After 48 hours, the relative *F5* mRNA expression was 70 000 and 50 000-fold higher for the pcDNA5/FRT-V and pMT2-V plasmids, respectively, compared to their corresponding empty vector controls (Figure 29A and B). After 72 hours, the *F5* mRNA expression decreased to 39 000-fold for cells transfected with the pcDNA5/FRT-V expression vector, compared to the empty vector control (Figure 29A). MCF-7 cells transfected with

pMT2 also showed a decrease in *F5* mRNA expression after 72 hours. The expression decreased to 14 000-fold, compared to the empty vector control, which corresponds to a 3.7-fold decrease compared to 48 hours (Figure 29B).

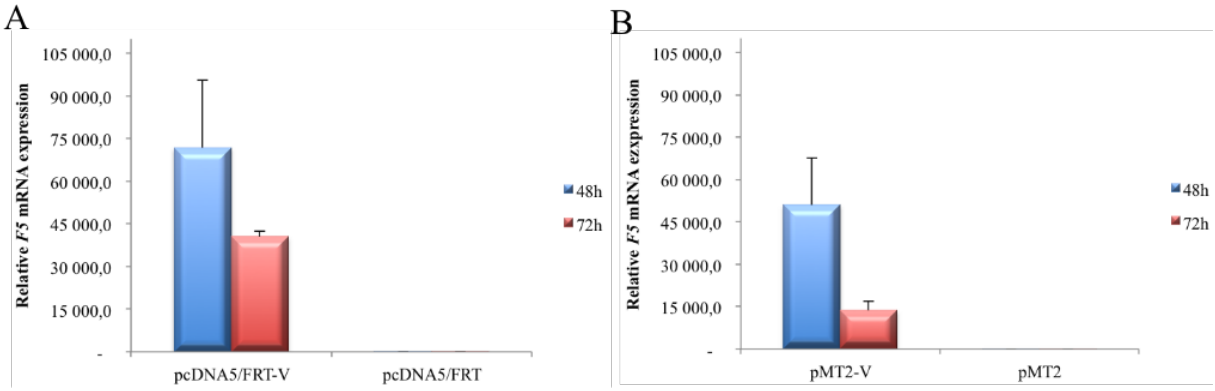


**Figure 29. Relative *F5* mRNA expression in MCF-7 cells.** The cells were transfected with the pcDNA5/FRT-V (A) and the pMT2-V (B) FV expression plasmids, and their empty vectors as a controls. *F5* mRNA expression is presented as mean RQ values, normalized against PMM1 as an endogenous control, and compared to the corresponding empty vector control. (A) Mean values + SD (n≥4) at 48h and (n=3) at 72h, and (B) mean values + SD (n=6) at 48h and (n=3) at 72 hours, from two independent experiments are shown.

We also evaluated if the two empty vector controls could be used interchangeably. However, due to differences in Ct values at both 48 and 72 hours (Figure 30), we considered that they could not. The two empty vectors were therefore only used as controls for their respective FV overexpression plasmids throughout this thesis.

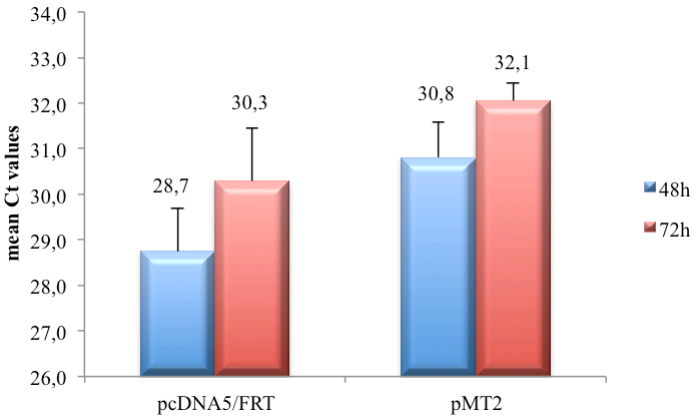


**Figure 30. RT-qPCR Ct values for *F5* for the two vector controls in transfected MDA-MB-231 cells.** The Ct values resulting from RT-qPCR with the *F5* assay were compared between the empty pcDNA5/FRT and pMT2 vectors in MDA-MB-231. Cells were harvested after 48 and 72 hours after transfection. Mean Ct values (n=3) + SD for one experiment is shown.

### 4.2.2 FV protein levels in MDA-MB-231 and MCF-7

To confirm the overexpression of FV at the protein level, ELISA was used to measure the FV protein in the cell media and cell lysate of the transfected MDA-MB-231 and MCF-7 cells.

FV protein levels were detectable in cell media from MDA-MB-231 cells transfected with both FV overexpression plasmids. However, the FV protein levels after transfection with the pMT2-V were 16.7-fold higher than for cells transfected with pcDNA5/FRT-V at 48 hours, and 13.3-fold higher after 72 hours (Figure 31). The empty pcDNA5/FRT and pMT2 plasmids were below the detection limit of the FV ELISA (data not shown).

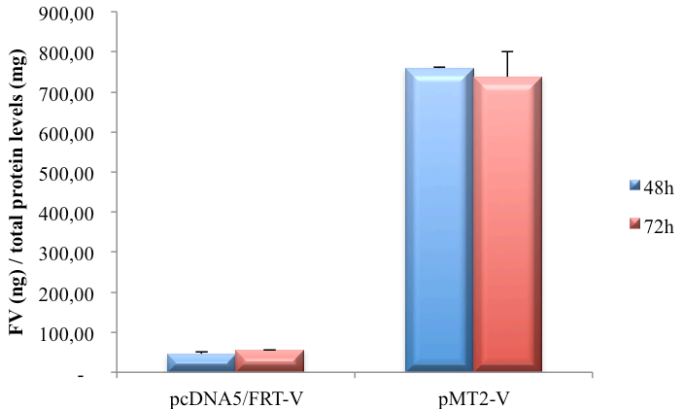


**Figure 31. FV protein levels in the cell media of MDA-MB-231 cells transfected with FV overexpression plasmids.** Cells were transfected with pcDNA5/FRT-V and pMT2-V, and harvested after 48 and 72 hours. FV protein levels in cell media was measured by FV ELISA, and corrected for total protein levels in cell lysate. Mean values (n=2) + SD from one representative experiment are shown.

Moreover, the FV ELISA also displayed present FV protein in the cell lysate from transfected MDA-MB-231 cells, showing the same patterns as in the cell media with a higher levels of FV for cells transfected with the pMT2-V plasmid (data not shown). This was further confirmed by western blotting of cell lysates (as described in 3.5.3). Expected bands for full length FV (330 kDa) (red arrows) established the FV overexpression for MDA-MB-231 cells transfected with the pMT2-V plasmid (Figure 32). There was a weak band for full length FV for cells transfected with pcDNA5/FRT-V, which is consistent to the low secretion of FV protein levels in the cell media (Figure 31).

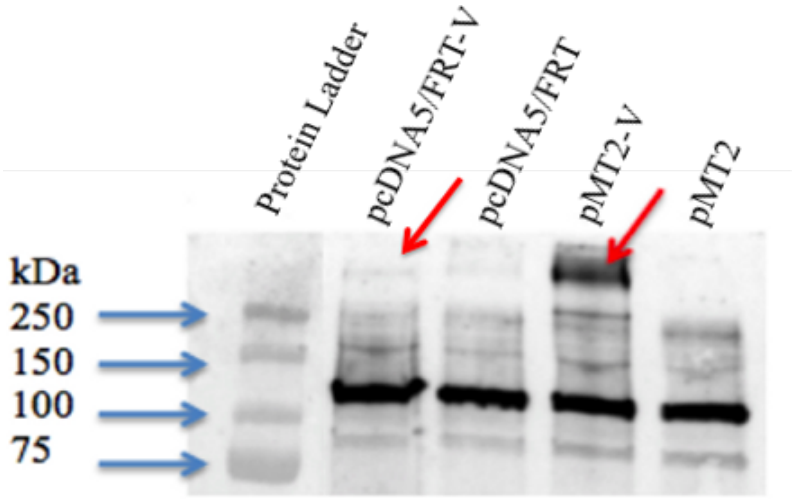


**Figure 32. Western blot analysis of FV protein in the cell lysate of transfected MDA-MB-231 cells.** Protein lysates (10 µg) harvested after 72 hours from cells transfected with the pcDNA5/FRT-V and pMT2-V FV expression plasmids and empty vector controls. The blot was stained with anti-human Factor V. Full length FV (330 kDa) is indicated with red arrows.

In transfected MCF-7 cells, the secretion of FV protein was generally lower compared to the MDA-MB-231 cells. However, similar to the MDA-MB-231 cells, MCF-7 cells transfected with pMT2-V secreted 15.5-fold higher amounts of FV protein than cells transfected with pcDNA5/FRT-V at 48 hours (Figure 33). After 72 hours, the secretion of FV decreased by 1.8-fold for cells transfected with the pMT2-V plasmid.

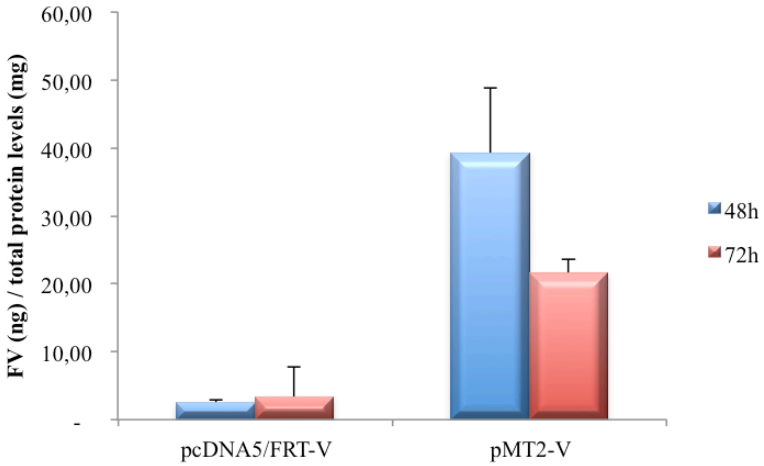


**Figure 33. FV protein levels in the cell media of MCF-7 cells.** Cells were transfected with pcDNA5/FRT-V and pMT2-V, and harvested after 48 and 72 hours. FV protein levels in cell media was measured by FV ELISA, and corrected for total protein levels in cell lysate. Mean values (n=2) + SD from one representative experiments are shown.

## 4.3 Functional effects of FV in MDA-MB-231 and MCF-7

The two FV overexpression plasmids were used to study the functional effects of FV in the MDA-MB-231 and MCF-7 breast cancer cells.

### 4.3.1 Effect on apoptosis (programmed cell death)

There were no differences in the effect of FV overexpression on apoptotsis in transfected MDA-MB-231 cells after 48 hours (Figure 34A and B). But, after 72 hours, FV overexpression with the pMT2-V plasmid resulted in a significantly ($P \leq 0.01$) reduced apoptosis, with a 28% lower DNA fragmentation than the empty pMT2 vector control (Figure 34B).

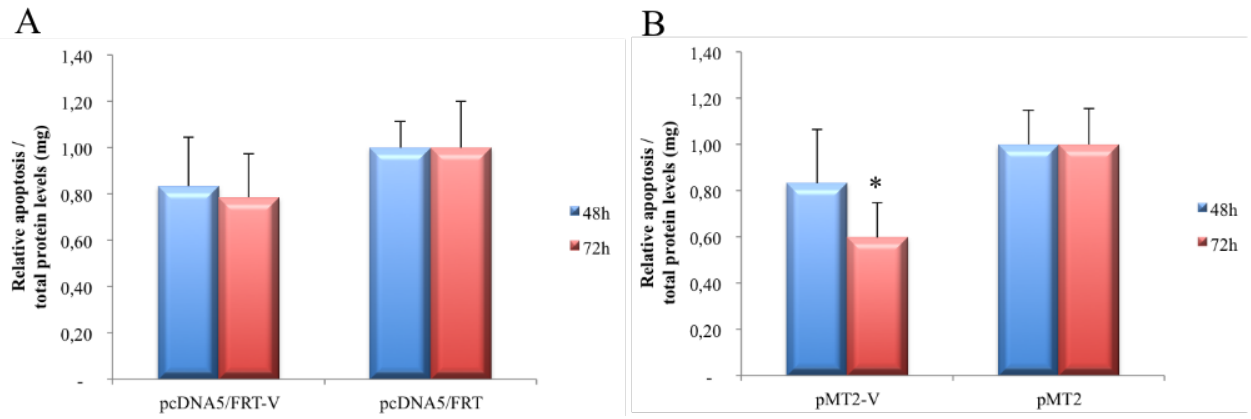


**Figure 34. Effect of FV overexpression on programmed cell death in MDA-MB-231.** Cells were transfected with pcDNA5/FRT-V (A) and PMT2-V (B) for overexpression of FV, and related to their empty vectors. Cell lysates were harvested after 48 and 72 hours. Relative apoptosis values + SD for (n=12) at 48 hours and (n=6) at 72 hours, for four independent experiments are shown. Significant difference ($P \leq 0.05$) to empty vector (B) is marked with *.

To further investigate the effect of FV overexpression on apoptosis the cell lysates of transfected MDA-MB-231 cells were used in western blotting (as described in 3.5.3). Separated proteins were stained with anti-poly(ADP-ribose) polymerase (PARP), an antibody marker selective for early apoptosis when cleaved. The blot showed bands for full length PARP (118 kDA) and cleaved PARP-1 (89 kDA) in all cell lysates of transfected MDA-MB-231 cells (Figure 35). There were no reduction in cleaved PARP for the pMT2-V expression plasmid, as what was seen in the programmed cell death assay (Figure 34B) was detected for all plasmids (Figure 35).

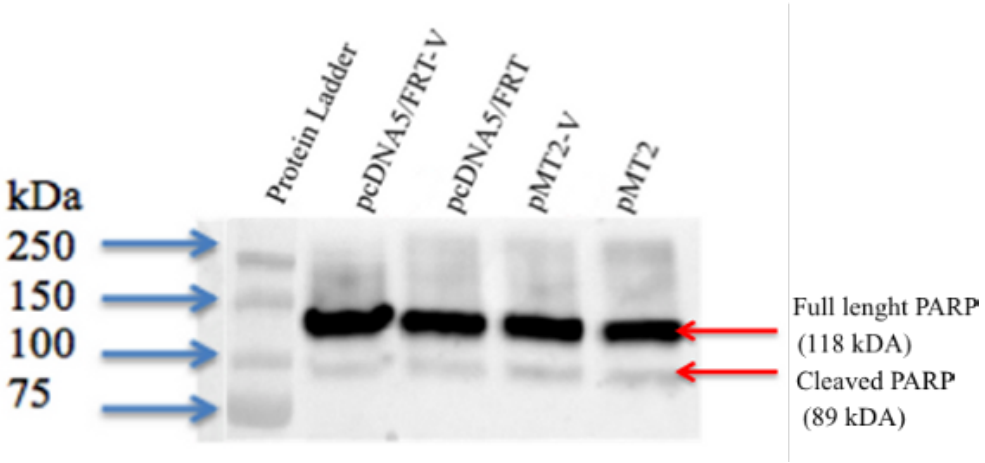


**Figure 35. Western blot analysis of PARP protein in the cell lysate of transfected MDA-MB-231 cells.** Protein lysates (10 µg) harvested after 72 hours from cells transfected with the pcDNA5/FRT-V and pMT2-V FV expression plasmids and empty vector controls. The blot was stained with anti-PARP, and full length PARP and cleaved PARP are indicated with red arrows.

MCF-7 cells transfected with the two FV overexpression vector systems showed no differences in DNA fragmentation, compared to the empty vector controls, at both 48 and 72 hours (Figure 36 A and B).

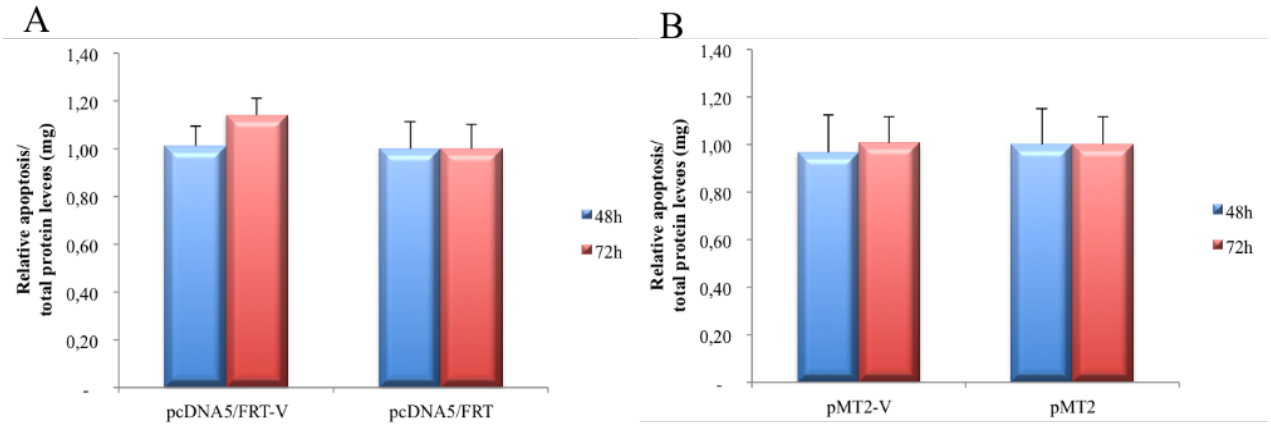


**Figure 36. Effect of FV overexpression on cell death in MCF-7.** Cells were transfected with pcDNA5/FRT-V (A) and PMT2-V (B) for overexpression of FV, and related to their empty vectors. Cell lysate were harvested after 48 and 72 hours. Relative apoptosis values +SD (n≥5) at 48 hours and (n=3) at 72 hours + SD for two independent experiments are shown.

### 4.3.2 Effect on cell growth

Effect of FV on cell growth in MDA-MB-231 and MCF-7 was studied through both reverse transfection of the cells with FV overexpression plasmids, and by addtion of exogenous human Factor V (hFV) directly to the cells. The cell growth was studied over a timeperiod of 0-72h for both cell lines.

#### *Effect of FV overexpression on cell growth*

MDA-MB-231 cells transfected with the pcDNA5/FRT-V plasmid showed no differences in cell growth compared to the empty pcDNA5/FRT vector (Figure 37). The untransfected cells showed higher cell growth after 48 and 72 hours, compared to the transfected cells.

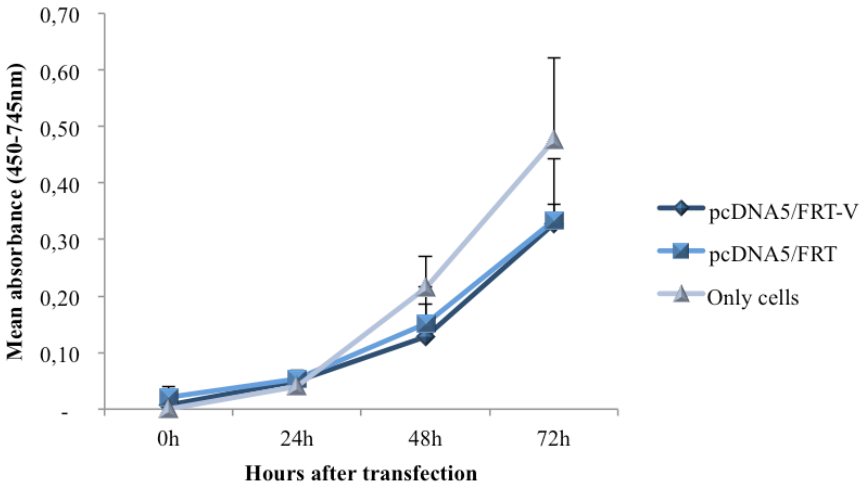


**Figure 37. Effect of FV on cell growth in transfected MDA-MB-231 cells.** Cells transfected with the pcDNA5/FRT-V FV expression plasmid and the empty pcDNA5/FRT vector control. Growth measurements were done with Wst-1 at OD (450-745nm), over 0-72h. Mean absorbance values (n=12) + SD for two independent experiments are shown.

MDA-MB-231 cells transfected with the pMT2-V plasmid showed a slightly higher cell growth compared to the empty pMT2 vector control, with significant differences ($P \leq 0.05$) at 24 and 72 hours after transfection (Figure 38A). The relative cell growth of MDA-MB-231 transfected with pMT2-V was 1.2-fold higher after both 24 and 72 hours, compared to the empty pMT2 vector control (Figure 38B).

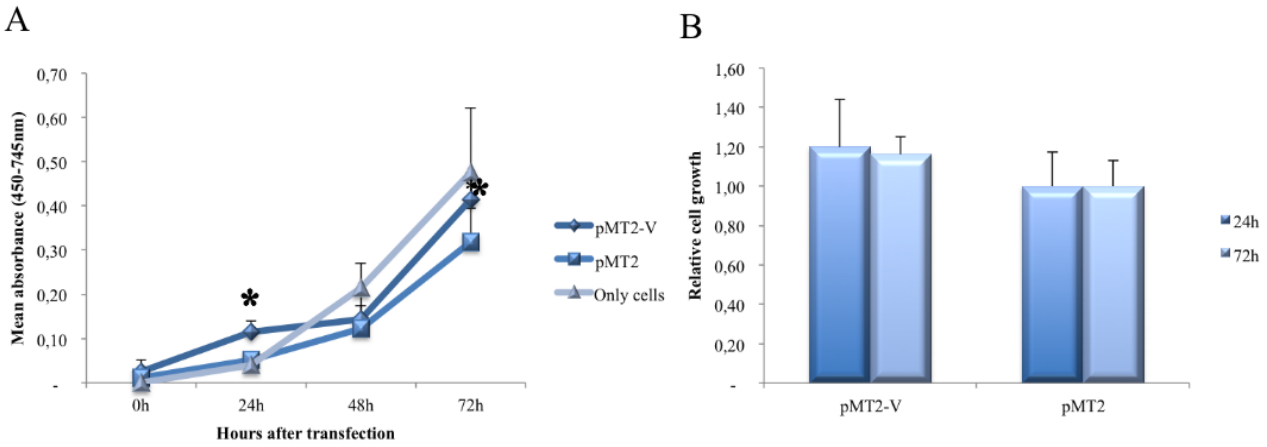


**Figure 38. Effect of FV on cell growth in transfected MDA-MB-231 cells.** (A) Cells transfected with the pMT2-V FV expression plasmid and the empty pMT2 vector control. Growth measurements were done with Wst-1 at OD (450-745 nm), over 0-72h. Mean absorbance values (n=12) + SD for two independent experiments are shown. (B) Relative fold increase in growth of MDA-MB-231 for time points with significant differences in (A), values are related to the empty pMT2 vector. Significant differences ($P \leq 0.05$) to the empty vector control (A) are marked with *. Only cells = non-transfected cells.

The growth of transfected MCF-7 cells was negligable after plasmid transfection, and the effect of FV overexpression could thus not be evaluated (Figure 39A and B). However, the effect of exogenous hFV on cell growth in MCF-7 was tested further.

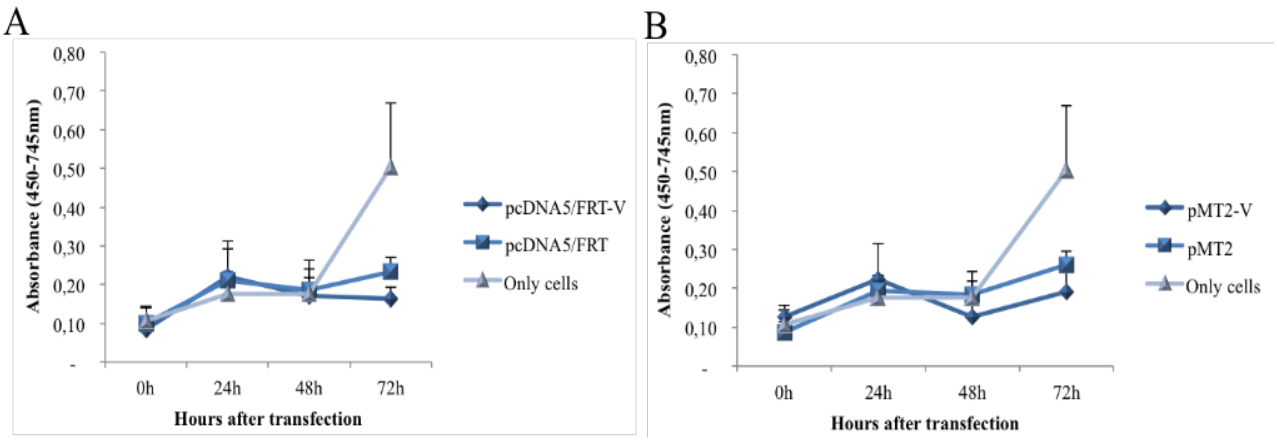


**Figure 39. Effect of FV on cell growth in transfected MCF-7 cells.** (A) Cells transfected with the pcDNA5/FRT-V FV expression plasmid and the empty pcDNA5/FRT vector control. (B) Cells transfected with the pMT2-V FV expression plasmid and the empty pMT2 vector control. Growth measurements were done with Wst-1 at OD (450-745 nm), over 0-72h. Mean absorbance values (n=12) + SD for two independent experiments are shown. Only cells = non-transfected cells.

### *Effect of exogenous human FV on cell growth*

In addition to test the effect of overexpression of FV, which is similar to the endogenous FV expression, it was of interest to investigate the effect of exogenous human Factor V(hFV) on cell growth in MDA-MB-231. The effect of exogenously added hFV was studied by incubating the cells with different concentrations of hFV for 72 hours, and a buffer solution was used as control. The cells incubated with hFV showed a slightly reduced growth rate, but only the lowest dose os hFV (0.1 µg/mL) showed a significant 12% growth reduction ($P$=0.03), compared to the buffer control (Figure 40). The effect of exogenous hFV on cell growth in MDA-MB-231 was also tested with different concentrations of hFV during culturing of cells in starvation media for 72h. The same effect of hFV on the cell growth was observed as without starvation (data not shown).

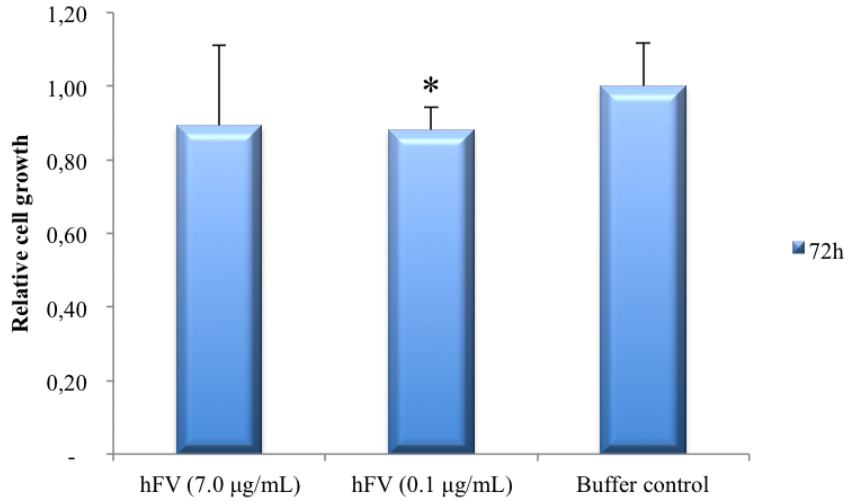


**Figure 40. Effect of hFV on cell growth in MDA-MB-231.** Cells were incubated with hFV (7.0 µg/mL and 0.1 µg/mL) and a buffer solution control. Growth measurements were done with Wst-1 at OD (450-745 nm) after 72h of incubation, and related to the buffer solution control. Mean relative growth values (n≥6) + SD for two independent experiments are shown. Significant differences ($P$≤0.05) to the buffer control are marked with *.

In MCF-7 cells, the highest concentration of hFV(7.0 µg/mL) showed a significant ($P$≤0.01) increase in cell growth, 1.5-fold higher than the buffer control (Figure 41). The purpose of incubating MCF-7 cells with hFV during culturing in starvation media, had no effect, as what was seen in MDA-MB-231.

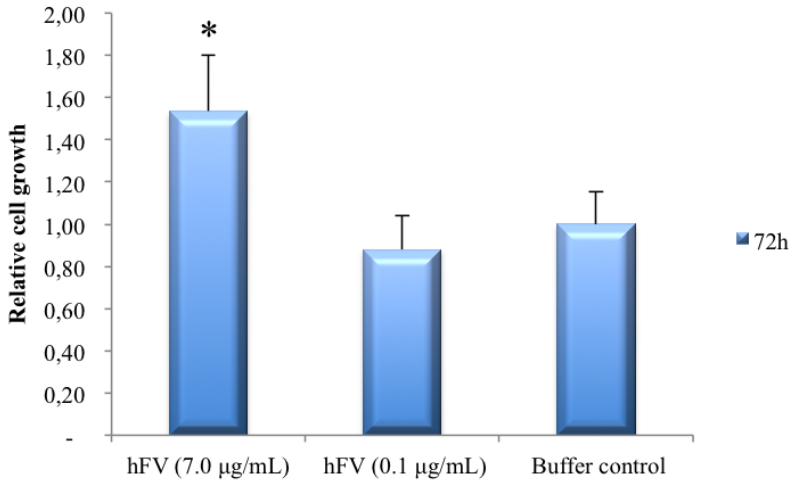


**Figure 41. Effect of hFV on cell growth in MCF7.** Cells were incubated with hFV (7.0 µg/mL and 0.1 µg/mL) and a buffer solution control. Growth measurements were done with Wst-1 at OD (450-745 nm) after 72h of incubation, and related to the buffer solution control. (A) Mean relative growth values (n=3) + SD for one representative experiments are shown. Significant differences ($P \leq 0.05$) to the buffer control are marked with *.

### 4.3.3 Effect of FV on cell migration in MDA-MB-231

#### *FV overexpression*

The effect of FV overexpression on cell migration in transfected MDA-MB-231 cells was studied by using a migration chamber assay (described in section 3.6.3).

MDA-MB-231 cells transfected with pMT2-V resulted in decreased cell migration compared to the empty pMT2 vector control and untransfected cells (Figure 42 and 43). After 17 hours, 44% of the wound was healed for cells transfected with the pMT2-V plasmid, compared to 56% for the empty pMT2 vector (Figure 43B). Whereas, after 24 hours, the pMT2-V plasmid resulted in a significant ($P$=0.03) 75% reduced wound closure, compared to the empty pMT2 vector control (Figure 43B).

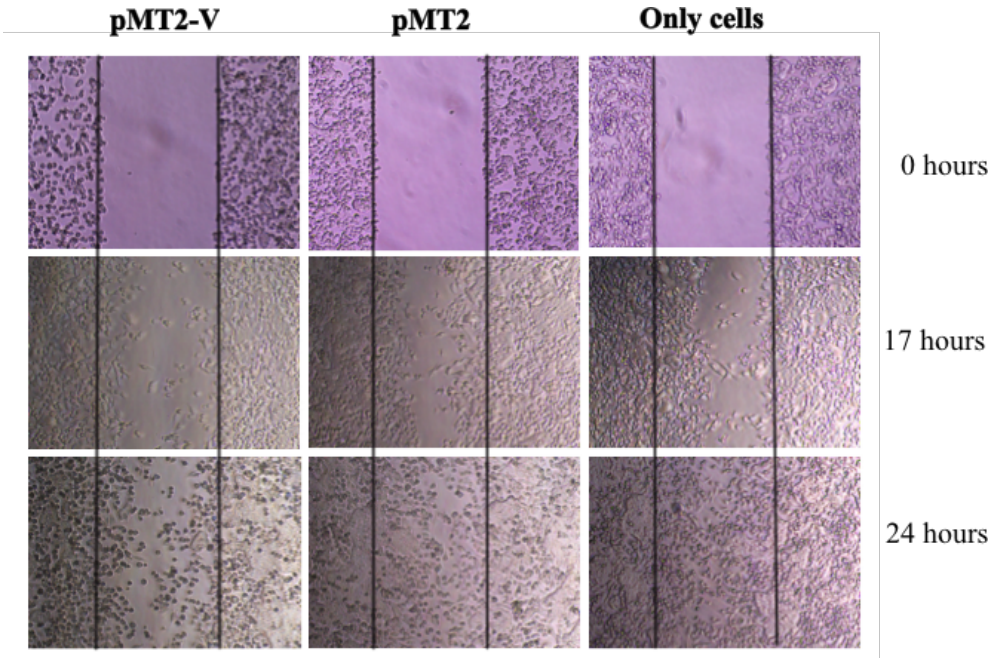


**Figure 42. Effect of FV overexpression on the cell migration of MDA-MB-231 cells.** Cells were reverse transfected with pMT2-V, and the empty pMT2 vector and untransfected cells (only cells) were used as controls. Images of the wound healing taken after 0, 17, and 24 hours are shown. One representative experiment of four is presented, with (n=6) at 17 hours and (n=12) at 0 and 24 hours.

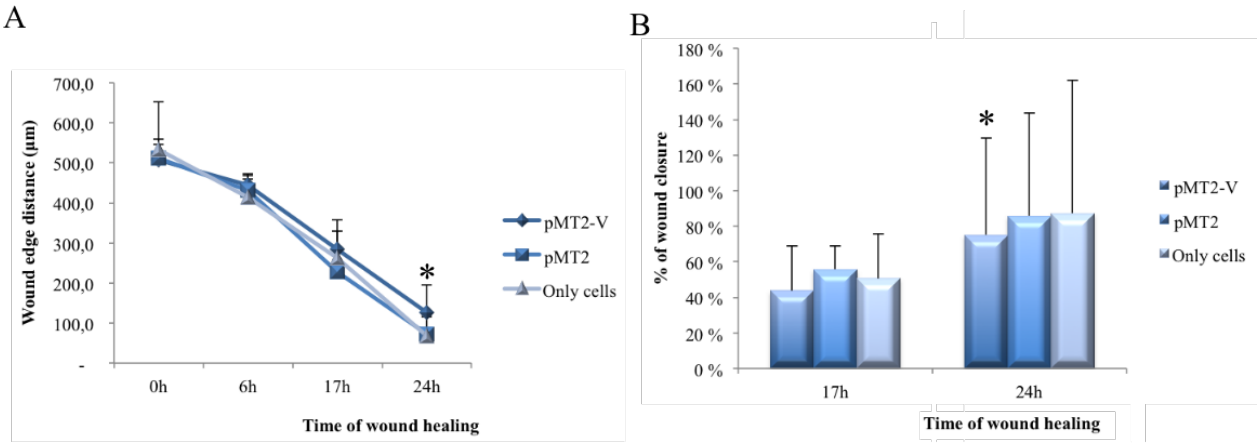


**Figure 43. Wound closure plot of transfected MDA-MB-231 cells.** The plot represents the wound closure of MDA-MB-231 cells transfected with pMT2-V, the empty pMT2 vector control and untransfected cells (only cells). (A) Wound edge distance plot (µM) of transfected MDA-MB-231 cells. (B) Wound closure (%) diagram of transfected MDA-MB-231 cells. Mean distance of wound edges + SD of four experiments are shown, (n=6) at 6 and 17 hours, (n=12) at 0 and 24 hours. Significant differences ($P \leq 0.05$) are marked with *.

The pcDNA5/FRT-V FV overexpression plasmid displayed no differences in wound healing compared to the empty pcDNA5/FRT vector control, in transfected MDA-MB-231 cells (Figure 44 and 45).

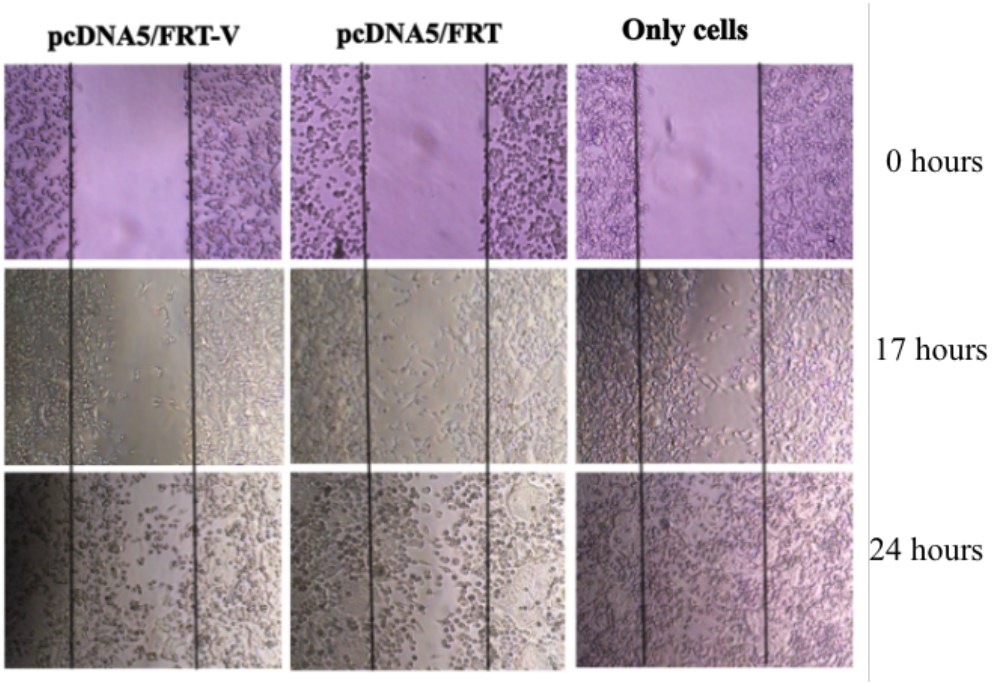


**Figure 44. Effect of FV overexpression on the cell migration of MDA-MB-231 cells.** Cells were reverse transfected with pcDNA5/FRT-V, and the empty pcDNA5/FRT vector and untransfected cells (only cells) were used as controls. Images of the wound healing after 0, 17, and 24 hours are shown. One representative experiment of four is presented, with (n=6) at 17 hours and (n=12) at 0 and 24 hours.

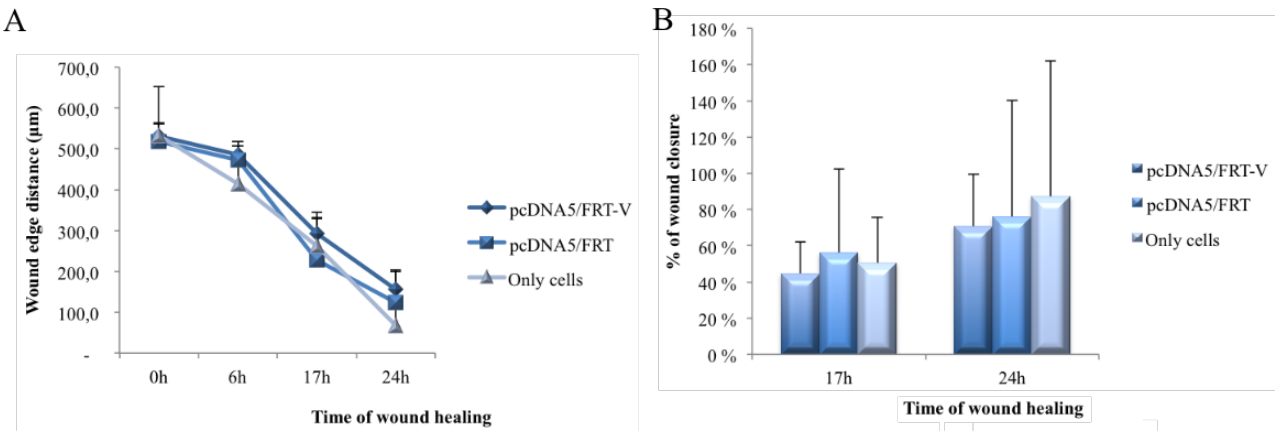


**Figure 45. Wound closure plot of transfected MDA-MB-231 cells.** The plot represents the wound closure of MDA-MB-231 cells transfected with pcDNA5/FRT-V, the empty pcDNA5/FRT vector control and untransfected cells (only cells). (A) Wound edge distance plot (µM) of transfected MDA-MB-231 cells. (B) Wound closure (%) diagram of transfected MDA-MB-231 cells. Mean distance of wound edges + SD of four experiments are shown, (n=6) at 6 and 17 hours, (n=12) at 0 and 24 hours.

### *Scratch-wound assay with exogenous human Factor V*

The effect of exogenous human Factor V on the cell migration of MDA-MB-231 cells was tested with different concentrations of hFV in a scratch-wound assay (described in section 3.6.3). The lowest dose of hFV (0.1 µg/mL) showed no differences in wound closure compared to the buffer control, at all time points (Figure 46 and 47). However, after 24 hours, the highest dose of hFV (7.0 µg/mL) resulted in a 1.3-fold significantly ($P \leq 0.01$) reduced wound closure compared to the buffer control (Figure 47). After 24 hours, the wound was healed 72% and 93%, respectively, for the hFV (7.0 µg/mL) and the buffer control (Figure 47)

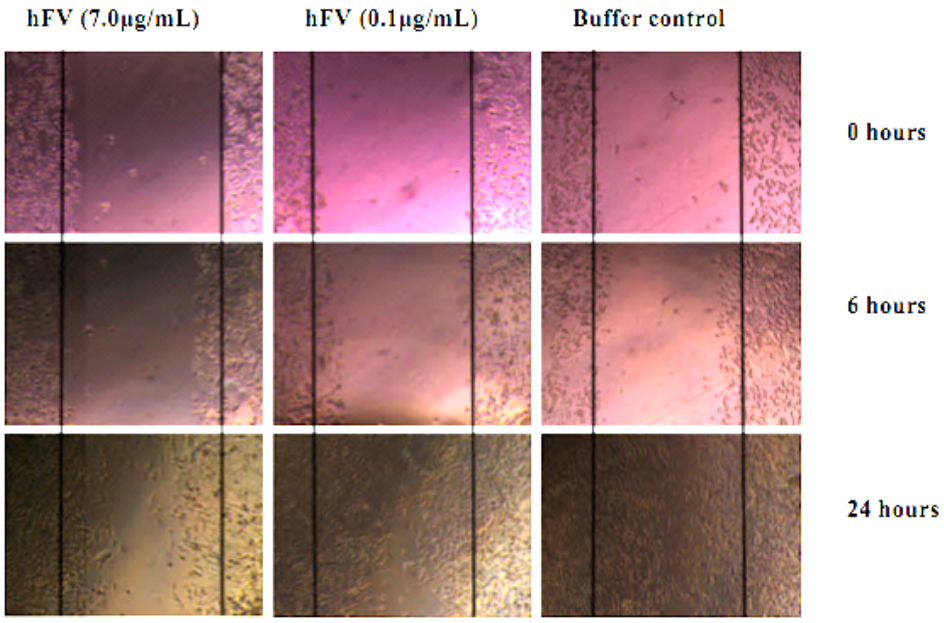


**Figure 46. Migration of MDA-MB-231 cells with exogenous human FV.** At 80-90% cell confluence a scratch-wound was made, and cells were incubated with different concentrations of hFV and a buffer control. Images were taken after 0, 6 and 24 hours. One representative experiment of three is presented, (n=6) at 6 hours and (n=9) at 0 and 24 hours.

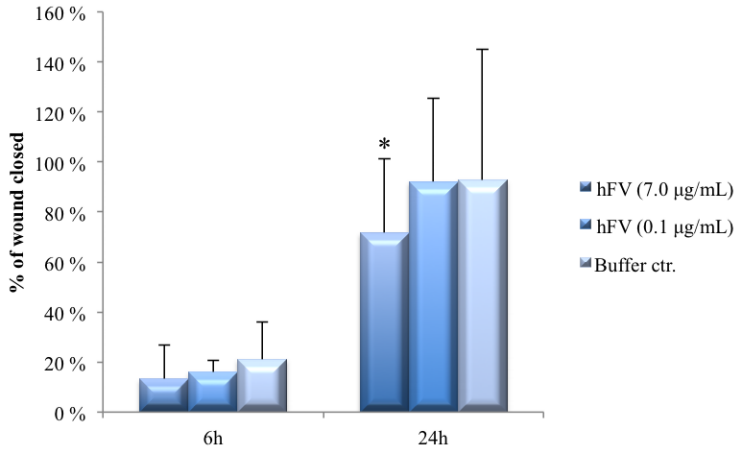


**Figure 47. Wound closure (%) of MDA-MB-231 cells incubated with exogenous human FV.** The % wound closure for three experiments are presented, (n=6) at 6 hours and (n=9) at 0 and 24 hours. Significant difference ($p \leq 0.05$) to the buffer control is marked with *.

The effect of hFV on the cell migration in MDA-MB-231 was also tested with starvation of cells during the incubation of hFV, resulting in no differences from what was seen without starvation (data not shown).

### 4.3.4 Effect on cancer-signalling pathways

The effect of FV on cancer-signalling pathways was studied *in vitro* with overexpression of FV and with addition of exogenous human Factor V in MDA-MB-231 and MCF-7. Ten different cancer-signalling pathways were investigated by measuring transcription factor activity in the breast cancer cell lines.

#### *Effect on cell-signalling pathways in MDA-MB-231*

The effect of overexpression of FV on cell-signalling pathways in MDA-MB-231 was tested with the pMT2-V overexpression plasmid, and the empty pMT2 vector as a negative control. The most upregulated pathway after overexpression of FV was the hypoxia pathway (HIF-1) with a 2.7-fold higher activity compared to the control (Figure 48), followed by the cell cycle (E2F/DPI), the Myc/Max (Myc/Max), and the MAPK/ERK (Elk-1/SRF) pathways with a 1.5-fold upregulation. The most downregulated cell-signalling pathways were Notch (RBK-Jκ) and p53/DNA Damage (p53) with 0.4-fold and 0.5-fold activity, respectively, compared to the control.

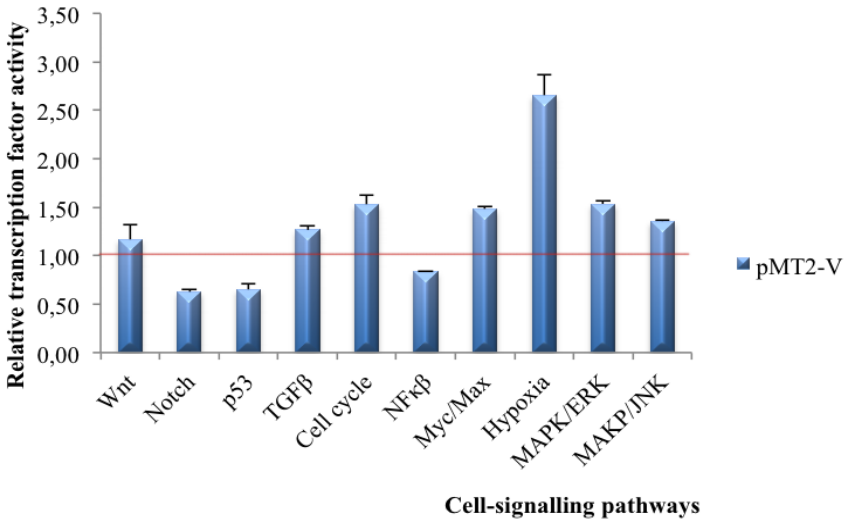


**Figure 48. Transcription factor activity in MDA-MB-231 cells transfected with pMT2-V.** The cells were transfected with pMT2-V and the empty pMT2 vector, and harvested after 48 hours for luciferase assay. The transcription factor activity is related to the empty pMT2 vector. Mean results of (n=2) + SD from one experiment are shown.

The effect of exogenous hFV on different signalling pathways in MDA-MB-231 was investigated by incubating the cells with hFV (1.0 µg/mL) and a buffer solution control. None of the ten signalling pathways seemed to be affected by hFV (Figure 49), compared to the buffer control.

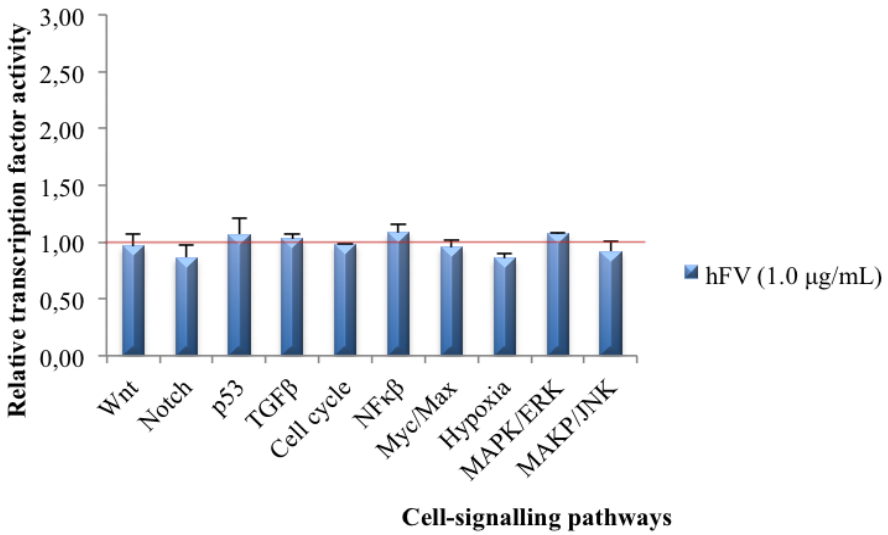


**Figure 49. Transcription factor activity in MDA-MB-231 cells incubated with hFV.** Cells were starved for six hours, then incubated with 1.0 µg/mL hFV and a buffer control, and cultured in starvation media. Cells were harvested after 24 hours of incubation with hFV for luciferase assay. The transcription factor activity is related to the buffer control solution. Mean results of (n=2) + SD from one experiment are shown.

### *Effect on cell-signalling pathways in MCF-7*

The effect of overexpression of FV on cell-signalling pathways in MCF-7 was tested with the pMT2-V overexpression plasmid, and the empty pMT2 vector as a negative control. The most upregulated pathways after overexpression of FV was the hypoxia pathway (HIF-1) and the Myc/Max (Myc/Max) pathway with a 1.3-fold and 1.2-fold higher activity, respectively, compared to the control (Figure 50).

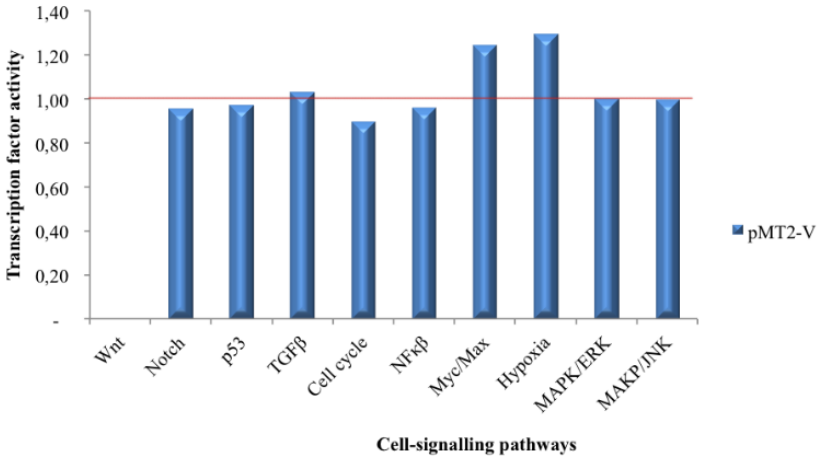


**Figure 50. Transcription factor activity in MCF-7 cells transfected with pMT2-V.** Cells were transfected with pMT2-V and the empty pMT2 vector, and harvested after 48 hours for luciferase assay. The transcription factor activity is related to the empty pMT2 vector. The transcription factor activity for the Wnt pathway is not presented in the figure, due to technical problems with the luciferase assay reading. Results from one experiment are shown.

Cell-signalling pathways in MCF-7 was screened for the effect of exogenous hFV by incubating the cells with hFV (1.0 µg/mL) and a buffer solution control. Cells were starved for six hours and during the incubation time. The only affected cancer-signalling pathway was the Wnt (TCF/LEF) pathway (Figure 51), which activity was 0.5-fold, compared to the buffer control.

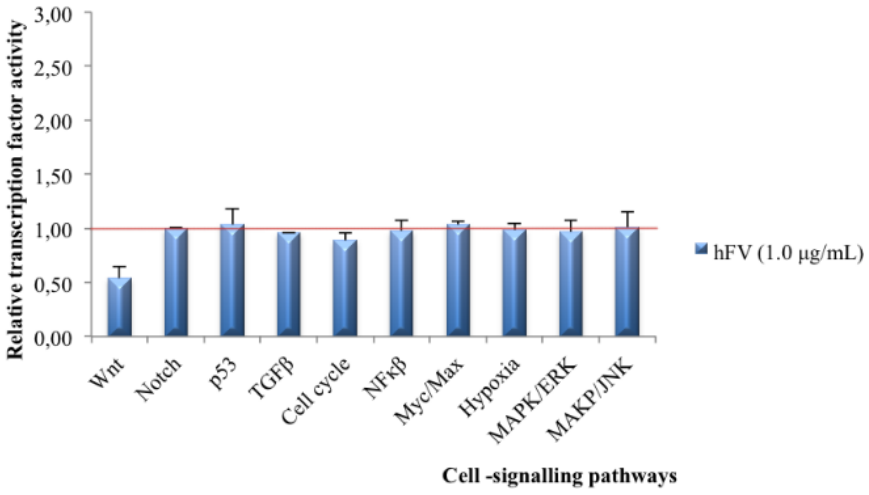


**Figure 51. Transcription factor activity in MCF-7 cells incubated with hFV.** Cells were starved for six hours, then incubated with 1.0 µg/mL hFV and a buffer control, and cultured in starvation media. Cells were harvested after 24 hours of incubation with hFV for luciferase assay. The transcription factor activity is related to the buffer control solution. Mean results of (n=2) + SD from one experiment are shown.

# 5 Discussion

The association between cancer and risk of thrombotic diseases has been well established (Elaymany et al. 2014). In fact, cancer patients are exposed to a 4-20% risk of evolving venous thrombosis (VT), and cancer-associated VT represents the second leading cause of death in cancer patients after the cancer itself (Hisada & Mackman 2017; Khorana et al. 2007). It has also been seen a correlation between coagulation and cancer progression for coagulation factors, such as tissue factor, tissue factor pathway inhibitors, and factor VII (Falanga et al. 2013; Jain et al. 2010). A better understanding of the relationship between cancer progression and blood coagulation could achieve an improved and more individualized treatment for both cancer and cancer-related thrombosis.

The role of coagulation factor V (FV) in cancer remains undiscovered. However, single nucleotide polymorphisms (SNPs) in the *F5* gene have been associated with breast cancer patients (Tinholt et al. 2014). Studies has also revealed a higher expression of *F5* in breast tumours of aggressive nature compared to normal tissue (Tinholt et al. 2018). Furthermore, breast cancer patients with basal-like tumours were also suggested to have a greater survival rate when expressing high levels of *F5* (Tinholt et al. 2018). This underlines the importance of developing new therapeutic strategies targeting the coagulation processes in cancer. The main purpose of this thesis was to characterize the role of coagulation factor V in breast cancer progression. FV overexpression models and exogenous FV were used to study the *in vitro* functional effects of FV in breast cancer cell lines.

## 5.1 Creation of FV overexpression vector systems

Expression vectors enable selectively expression of a gene of interest, and are commonly used to study the *in vitro* functional effects of the gene regulation and the protein synthesis in eukaryotic cells (Prelich 2012). One of the specific aims in this thesis was to construct two plasmid-based vector systems for FV overexpression in cell lines.

We already possessed a commercial expression vector containing the *F5* gene: pMT2-V. As no empty pMT2 vector was available, we successfully created an empty version of the pMT2-V plasmid in order to use this as a vector control in cell experiments. Since the pMT2-V expression vector lack eukaryotic selection markers, the *F5* sequence was subcloned from the pMT2-V vector into the pcDNA5/FRT mammalian expression vector. Unlike the pMT2

vector, the pcDNA5/FRT contains a mammalian antibiotic resistance gene (*Hygromycin*), and could be used for selection of cell lines with stable overexpression FV. As there were no compatible restriction sites for the pMT2-V vector and the pcDNA5/FRT destination vector, the *F5* cDNA was amplified with long-range PCR using *F5* specific primer pairs. Amplification of larger DNA fragments can be problematic due to limited size amplification and incomplete proofreading by the *DNA polymerase* (Jia et al. 2014). Long-range PCR is developed to improve these conditions, and was chosen as a suitable amplification procedure of the ~7 kb long *F5* cDNA sequence. Several conformational steps established a successful subcloning of the amplified *F5* cDNA into the destination vector (pcDNA5/FRT). Sequencing of the constructed pcDNA5/FRT-V plasmid displayed a *F5* sequence without any novel mutations due to polymerase errors, and the revealed SNPs in exon 13 were already present in the *F5* cDNA sequence template in the pMT2-V vector.

After a successful creation of the two FV overexpression plasmid-based vector systems, the plasmids were used further in this thesis for overexpression studies of FV in breast cancer cell lines.

## 5.2 Breast cancer cell lines

*In vitro* cell models are widely used to study the biological responses and mechanisms related to human health and disease. There are several advantages by using cell lines as *in vitro* models compared to primary cells. Removing cells from its original context enables a more detailed and specified study. Moreover, the *in vitro* cell models are easily acquired, they have an infinite potential of cell division, it is cost-effective, and the cells can be stored in a frozen condition until they are required. However, it is necessary to be aware of the transition from an *in vitro* to an *in vivo* experiment. *In vitro* cell lines are cultured outside its natural environment, and the complexity of an *in vivo* experiment may be absent. Hence, the results should only be used as a possible prediction for further studies and not to draw clear conclusions about the functional effects in humans.

The two breast cancer cell lines used in this thesis, the MDA-MB-231 and the MCF-7, has a low endogenous expression of *F5* mRNA levels, and were therefore suitable to study the *in vitro* effect of FV overexpression. In addition, MDA-MB-231 cells are characterized as basal-like and triple negative, matching the aggressive tumour characteristics found to be associated

with a greater survival rate when expressing high levels of *F5* (Tinholt et al. 2018). The MCF-7 cancer cell line has the ability to generate unlimited amounts of RNA/DNA, facilitating validation and downstream functional studies (Lee et al. 2015). Hence, the MCF-7 cells are widely used in genomic studies, and have contributed to an improved treatment of breast cancer patients. It was of interest to study the functional effects of FV in MCF-7, as the luminal cell line possesses other characteristics than the basal-like and triple negative MDA-MB-231 breast cancer cell line. The MCF-7 cell line is characterized as ER and PR positive, and HER2 negative (section 3.3.5).

## 5.3 Overexpression of FV in MDA-MB-231 and MCF-7

MDA-MB-231 and MCF-7 breast cancer cell lines were transiently transfected with the two created plasmid-based vector systems for FV overexpression.

Cells transfected with the pMT2-V plasmid resulted in high levels of *F5* mRNA expression compared to the empty vector control, as predicted in previous studies in the research group without the corresponding vector control (data not shown). The relative *F5* mRNA expression in MDA-MB-231 increased 26 000-fold to 40 000-fold from 48 to 72 hours, compared to the empty vector control. While transfected MCF-7 cells had a higher relative *F5* mRNA expression at 48 hours than MDA-MB-231, the *F5* expression decreased from 50 000-fold to 13 000-fold.

The newly constructed pcDNA5/FRT-V FV overexpression vector likewise displayed high levels of *F5* mRNA expression in both cell lines, compared to the empty vector control. Moreover, the *F5* mRNA expression decreased from 48 to 72 hours in both cell lines transfected with the pcDNA5/FRT-V expression vector, respectively from 25 000-fold to 18 000-fold in MDA-MB-231, and from 70 000-fold to 39 000-fold in MCF-7.

Since both cell lines transfected with the pcDNA5/FRT-V plasmid resulted in high expression of *F5* at the mRNA level, it was unexpected that the levels of secreted FV in cell media and cell lysate from the transfected cells were low. There is a possibility that the cells did not secrete the expected levels of FV, or the low secretion was a result of translation problems. In contrast, the secretion of FV in cell media from cells transfected with the pMT2-V plasmid was up to 16-fold higher, than for cells transfected with the pcNDA5/FRT-V plasmid. The

sequencing of the pcDNA5/FRT-V plasmid after subcloning showed a matching *F5* cDNA sequence as in the pMT2-V template. Thus, the expected expression and secretion of FV should be similar for the plasmids. Post-translational modifications may lead to differences at the mRNA and the protein level, derived from the same gene (Greenbaum et al. 2003). Cells transfected with the pMT2-V plasmid showed high levels of secreted FV as well as *F5* mRNA expression compared to the empty vector control, thus it should not suggest alterations at the translational level. However, this could anyhow be a problem with the pcDNA5/FRT-V plasmid.

Further, the variation in FV secretion between the two plasmids might be explained by the features the plasmids possess. The knowledge about the pMT2-V plasmid's features is limited, but it contains a different promoter than the pcDNA5/FRT plasmid. The pcDNA5/FRT vector was initially chosen to construct a new FV overexpression vector, as it is a mammalian expression vector and contain a mammalian antibiotic resistance gene. In addition, the pcDNA5/FRT plasmid is constructed with an Flp-In™ System from the manufacturer, which engages introduction of a Flp Recombination Target (FRT) site into the genome of the mammalian cell line. The site-specific recombinase technology is based on the *Flp* recombinase binding to the FRT site of the vector, and enables integration and expression of the desired gene at a specific genomic location in the mammalian cell line of choice (Craig 1988; Sauer 1994). According to the manufacturer, the Flp-In™ system for pcDNA5/FRT includes several components to obtain the site-specific recombinase technology. An important note is that the pcDNA5/FRT plasmid lacks a promoter for the *Hygromycin* gene, and need to be co-transfected fro the host cell to obtain the *Hygromycin* resistance gene. Although, the transfected cells with pcDNA5/FRT-V resulted in high *F5* mRNA expression, and an insufficient transfection of the pcDNA5/FRT-V plasmid alone is therefore difficult to explain.

The results suggest that the features of the plasmids needs to be investigated further, and that it might be a translational problem for cells transfected with the pcDNA5/FRT-V plasmid. Further research should be conducted with minimal differences between plasmid features, but with the same benefits of an eukaryotic selection marker as what is possessed in the pcDNA5/FRT mammalian expression vector.

## 5.3 Functional effects of FV overexpression in MDA-MB-231 and MCF-7

The biological hallmarks of acquired cancer capabilities were proposed to gain a better understanding of the underlying molecular mechanisms of cancer pathogenesis (Hanahan & Weinberg 2000; Hanahan & Weinberg 2011). Since the proposed characteristics of cancer cell proliferation includes sustaining proliferative signalling, evading cell growth suppressors, the ability to resist programmed cell death, and induce angiogenesis, the functional effect of FV overexpression were investigated on cell growth, cell death, cell migration, and cancer-signalling pathways.

### 5.3.1 Effect of FV overexpression on programmed cell death

Apoptosis is an intrinsic cellular mechanism of programmed cell death present in every cell of the human body, and highly conserved due to its critical role in the regulation of important physiological and pathophysiological processes (Fulda 2013). One of the hallmarks of human cancers is the tumour's ability to resist induction of cell death, as a result of disrupted signalling of death receptors, loss of caspase activity, and an imbalance between anti- and pro-apoptotic proteins. FV overexpression in the transfected breast cancer cell lines showed no clear differences in apoptotic effect compared to the empty vector controls, except from a significant reduced DNA fragmentation for the pMT2-V plasmid after 72 hours in MDA-MB-231. However, awareness of the amount of biological replicates at this time point should be taken in care before drawing conclusions of the effect. Western blot analysis with PARP was performed to confirm the apoptotic effect in cell lysates of transfected MDA-MB-231 cells. PARP is an antibody marker selective for early apoptosis when cleaved, and showed bands for both full length and cleaved PARP for all samples. The reduced effect of pMT2-V was not confirmed with the western blot analysis, as the same amount of cleaved PARP was present in this sample. This could be due to the sensitivity of the blotting. A loading control should have been implemented in this analysis, but was not performed due to time limitations. Therefore, the cleavage of PARP is only presented as a potential predictive marker of the apoptotic effect, and further analysis should be performed.

Normally, apoptosis is evaded in a tumour environment, and the breast cancer cells seems to be unaffected by the FV overexpression. Supplementary DNA fragmentation assays must be performed to confirm the apoptotic effect of FV overexpression, suggesting additional experiments to reproduce a consistency of the apoptotic effect in both independent

experiments and biological replicates. The programmed cell death can then further be analysed by the caspase activity, targeting either the cell's extrinsic (receptor) pathway or intrinsic (mitochondrial) pathway of apoptosis (Fulda 2013).

### 5.3.2 Effect of FV overexpression on cell growth

MDA-MB-231 cells transfected with the pcDNA5/FRT-V FV overexpression plasmid showed no differences in cell growth compared to the empty vector control. While the pMT2-V plasmid had a significant 1.2-fold increase in cell growth at both 24 and 72 hours after transfection, compared to the empty vector control. This can be related to the unaffected apoptotic effect of pcDNA5/FRT-V plasmid at 48 and 72 hours, and the reduced apoptotic effect of pMT2-V at 72 hours. However, the untransfected cells showed a consistent elevated cell growth over time, compared to the transfected cells and empty vector control. Indicating that the transfection itself had an impact on the cell's growth. In MCF-7, the growth was negligible after transfection, and the effect of FV overexpression on cell growth could thus not be elevated. In addition, a minimal cell growth of untransfected cells was observed until 48 hours of culturing. The reason for this is undetermined, but might be caused by the experimental design in a 96-well plate. From out knowledge, there are no available reported results of previous studies with the focus on effect of FV overexpression on cell growth. Other methods should be carried out to estimate the effect of FV overexpression on cell growth. Cell count, total protein quantification, and cell cycle arrest studies are examples of other methods that can be of interest for this purpose. To limit the possible impact of transfection reagents on the cell growth, the effect of exogenous human FV was tested further in the breast cancer cell lines (5.4.1).

### 5.3.3 Effect of FV overexpression on cell migration

Tumours have the opportunity to induce angiogenesis, which is one of the proposed hallmarks of cancer by Hannahan & Weinberg. Angiogenesis is the process of sprouting, cell division, migration, and assembly of endothelial cells from pre-existing vessels (Fouad & Aanei 2017). Angiogenesis is an important process in embryogenesis to recreate and expand vascular networks, in addition to its presence in postnatal events such as wound healing, the female reproductive cycle, and chronic inflammation (Ribatti et al. 2015). These processes are regulated by pro- and anti-angiogenic factors, but in malignancy these events of angiogenesis are continuously activated. Initiation of pro-angiogenic factors in cancer tumours stimulates

migration of endothelial cells for blood vessel development, supporting increased blood flow to the tumour (Hanahan & Weinberg 2000).

A migration chamber assay was used to investigate the effect of FV overexpression on cell migration in transfected MDA-MB-231 cells over time. Cells transfected with pMT2-V resulted in decreased cell migration, compared to the empty pMT2 vector control and untransfected cells. The pcDNA5/FRT-V overexpression plasmid displayed a lower difference in wound healing than the pMT2-V plasmid. When cells are exposed to a wound, the disruption initiates a response of the cell monolayer and increase growth factor concentrations at the wound edge. This results in a healing of the wound through a combination of proliferation and migration (Yarrow et al. 2004). Previous experiments of cell migration assays in combination with FV have not been reported. Our results suggest that FV overexpression may reduce the cell's ability to initiate migration or proliferation, proposing FV towards a potentially role in cancer angiogenesis. However, the experiment should be reproduced with supplementary experiments with the focus on time points between 6 to 24 hours, in addition to other confirming methods. This can be performed with a Boyden chamber assay to provide more certain results, and exclude the difference in migration due to growth. In addition, the underlying cellular response of migration can be analysed with western blotting, by testing the presence of for example p-FAK (Focal adhesion kinase 1) and CD49b antibodies. P-FAK is a tyrosine kinase that can act as a signal protein, controlling cellular response of cell migration, proliferation, survival, and repair of epithelial tissue after DNA damage. The CD49b is a glycoprotein, expressed on NK cells, and plays a role in cell adhesion and lymphocyte activation.

### 5.3.4 Effect of FV overexpression on cancer cell-signalling pathways

Cell signalling is an essential communication pathway and a highly complex control of cell activity, including regulation of cell growth, migration, metabolism, differentiation, and cell death. MDA-MB-231 and MCF-7 cells were transfected with the pMT2-V overexpression plasmid, and the empty pMT2 vector control, to test the effect of FV overexpression on ten different cancer-signalling pathways.

FV overexpression in MDA-MB-231 resulted in upregulation of several pathways, where the most upregulated pathways after overexpression of FV was the hypoxia pathway with a 2.7-

fold higher activity compared to the empty control. Followed by the cell cycle, the Myc/Max, and the MAPK/ERK pathways with a 1.5 fold upregulation. Transfected MCF-7 cells with the pMT2-V overexpression plasmid also resulted in an upregulation of the hypoxia and the Myc/Max pathway, with a 1.3-fold and 1.2-fold higher activity, respectively, compared to the control. Due to technical problems with the luciferace assay reading, the transcription factor activity for the wnt pathway could not be presented for transfected MCF-7 cells.

Hypoxia is one of the most important triggers of angiogenesis (Fouad & Aanei 2017). Oxygen mechanisms of endothelial cells respond to hypoxia-inducible transcription factors (HIF), and regulate expression of genes involved in angiogenesis, cell survival, metabolism, and inflammation. One of the biological hallmarks of cancer is the cancer cell's ability to enter the cell cycle in the absence of mitogenic signals. A mutation in the pRB tumour suppressor gene may cause the cells to enter the cell cycle unintentionally. Cancer cells also have the ability to produce their own growth signals, such as platelet-derived growth factor (PDGF), which can initiate proliferation signals like mitogen-activated protein kinases (MAPK) (Holland et al. 2000). The MYC proto-oncogene interact with several growth promoting signal pathways, and is an early response of membrane bound receptor complexes. Upon activation of MYC, the Myc-Max binds to E-box genes which regulates metabolism, ribosomal biogenesis, and cell mass accumulation (Dang 2012). Interestingly, deregulation of MYC has shown to be sufficient to reverse *in vivo* tumourigenesis in some cases (Jain et al. 2002), but not in others (Boxer et al. 2004; Jonkers & Berns 2004), suggesting that tumour specificity affect the tumorigenesis upon MYC suppression. The suppression of MYC may also trigger an imbalance between apoptotic and anti-apoptotic gene expression.

FV overexpression also resulted in downregulation of the notch and the p53 pathways in MDA-MB-231. The notch pathway promotes proliferative signalling during neurogenesis, and is involved in the regulation of embryonic development and homeostasis in various tissues (Baron 2003). Depending on the tissue and cellular context, notch can be either oncogenic or tumour suppressive (Nowell & Radtke 2017). Expression of p53 is involved in DNA damage, and inhibits the cell to enter the cell cycle, preventing cell growth and cell division. Tumour cells often carry a missense mutation in the *TP53* tumour suppressor gene, enabling tumour cell resistance to normal cell cycle prevention.

The role of FV in these up- or downregulated pathways should be investigated further before drawing clear conclusions. Suggesting transfection of cells with the pMT2-V FV overexpression plasmid systems with the addition of an inhibitor or activator of the up- or downregulated pathway, following analysis at the mRNA and the protein level.

## 5.4 Functional effects of exogenous FV in MDA-MB-231 and MCF-7

Exogenous haemostatic factor are commonly used in biotechnological and pharmaceutical research and applications (Tavassi et al. 2014). An example is the use of exogenous factors in diagnostic kits to detect haemostatic deficiency of a clotting factor, due to the specific activities of the factor. Exogenous factors have been suggested as therapeutic agents for treatment of various imbalances in the haemostatic system, including thrombosis, stroke, clotting factor deficiencies, cancer, and bleeding (Andrade et al. 2012).

Based on the experiments performed with the FV overexpression vector systems, it was of interest to investigate the functional effects of FV further, without the possible limitations in transfection efficiency, cell's sensitivity to the transfection reagents, or possible translational problems of the *F5* mRNA sequence. The *in vitro* overexpression of FV can be related to the endogenous expression of FV, thus it was of interest to test the effects of exogenously added FV. A commercial native human Factor V protein (330 kDA), derived from human blood/plasma was used for this purpose. Single-chain FV protein (330 kDA) circulates in blood in its inactive form, whereas 80% of FV circulates in plasma at a concentration of approximately 20 nM (7.0 µg/mL) (Asselta et al. 2006; Duga et al. 2004). The remaining 20% of FV present in whole blood is contained in platelet α-granules. The *in vitro* functional effects of exogenously added human Factor V (hFV), was studied by the use of different hFV concentrations. The highest concentration of hFV (7.0 µg/mL) was based on the circulating plasma concentration of FV in humans, followed by decreasing concentrations towards 0.1 µg/mL. A buffer solution control was made according to the storage buffer of the native hFV, consisting of 50% water with 50% glycerol. The functional effect of hFV was studied on cell growth, cell migration, and cell signalling in breast cancer cell lines.

### 5.4.1 Effect on cell growth

To study the effect of exogenously added hFV on cell growth in MDA-MB-231 and MCF-7, the cells were incubated with two different concentrations of hFV for 72 hours, and a buffer solution as control.

MDA-MB-231 cells incubated with the lowest dose of hFV (0.1 µg/mL) showed a significant growth reduction ($P$=0.03) compared to the buffer control. There were no difference in cell growth between the highest dose of hFV and the buffer control. Additionally, the effect of exogenous hFV was studied by culturing the cells in starvation media during the incubation time of hFV. The same results were obtained by starvation as with only hFV incubation (data not shown). Despite the significant reduced cell growth by hFV in MDA-MB-231, the differences were anyhow small compared to the buffer control, and should be evaluated further.

In MCF-7, the incubation with exogenous hFV resulted in a significant ($P$≤0.01) increase in cell growth for the highest concentration of hFV (7.0 µg/mL), compared to the buffer control. While cell growth of the lowest dose of hFV (0.1 µg/mL) was equal to the buffer control. MCF-7 cells were also tested with starvation during incubation with hFV, and showed no differences in the cell growth as without starvation, similar to what was observed in MDA-MB-231. Further experiments with high concentrations of hFV are of interest to test the significance of the effect of hFV on cell growth.

The effect of exogenously added hFV compared to the effect of FV overexpression on cell growth, seems to be either unaffected or FV increase the growth of the breast cancer cells. The effect of exogenous hFV should also be studied further on the apoptotic effect, to test the differences between endogenous and exogenous expression of FV.

### 5.4.2 Effect on cell migration

The effect of exogenous human factor V on cell migration was studied in the MDA-MB-231 breast cancer cell line, with different concentrations of hFV in a scratch-wound assay. There were no differences in the lowest dose of hFV (0.1 µg/mL) over the observed time period. However, incubation with the highest concentration of hFV (7.0 µg/mL) resulted in a significant 1.3-fold reduced cell migration after 24 hours compared to the buffer control. As

for the effect of hFV on cell growth during starvation, there was no effect on cell migration by starving the cells during incubation with hFV (data not shown). After testing the effect of FV overexpression and exogenously added hFV on cell migration, the results suggest that FV reduce cell migration in the MDA-MB-231 breast cancer cell line.

Further, several repeated experiments should be performed to confirm the findings. Different concentrations of hFV ranging from (0.1 – 7.0 µg/mL) could be used, as well as measuring the wound healing with specific interest of wound closure after 6 hours and up to 24 hours. In addition, investigating the possible involved cellular mechanisms in cell migration would be of interest, as for the overexpression of FV with western blot analysis. The scratch-wound assay is a relative simple procedure, and has a rapid setup and easy analysis. However, there are several limitations by using this method. The scratch is made manually by a pipette tip or needle. Cell migration is often increased prior to the wound, resulting in a critical start if the wound gap is uneven. In addition, some cells may loosen from the wound edges during the scratch making. Those cells have the possibility to adhere to the plate and move into the wound area, causing an uneven wound closure. In this thesis, a scratch wound assay in a 96-well plate was chosen to obtain the highest concentration of hFV, due to the limits of commercial hFV concentration and culture area. Other suggested migration assays that can be performed with an optimized wound edges in small culturing areas are; an electric cell substrate impedance sensing (ECIS), or introducing an electric fence into a 96-well plate (Kramer et al. 2013).

### 5.4.3 Effect on cancer cell-signalling pathways

The effect of human Factor V on cancer-signalling pathways was tested in MDA-MB-231 and MCF-7, by using a concentration of 1.0 µg/mL of hFV and starving the cells for six hours in advance of the addition of hFV. None of the ten signalling pathways seemed to be affected by hFV in the MDA-MB-231 breast cancer cell line. While in MCF-7, the only affected cancer-signalling pathway was the Wnt pathway, which activity was 0.5-fold, compared to the buffer control.

The Wnt pathway controls cell-to-cell interactions, and has an important role in tissue homeostasis in several organ systems (Tabatabai et al. 2017), cellular proliferation, differentiation, and migration (Logan & Nusse 2004). Malfunction of the Wnt pathway is

related to several forms of human disease, including cancer (Katoh 2005). Different genetic defects may lead to tumour elevation through Wnt signalling, and is most likely caused by inappropriate gene activation mediated by β-catenin (Polakis 2000). Targeting the abnormalities in the Wnt pathway in cancer has emerged as a potential treatment of cancer. Based on this knowledge, it is of interest to investigate further the role hFV in the regulation of the Wnt pathway in MCF-7, as the signalling pathway has an impact on the tumour cell proliferation, differentiation, and migration.

## 5.5 Limitations

In this thesis, there are several present limitations. Cell type specific properties may result in different influence on the functional effect of FV, and should be noted when comparing experiments from different cell lines. Some of the experiments performed in this thesis do not follow the norm of performing at least three individual experiments, each with biological replicates, for a consistency in reproductive results. This includes particularly the variation and number of replicates presented at 72 hours, in RT-qPCR analysis of *F5* mRNA expression in MDA-MB-231 and MCF-7, and in apoptotic effect of FV in MCF-7. Nevertheless, functional studies contain biological replicates, but lack repetition of independent experiments (cell growth). Thus, care should be taken when drawing conclusions from those results presented in this thesis. In addition to the statistics, which is provided as an estimate of significance. Other methods should be performed to confirm the effect of FV on cell growth, apoptosis, and migration. Particularly, there is a need of an improved migration assay for experiments with exogenous human Factor V.

# 6 Conclusions

In this thesis, two plasmid-based vector systems were constructed to study the *in vitro* functional effects of overexpression of FV in breast cancer cell lines. Moreover, the effects of exogenously added human FV was studied *in vitro* in breast cancer cell lines.

The main conclusions from these studies are as follows:

I. Expression and functional effects of FV overexpression in MDA-MB-231 and MCF-7 *in vitro*:
   - Two plasmid-based vector systems were created for *in vitro* experiments of FV overexpression in cell lines. The *F5* cDNA sequence was successfully subcloned to the pcDNA5/FRT vector, without any novel mutations.
   - The constructed pcDNA5/FRT-V FV overexpression vector showed an increased expression of *F5* mRNA in MDA-MB-231 and MCF-7, but low levels and secretion of FV protein in comparison to the pMT2-V vector.
   - FV overexpression resulted in unaffected apoptosis and cell growth, except for cells transfected with the pMT2-V FV overexpression plasmid, which showed reduced apoptotic effect and an increase in cell growth after 72 hours.
   - FV overexpression resulted in a decreased cell migration in transfected MDA-MB-231 cells. Proposing that FV has a role in breast cancer angiogenesis.
   - FV overexpression caused an upregulation of the hypoxia, cell cycle, Myc/max, and MAPK/ERK cancer-signalling pathways in MDA-MB-231, and an upregulation of the hypoxia and the Myc/max pathways in MCF-7. The signalling pathways activated by FV overexpression are essential for tumour development, cell proliferation, and enabling the cell to enter the cell cycle.
   - FV overexpression lead to downregulation of the notch and the p53 pathways in MDA-MB-231, which is important for proliferative signalling, DNA damage, and prevention of the cell to enter the cell cycle.

II. Functional effects of exogenous human FV in MDA-MB-231 and MCF-7 *in vitro*:
   - Exogenous hFV leads to small effects on cell growth in the MDA-MB-231 breast cancer cell line. While, a high concentration of hFV significantly increased the growth of MCF-7 cells.

- A higher concentration of exogenously added hFV decreased the cell migration of MDA-MB-231, confirming the effects of overexpression of FV on cell migration in the breast cancer cell line.
- None of the ten cell-signalling pathways was remarkably affected by hFV in the MDA-MB-231 breast cancer cell line. While in the MCF-7 breast cancer cell line, the Wnt pathway was down regulated. These pathways are involved in cell proliferation, differentiation, and migration.

# 7 Further perspectives

- The features of the FV overexpression vectors needs to be investigated further, to determine the differences of FV expression at the protein level between the two plasmid-based vector systems. Further experiments of FV overexpression should be performed with a new expression vector, containing the same benefits as the pcDNA5/FRT vector.
- Supplementary studies, with several independent experiments and biological replicates, to confirm the observed effect of FV overexpression on apoptosis (by DNA fragmentation through western blot analysis, or assays measuring membrane alterations or caspace activity) and cell growth (by living cell count or total protein quantification).
- Use exogenous human Factor V to study the effect on programmed cell death.
- Further study the effect of FV overexpression and exogenous human FV on cell migration with and optimized migration assay. With the focus on time points between 6 to 24 hours, and high concentrations of exogenous hFV. In addition, the results should be confirmed by western blot analysis with specific antibodies targeting the underlying cellular response of migration.
- Further investigate the role of FV overexpression on the upregulated and downregulated cancer-signalling pathways presented in this thesis.

.

# 8 References


Anand, P., Kunnumakkara, A. B., Sundaram, C., Harikumar, K. B., Tharakan, S. T., Lai, O. S., Sung, B. & Aggarwal, B. B. (2008). Cancer is a preventable disease that requires major lifestyle changes. *Pharm Res*, 25 (9): 2097-116. doi: 10.1007/s11095-008-9661-9.

Anderson, K. N., Schwab, R. B. & Martinez, M. E. (2014). Reproductive risk factors and breast cancer subtypes: a review of the literature. *Breast Cancer Research and Treatment*, 144 (1): 1-10. doi: https://doi.org/10.1007/s10549-014-2852-7.

Andrade, S. A., Carrijo-Carvalho, L. C., Peceguini, L. A., Wlian, L., Sato, A. C., Luchiari, C., Silva, E. D., Maffei, F. H. & Chudzinski-Tavassi, A. M. (2012). Reversal of the anticoagulant and anti-hemostatic effect of low molecular weight heparin by direct prothrombin activation. *Braz J Med Biol Res*, 45 (10): 929-34.

Asselta, R., Tenchini, M. L. & Duga, S. (2006). Inherited defects of coagulation factor V: the hemorrhagic side. *J Thromb Haemost*, 4 (1): 26-34. doi: 10.1111/j.1538-7836.2005.01590.x.

B., D. (2017). Novel insights into the regulation of coagulation by factor V isoforms, tissue factor pathway inhibitorα, and protein S. *Journal of Thrombosis and Haemostasis*, 15 (7): 1241-1250. doi: doi:10.1111/jth.13665.

Baron, M. (2003). An overview of the Notch signalling pathway. *Seminars in Cell & Developmental Biology*, 14 (2): 113-119. doi: https://doi.org/10.1016/S1084-9521(02)00179-9.

Berridge, M. V., Tan, A. S., McCoy, K. D. & Wang, R. (1996). The biochemical and cellular basis of cell proliferation assays that use tetrazolium salts. *Biochemica*, 4 (1): 14-19.

Boxer, R. B., Jang, J. W., Sintasath, L. & Chodosh, L. A. (2004). Lack of sustained regression of c-MYC-induced mammary adenocarcinomas following brief or prolonged MYC inactivation. *Cancer Cell*, 6 (6): 577-86. doi: 10.1016/j.ccr.2004.10.013.

Brose, K. M. & Lee, A. Y. (2008). Cancer-associated thrombosis: prevention and treatment. *Curr Oncol*, 15 (Suppl 1): S58-67.

Chae, Y. K., Anker, J. F., Carneiro, B. A., Chandra, S., Kaplan, J., Kalyan, A., Santa-Maria, C. A., Platanias, L. C. & Giles, F. J. (2016). Genomic landscape of DNA repair genes in cancer. *Oncotarget*, 7 (17): 23312-23321. doi: 10.18632/oncotarget.8196.

Chavez, K. J., Garimella, S. V. & Lipkowitz, S. (2011). Triple negative breast cancer cell lines: One tool in the seach for better treatment of triple negative breast cancer. *Breast Disease*, 32 (1-2): 35-48. doi: 10.3233/BD-2010-0307.

Coussens, L. M. & Werb, Z. (2002). Inflammation and cancer. *Nature*, 420: 860. doi: 10.1038/nature01322.

Craig, N. L. (1988). The mechanism of conservative site-specific recombination. *Annu Rev Genet*, 22: 77-105. doi: 10.1146/annurev.ge.22.120188.000453.

Cramer, T. J. & Gale, A. J. (2012). The anticoagulant function of coagulation factor V. *Thromb Haemost*, 107 (01): 15-21. doi: 10.1160/TH11-06-0431.

Cripe, L. D., Moore, K. D. & Kane, W. H. (1992). Structure of the gene for human coagulation factor V. *Biochemistry*, 31 (15): 3777-3785. doi: 10.1021/bi00130a007.

Dahlback, B. (2016). Pro- and anticoagulant properties of factor V in pathogenesis of thrombosis and bleeding disorders. *Int J Lab Hematol*, 38 Suppl 1: 4-11. doi: 10.1111/ijlh.12508.

Dang, C. V. (2012). MYC on the Path to Cancer. *Cell*, 149 (1): 22-35. doi: 10.1016/j.cell.2012.03.003.

Dashty, M., Akbarkhanzadeh, V., Zeebregts, C. J., Spek, C. A., Sijbrands, E. J., Peppelenbosch, M. P. & Rezaee, F. (2012). Characterization of coagulation factor synthesis in nine human primary cell types. *Sci Rep*, 2: 787. doi: 10.1038/srep00787.

Davalos, D. & Akassoglou, K. (2012). Fibrinogen as a key regulator of inflammation in disease. *Semin Immunopathol*, 34 (1): 43-62. doi: 10.1007/s00281-011-0290-8.

Denkert, C., Liedtke, C., Tutt, A. & von Minckwitz, G. (2017). Molecular alterations in triple-negative breast cancer—the road to new treatment strategies. *The Lancet*, 389 (10087): 2430-2442. doi: https://doi.org/10.1016/S0140-6736(16)32454-0.

Drugbank. (2005). *Doxorubicin*. DRUGBANK. Available at: https://www.drugbank.ca/drugs/DB00997 (accessed: December 04, 2017).

Duga, S., Asselta, R. & Tenchini, M. L. (2004). Coagulation factor V. *Int J Biochem Cell Biol*, 36 (8): 1393-9. doi: 10.1016/j.biocel.2003.08.002.

Eiró, N. & Vizoso, F. J. (2012). Inflammation and cancer. *World Journal of Gastrointestinal Surgery*, 4 (3): 62-72. doi: 10.4240/wjgs.v4.i3.62.

Elaymany, G., Alzahrani, A. M. & Bukhary, E. (2014). Cancer-Associated Thrombosis: An Overview. *Clinical Medicine Insights: Oncology*, 8: 129-137.

Falanga, A., Marchetti, M. & Vignoli, A. (2013). Coagulation and cancer: biological and clinical aspects. *J Thromb Haemost*, 11 (2): 223-33. doi: 10.1111/jth.12075.

Falanga, A., Russo, L., Milesi, V. & Vignoli, A. (2017). Mechanisms and risk factors of thrombosis in cancer. *Crit Rev Oncol Hematol*, 118: 79-83. doi: 10.1016/j.critrevonc.2017.08.003.

Ferlay, J., Soerjomataram, I., Dikshit, R., Eser, S., Mathers, C., Rebelo, M., Parkin, D. M., Forman, D. & Bray, F. (2015). Cancer incidence and mortality worldwide: sources, methods and major patterns in GLOBOCAN 2012. *Int J Cancer*, 136 (5): E359-86. doi: 10.1002/ijc.29210.

Fouad, Y. A. & Aanei, C. (2017). Revisiting the hallmarks of cancer. *American Journal of Cancer Research*, 7 (5): 1016-1036.

Fulda, S. (2013). Regulation of cell death in cancer—possible implications for immunotherapy. *Frontiers in Oncology*, 3: 29. doi: 10.3389/fonc.2013.00029.

Greenbaum, D., Colangelo, C., Williams, K. & Gerstein, M. (2003). Comparing protein abundance and mRNA expression levels on a genomic scale. *Genome Biol*, 4 (9): 117. doi: 10.1186/gb-2003-4-9-117.

Hanahan, D. & Weinberg, R. A. (2000). The Hallmarks of Cancer. *Cell*, 100 (1): 57-70. doi: https://doi.org/10.1016/S0092-8674(00)81683-9.

Hanahan, D. & Weinberg, R. A. (2011). Hallmarks of Cancer: The Next Generation. *Cell*, 144 (5): 646-674. doi: https://doi.org/10.1016/j.cell.2011.02.013.

Hisada, Y. & Mackman, N. (2017). Cancer-associated pathways and biomarkers of venous thrombosis. *Blood*, 130 (13): 1499-1506. doi: 10.1182/blood-2017-03-743211.

Holland, E. C., Celestino, J., Dai, C., Schaefer, L., Sawaya, R. E. & Fuller, G. N. (2000). Combined activation of Ras and Akt in neural progenitors induces glioblastoma formation in mice. *Nat Genet*, 25 (1): 55-7. doi: 10.1038/75596.

Jain, M., Arvanitis, C., Chu, K., Dewey, W., Leonhardt, E., Trinh, M., Sundberg, C. D., Bishop, J. M. & Felsher, D. W. (2002). Sustained Loss of a Neoplastic Phenotype by Brief Inactivation of <em>MYC</em&gt. *Science*, 297 (5578): 102.

Jain, S., Harris, J. & Ware, J. (2010). Platelets: linking hemostasis and cancer. *Arterioscler Thromb Vasc Biol*, 30 (12): 2362-7. doi: 10.1161/ATVBAHA.110.207514.

Jia, H., Guo, Y., Zhao, W. & Wang, K. (2014). Long-range PCR in next-generation sequencing: comparison of six enzymes and evaluation on the MiSeq sequencer. *Scientific Reports*, 4: 5737. doi: 10.1038/srep05737

https://www.nature.com/articles/srep05737 - supplementary-information.

Jonkers, J. & Berns, A. (2004). Oncogene addiction: sometimes a temporary slavery. *Cancer Cell*, 6 (6): 535-8. doi: 10.1016/j.ccr.2004.12.002.

Kao, J., Salari, K., Bocanegra, M., Choi, Y. L., Girard, L., Gandhi, J., Kwei, K. A., Henrandez-Boussard, T., Wang, P. & Gazdar, A. F. (2009). Molecular profiling of breast cancer cell lines defines relevant tumor models and provides a resource for cancer gene discovery. . *PLoS One*, 4 (7).

Katoh, M. (2005). WNT/PCP signaling pathway and human cancer (review). *Oncol Rep*, 14 (6): 1583-8.

Khorana, A. A., Francis, C. W., Culakova, E., Kuderer, N. M. & Lyman, G. H. (2007). Thromboelism is a leading cause of death in cancer patients receiving outpatient chemotherapy. *Journal of Thromboelism and Haemostasis*, 5 (3): 632-634. doi: https://doi.org/10.1111/j.1538-7836.2007.02374.x.

Khorana, A. A. (2012). Cancer-associated thrombosis: updates and controversies. *Hematology Am Soc Hematol Educ Program*, 2012: 626-30. doi: 10.1182/asheducation-2012.1.626.

Kim, T. K. & Eberwine, J. H. (2010). Mammalian cell transfection: the present and the future. *Analytical and Bioanalytical Chemistry*, 397 (8): 3173-3178. doi: 10.1007/s00216-010-3821-6.

Klee, E. W., Bondar, O. P., Goodmanson, M. K., Dyer, R. B., Erdogan, S., Bergstralh, E. J., Bergen, H. R., 3rd, Sebo, T. J. & Klee, G. G. (2012). Candidate serum biomarkers for prostate adenocarcinoma identified by mRNA differences in prostate tissue and verified with protein measurements in tissue and blood. *Clin Chem*, 58 (3): 599-609. doi: 10.1373/clinchem.2011.171637.

Kolonel, L. N., Altschuler, D. & Henderson, B. E. (2004). The multiethnic cohort study: exploring genes, lifestyle and cancer risk. *Nature Reviews. Cancer.*, 4 (7): 519-527. doi: http://dx.doi.org/10.1038/nrc1389.

Kramer, N., Walzl, A., Unger, C., Rosner, M., Krupitza, G., Hengstschläger, M. & Dolznig, H. (2013). In vitro cell migration and invasion assays. *Mutation Research/Reviews in Mutation Research*, 752 (1): 10-24. doi: https://doi.org/10.1016/j.mrrev.2012.08.001.

Krishnaswamy, S. (2013). The transition of prothrombin to thrombin. *J Thromb Haemost*, 11 Suppl 1: 265-76. doi: 10.1111/jth.12217.

L., M. L. (2017). Cancer and inflammation. *Wiley Interdisciplinary Reviews: Systems Biology and Medicine*, 9 (2): e1370. doi: doi:10.1002/wsbm.1370.

Larsen, M. J., Thomassen, M., Gerdes, Anne-Marie & Kruse, T. A. (2014). Hereditary Breast Cancer: Clinical, Pathological and Molecular Characteristics. *Breast Cancer (Auckl)*, 8: 145-155. doi: 10.4137/BCBCR.S18715.

Lea, T. (2013). *Immunologi og immunologiske teknikker*. 3 ed., vol. 3. Bergen: Fagbokforlaget Vigmostad & Bjerke AS.

Lee, A. V., Oesterreich, S. & Davidson, N. E. (2015). MCF-7 Cells—Changing the Course of Breast Cancer Research and Care for 45 Years. *JNCI: Journal of the National Cancer Institute*, 107 (7): djv073-djv073. doi: 10.1093/jnci/djv073.

Lee, C. D. & Mann, K. G. (1989). Activation/inactivation of human factor V by plasmin. *Blood*, 73 (1): 185-90.

Lee, P. Y., Costumbrado, J., Hsu, C. Y. & Kim, Y. H. (2012). Agarose gel electrophoresis for the separation of DNA fragments. *J Vis Exp* (62). doi: 10.3791/3923.

Lodish, H., Berk, A. & Zipursky, S. (2000). Section 7.1 DNA Cloning with Plasmid Vectors. In *Molecular Cell Biology*. New York: W. H. Freeman.

Logan, C. Y. & Nusse, R. (2004). THE WNT SIGNALING PATHWAY IN DEVELOPMENT AND DISEASE. *Annual Review of Cell and Developmental Biology*, 20 (1): 781-810. doi: 10.1146/annurev.cellbio.20.010403.113126.

Mahmood, T. & Yang, P.-C. (2012). Western Blot: Technique, Theory, and Trouble Shooting. *North American Journal of Medical Sciences*, 4 (9): 429-434. doi: 10.4103/1947-2714.100998.

Mann, K. G. & Kalafatis, M. (2003). Factor V: a combination of Dr Jekyll and Mr Hyde. *Blood*, 101 (1): 20-30. doi: 10.1182/blood-2002-01-0290.

Moses, C., Garcia-Bloj, B., Harvey, A. R. & Blancafort, P. (2018). Hallmarks of cancer: The CRISPR generation. *European Journal of Cancer*, 93: 10-18. doi: https://doi.org/10.1016/j.ejca.2018.01.002.

Nowell, C. S. & Radtke, F. (2017). Notch as a tumour suppressor. *Nature Reviews Cancer*, 17: 145. doi: 10.1038/nrc.2016.145.

Owren, P. (1947). PARAHÆMOPHILIA: HÆMORRHAGIC DIATHESIS DUE TO ABSENCE OF A PREVIOUSLY UNKNOWN CLOTTING FACTOR. *The Lancet*, 249 (6449): 446-448. doi: https://doi.org/10.1016/S0140-6736(47)91941-7.

Polakis, P. (2000). Wnt signaling and cancer. *Genes Dev*, 14 (15): 1837-51.

Prelich, G. (2012). Gene Overexpression: Uses, Mechanisms, and Interpretation. *Genetics*, 190 (3): 841-854. doi: 10.1534/genetics.111.136911.

Ribatti, D., Nico, B. & Crivellato, E. (2015). The development of the vascular system: a historical overview. *Methods Mol Biol*, 1214: 1-14. doi: 10.1007/978-1-4939-1462-3_1.

Sauer, B. (1994). Site-specific recombination: developments and applications. *Current Opinion in Biotechnology*, 5 (5): 521-527. doi: https://doi.org/10.1016/0958-1669(94)90068-X.

Smith, L., Watson, M. B., O'Kane, S. L., Drew, P. J., Lind, M. J. & Cawkwell, L. (2006). The analysis of doxorubicin resistance in human breast cancer cells using antibody microarrays. *Mol Cancer Ther*, 5 (8): 2115-20. doi: 10.1158/1535-7163.MCT-06-0190.

Smith, S. A. (2009). The cell-based model of coagulation. *J Vet Emerg Crit Care (San Antonio)*, 19 (1): 3-10. doi: 10.1111/j.1476-4431.2009.00389.x.

Sun, H. (2015). Factor V: an active player in inflammation. *Blood*, 126 (21): 2352-2353. doi: 10.1182/blood-2015-09-669077.

Tabatabai, R., Linhares, Y., Bolos, D., Mita, M. & Mita, A. (2017). Targeting the Wnt Pathway in Cancer: A Review of Novel Therapeutics. *Targeted Oncology*, 12 (5): 623-641. doi: 10.1007/s11523-017-0507-4.

Tavassi, A. M. C., Carvalho, L. C. C., Alvarez-Flores, M. P. & Andrade, S. A. (2014). Exogenous Procoagulant Factors as Theurapeutic and Biotechnological Tools. *Journal of Blood Disorders & Transfusion*, 5 (5). doi: 10.4172/2155-9864.1000209.

Tinholt, M., Viken, M. K., Dahm, A. E., Vollan, H. K. M., Sahlberg, K. K., Garred, Ø., Børresen-Dale, A.-L., Jacobsen, A. F., Kristensen, V., Bukholm, I., et al. (2014). Increased coagulation activity and genetic polymorphisms in the F5, F10 and EPCRgenes are associated with breast cancer: a case-control study. *BMC Cancer*, 14 (1): 845. doi: 10.1186/1471-2407-14-845.

Tinholt, M., Garred, Ø., Borgen, E., Beraki, E., Sletten, M., Kleivi Sahlberg, K., Sandset, P. M. & Iversen, N. (2018). Coagulation factor V is expressed in tumors and predicts favorable outcome in aggressive breast cancer. *Thrombosis Research*, 164: S183. doi: https://doi.org/10.1016/j.thromres.2018.02.019.

Veeraraghavan, J., De Angelis, C., Reis-Filho, J. S., Pascual, T., Prat, A., Rimawi, M. F., Osborne, C. K. & Schiff, R. (2017). De-escalation of treatment in HER2-

positive breast cancer: Determinants of response and mechanisms of resistance. *The Breast*, 34: S19-S26. doi: 10.1016/j.breast.2017.06.022.

Versteeg, H. H., Heemskerk, J. W. M., Levi, M. & Reitsma, P. H. (2013). New Fundamentals in Hemostasis. *Physiological Reviews*, 93 (1): 327-358. doi: 10.1152/physrev.00016.2011.

Vossen, C. Y., Hoffmeister, M., Chang-Claude, J. C., Rosendaal, F. R. & Brenner, H. (2011). Clotting factor gene polymorphisms and colorectal cancer risk. *J Clin Oncol*, 29 (13): 1722-7. doi: 10.1200/jco.2010.31.8873.

Vuong, D., Simpson, P. T., Green, B., Cummings, M. C. & Lakhani, S. R. (2014). Molecular classification of breast cancer. *Virchows Arch*, 465 (1): 1-14. doi: 10.1007/s00428-014-1593-7.

Walker, A. J., West, J., Card, T. R., Crooks, C., Kirwan, C. C. & Grainge, M. J. (2016). When are breast cancer patients at highest risk of venous thromboelism? A cohort study using English health care data. *Blood*, 127 (7): 849-857. doi: 10.1182/blood-2015-01-625582.

Waring, M. J., Arrowsmith, J., Leach, A. R., Leeson, P. D., Mandrell, S., Owen, R. M., Pairaudeau, G., Pennie, W. D., Pickett, S. D., Wang, J., et al. (2015). An analysis of the attrition of drug candidates from four major pharmaceutical companies. *Nature Reviews Drug Discovery*, 14: 475. doi: 10.1038/nrd4609 https://www.nature.com/articles/nrd4609 - supplementary-information.

Weinstein, B. & Joe, A. K. (2006). Mechanisms of Disease: oncogene addiction-a rational for molecular targetin in cancer therapy. *Nature*, 4 (8): 448-457.

Welsh, J. (2013). Chapter 40 - Animal Models for Studying Prevention and Treatment of Breast Cancer A2 - Conn, P. Michael. In *Animal Models for the Study of Human Disease*, pp. 997-1018. Boston: Academic Press.

Yarrow, J. C., Perlman, Z. E., Westwood, N. J. & Mitchison, T. J. (2004). A high-throughput cell migration assay using scratch wound healing, a comparison of image-based readout methods. *BMC Biotechnology*, 4 (1): 21. doi: 10.1186/1472-6750-4-21.

Zeibdawi, A. R. & Pryzdial, E. L. (2001). Mechanism of factor Va inactivation by plasmin. Loss of A2 and A3 domains from a Ca2+-dependent complex of fragments bound to phospholipid. *J Biol Chem*, 276 (23): 19929-36. doi: 10.1074/jbc.M004711200.

Zhang, S., Garcia-D'Angeli, A., Brennan, J. P. & Huo, Q. (2014). Predicting detection limits of enzyme-linked immunosorbent assay (ELISA) and bioanalytical techniques in general. *Analyst*, 139 (2): 439-45. doi: 10.1039/c3an01835k.

# Appendix A

## A.1 Reagents and chemicals

| Reagent/chemical | Supplier | Catalogue number |
|---|---|---|
| Agar-Agar | Merck, Darmstadt, Germany | 101614 |
| Ampicillin, Sodium Salt | Millipore S.A.S., Molsheim, France | 171254 |
| BlueJuice™ Gel Loading Buffer (10X) | Thermo Fisher Scientific, Waltham, MA, USA | 10816015 |
| Bovine Serum Albumin | Thermo Fisher Scientific, Waltham, MA, USA | A7906 |
| Dulbecco's Modified Eagle's Medium 4.5g/L Glucose w/L-Glutamine 500mL | Lonza, Verviers, Belgium | BE-12-614F |
| Dulbecco's Phosphate Buffered Saline | Gibco® Life Technologies | 14190-094 |
| Fetal Bovine Serum Ultra-Low Endotoxin Heat Inactivated | Biowest, Nuaillé, France | Si86H-500 |
| GeneRuler 1kb DNA Ladder Mix | Fermentas, Vilnius, Lithuana | SM0311 |
| GelRed Nucleic Acid Gel Stain | VWR, Oslo, Norway | 730-2958 |
| Glycine | BioRad, CA, USA | 161-0718 |
| Glycerol | LBH Laboratory Supplies, Alberta, Canada | 101184K |
| Halt™ Protease & Phosphatase Inhibitor Coctail (x100) | Thermo Fisher Scientific, Waltham, MA, USA | 78440 |
| Lipoafectamine®3000 Transfection Reagent | Thermo Fisher Scientific, Waltham, MA, USA | L3000008 |
| Magermilchpulver | Applichem GmBH, Darmstadt, Germany | A0830 |
| Methanol | Merck, Darmstad, Germany | 1677909313 |
| NaOH | Merck, Damstadt, Germany | 1064951000 |
| Opti-MEM® Reduced Serum Medium | Thermo Fisher Scientific, Waltham, MA, USA | 31985-062 |
| Peptone from casein (Tryptone) | Merck, Darmstadt, Germany | 119311000 |
| Precision Plus Protein ™ Dual Xtra Standards | BioRad, CA, USA | 161-0374 |
| Reagent A100 Lysis Buffer | ChemoMetec, Allerød, Denmark | 910-0003 |
| Reagent B Stabilizing Buffer | ChemoMetec, Allerød, Denmark | 910-0003 |
| Recombinant FV | Hematologic Technologies Inc., VT, USA | HCV-0100 |
| RIPA Buffer | Sigma-Aldrich, St. Louis, USA | R0278 |
| SDS solution (20%) | BioRad, CA, USA | 161-0418 |
| SeaKem® LE Agarose | BioNordika Norway AS, Oslo, Norway | 50004 |
| S.O.C medium | Thermo Fischer Scientic, Waltham, MA, USA | 15544034 |
| TaqMan® Gene Expression Master Mix | Applied Biosystems, Foster City, USA | 4369016 |

| | | |
|---|---|---|
| Tris buffered Saline (TBS) (10X) | BioRad, CA, USA | 170-6435 |
| Tris/Glycine/SDS (TGS)(10X) | BioRad, CA, USA | 161-0732 |
| Trizma ® Base | Sigma-Aldrich, St. Louis, USA | T1503-1KG |
| Trypsin EDTA | Lonza, Verviers, Belgium | BE17-711E |
| Tween ® 20 viscous liquid | Sigma-Aldrich, St. Louis, USA | P1379 |
| UltraPure™ 10X TAE buffer | Thermo Fischer Scientic, Waltham, MA, USA | 15558-042 |
| WST-1 Cell Proliferation Reagent | Abcam, UK | Ab155902 |
| Yeast Extract | Thermo Fischer Scientic, Waltham, MA, USA | Y1625-250G |

## A.2 Solutions

### *LB (Luria Broth) medium*

10.0 g Peptone from casein (Tryptone)

5.0 g Yeast Extract

10.0 g Sodium Chloride (NaCl)

950.0 mL $H_2O$ milli-Q for a total solution of 1.0 L

pH adjusted to 7.0 with Sodium Hydroxide (NaOH), and autoclaved.

1000 µL Ampicillin (100 µg/µL) was added before use.

### *LB (Luria Broth) medium agar*

7.5 g Agar-Agar

5.0 g Peptone from casein (Tryptone)

2.5 g Yeast Extract

5.0 g Sodium Chloride (NaCl)

500.0 mL $H_2O$ milli-Q for a total solution of 0.5 L

pH adjusted to 7.0 with Sodium Hydroxide (NaOH), and autoclaved.

500 µL Ampicillin (100 µg/µL) was added before use.

### *1% Agarose gel*

1.0 g SeaKem® LE Agarose

100 mL (1:10) 10X TAE Buffer

Boiled until homologous solution. 10 µL Gel Red Dye was added.

### *RIPA Lysis Buffer with inhibitors*

1x RIPA Lysis Buffer

1:100 Halt™ Protease and Phosphatase Inhibitor Cocktail (x100)

### *1x TGS (running) buffer – Western blot*

100 mL 10X TGS (Tris/Glycine/SDS)

900 mL $H_2O$ milli-Q

### *Blotting buffer – Western blot*

3.0 g Trizma base

14.4 g Glycine

900 mL $H_2O$ milli-Q

100 mL Methanol

0.01% SDS

### *1x TBS – Tween (TBST) buffer – Western blot*

100 mL 10X TBS

900 mL $H_2O$ milli-Q

1.0 mL Tween ® 20

### *5% Bovine Serum Albumin (BSA) – Western blot*

2.5 g Bovine Serum Albumin

50 mL TBST

### *Primary Antibody solution – Western blot*

1.0 mL 5% BSA

4.0 mL TBST

Antibody (PARP 1:1000 dilution or 10 µg/mL Anti-Human Factor V)

## A.3 Kits

| Kit | Supplier | Catalogue number |
|---|---|---|
| Agencourt® CleanSEQ® | Beckmann Coulter, CA, USA | A29154 |
| AmpliTaq Gold™ 360 Masyer Mix Kit | Thermo Fischer Scientific, Waltham, MA, USA | 439881 |
| Amersham™ ECL™ Prime Western Blotting Detection Reagents | GE Healthcare, Buckinghamshire, UK | RPN2232 |
| BigDye® Terminator v3.1 Cycle Sequencing Kit | Thermo Fischer Scientific, Waltham, MA, USA | 4337455 |
| Cancer 10-Pathway Reporter Luciferace Kit | Qiagen, Alameda, CA, USA | 301005 |
| Cell Death Detection Kit ELISA $^{PLUS}$ | Roche Applied Science, IN, USA | 11774425001 |
| High Capacity® cDNA Reverse Transcription Kit | Thermo Fischer Scientific, Waltham, MA, USA | 4368813 |
| MycoAlert™ Assay Control Set | Lonza, Verviers, Belgium | T07-518 |
| Pierce® BCA Protein Assay Kit | Thermo Fischer Scientific, Waltham, MA, USA | 23225 |
| RNAqeuous® Total RNA Isolation Kit | Thermo Fischer Scientific, Waltham, MA, USA | AM1912 |
| Thermo Scientific™ FastDigest Kit | Thermo Fischer Scientific, Waltham, MA, USA | FD0504, FD0593, FD0644 |
| Thermo Scientific™ Rapid DNA Ligation Kit | Thermo Fischer Scientific, Waltham, MA, USA | K1422 |
| Wizard® SV Gel and PCR Clean-Up System | Promega Biotech AB, Sweden | A9281 |
| Zyppy™ Plasmid Miniprep Kit | Zymo Research, Irvine, CA, USA | D4036 |
| ZymoPURE™ Plasmid Maxiprep Kit | Zymo Research, Irvine, CA, USA | D4202 D4203 |
| ZYMUTEST Factor V Kit | Hyphen BioMed, CoaChrom Diagnostica GmbH, Germany | RK009A |
| Q5® High Fidelity PCR Kit | New England BioLabs® Inc., MA, USA | E0555S |

## A.4 Instruments and equipment

| Instrument/equipment | Supplier |
|---|---|
| Alamut ® Visual Software database | Interactive Biosoftware |
| Eppendorf Centrifuge 5810 | Eppendorf AG |
| Eppendorf miniSpin plus | Eppendorf AG |
| Wallac DELFIA® Plate Shaker | Perkinelmer |
| Direct-Q® 3UV-R Water Purification System | Merk |
| Grant Optima T100, TC120 Waterbath | Grant Instruments Ltd. |
| ImageQuant LAS 4000 Imaging System | GE Healthcare Life Sciences |
| ImageQuant™ TL 1D v8.1 software | GE Healthcare Life Sciences |
| Incubator | Termaks A/S |
| Infors Multitron Incubation Shaker | Infors HT |
| LAAF Sterile Bench, KR-160 Safety | Kojair® Tech Oy |
| Lucetta™ Luminometer | Lonza |
| Mini-PROTEAN ® TGX ™ Gels (10%) 10-well comb | BioRad |
| NanoDrop® ND-1000 Spectrophotometer | NanoDrop Technologies |
| Nikon Ecplipse TE 300 microscope | Nikon |
| Nikon Ecplipse Ts2-S-SM microscope | Nikon |
| NucleoCasette ™ | ChemoMetec A/S |
| NucleoCounter ® System | ChemoMetec A/S |
| Nunc™ Cell Culture Treated Flasks ($25cm^2$, $75cm^2$, $125cm^2$) | Thermo Scientific |
| Nunc™ Cell Culture Treated Multidishes (6, 12, 24 and 96 well) | Thermo Scientific |
| pHenomenal | VWR |
| QuantStudio 12k Flex | Applied Biosystems |
| SecScape® Software | Applied Biosystems |
| SoftMax Pro6.4 software | Molecular Devices |
| Sartorius weight | Sartorius |
| Steri-Cycle CO2 Incubator, HEPA class100 | Thermo Electron Corporation |
| Thermal Cycler 2720 | Applied Biosystems |
| Veriti 96 well Thermal Cycler | Applied Biosystems |
| VersaMax microplate reader | Molecular Devices |
| Whatman® PROTRAN Nictrocellulose Transfer Membrane | Sigma-Aldrich |

## A.5 Cells

| Cell type | Supplier | Catalogue number |
|---|---|---|
| OneShot® TOP10 Chemically Competent Cells, *Escherichia coli* | Invitrogen, Carlsbad, CA, USA | C4040-03 |
| MDA-MB-231 | ATCC, Manassas, USA | ATCC® HTB-26™ |
| MCF-7 | ATCC, Manassas, USA | ATCC® HTB-22 |

## A.6 Vectors

| Vector | Supplier | Catalogue number |
|---|---|---|
| pMT2-V | LGC Standards GmbH, Wesel, Germany | ATCC ® 40515 ™ |
| pcDNA5/FRT Mammalian Expression Vector | Thermo Fischer Scientific, Waltham, MA, USA | V601020 |

## A.7 Antibodies

| | Antibody | Supplier | Catalogue number | Dilution |
|---|---|---|---|---|
| Primary antibody | Anti-Human Factor V antibody, monoclonal mouse | Hematologic Technologies Inc. | AHV-5146 | (1:1000) |
| Primary antibody | Anti-PARP-1, Polyclonal mouse | Cell Signalling Technology | #9542 | (1:1000) |

## A.8 TaqMan assays used in RT-qPCR

| TaqMan Assay Name | ID | Sequence 5'→3' |
|---|---|---|
| Factor V (FV) | Hs0091412_m1 Thermo Scientific | - |
| Phosphomannomutase 1 (PMM1) | PMM1-80 Forward primer | CCGGCTCGCCAGAAAATT |
| | PMM1-149 Reverse primer | CGATCTGCACTCTACTTCGTAGCT |
| | PMM1-99 Probe | ACCCTGAGGTGGCCGCCTTCC |

## A.9 Primers

All primers were obtained from Eurogentec.

**Table A.9.1 Primers used in AmpliTaq® Gold 360 PCR.**

| Primer name | Sequence 5'→3' |
|---|---|
| F5 – 7F | GGAAGAGGTCCAGAGCAGTGAAGA |
| F5 – 9F | GGCCCCTTCTGCCTGGTTCA |
| F5 – 7R | GGATAACATCATCCACTTCAGCTCTGA |
| F5 – 9R | TCCCTGCTCACTGTAGTGGATGGTAT |

**Table A.9.2 Primers used in Q5® High-Fidelity long-range PCR of *F5*.**

| Primer name | Sequence 5'→3' |
|---|---|
| pMT2-V_HindIII_F | ATTCGTAAGCTTGATCTGCCCAGGT |
| pMT2-V_NotI_R | TGCTTAGCGGCCGCAACATTTAACACAGCGTAAAATACA |

Primers tailed with *HindIII* and *NotI* restriction sites. Red colour represents the restriction site of the enzymes, while the black colour is part of the *F5* sequence. Blue colour represents extra base pairs of the primer sequence.

**Table A.9.3 Primers used in BigDye® Sequencing reaction.**

| Primer name | Sequence 5'→3' |
|---|---|
| F5 – 1F | TGGGGGAGCCAAGGGACAGA |
| F5 – 2F | CTCGGGGCCAGAATTATTCTCCATTCA |
| F5 – 3F | CATCGCCTCTGGGCTAATAGG |
| F5 – 4F | AGATTTTTGAACCTCCAGAATCTACAGTCA |
| F5 – 5F | GGAGGAAAGAGTAGACTGAAGAAAAGCCA |
| F5 – 6F | ATGACTCTCTCTCCAGAACTCAGTCAG |
| F5 – 7F | GGAAGAGGTCCAGAGCAGTGAAGA |
| F5 – 8F | TGGTTTAAGGAAGATAATGCTGTTCAGCCA |
| F5 – 9F | GGCCCCTTCTGCCTGGTTCA |
| F5 – 10F | AGAGAATCAGTTTGACCCACCTATTGT |
| F5 – 11F | CCCCCAATCATTTCCAGGTTTATCCGT |
| F5 – 1R | AGGTGTATTCTCGGCCTGGAGC |
| F5 – 2R | ATGCTATAGGGGCGGCTGGC |
| F5 – 3R | CCACGCATGGGGAAGAGGGT |
| F5 – 4R | AGCCAAATGCCATCTCCCAACCA |
| F5 – 5R | AGGATCTGTGACTGGGGTCTGA |
| F5 – 6R | TCCGGGAGAAGGGTGGTGTCA |
| F5 – 7R | GGATAACATCATCCACTTCAGCTCTGA |
| F5 – 8R | ACACTCCAAGCATTATAAGATCCACCA |
| F5 – 9R | TCCCTGCTCACTGTAGTGGATGGTAT |
| T7-F | TAATACGACTCACTATAGGG |
| BGH-R | TAGAAGGCACAGTCGAGG |

# Appendix B

## B.1 Standard curve of Albumin concentrations

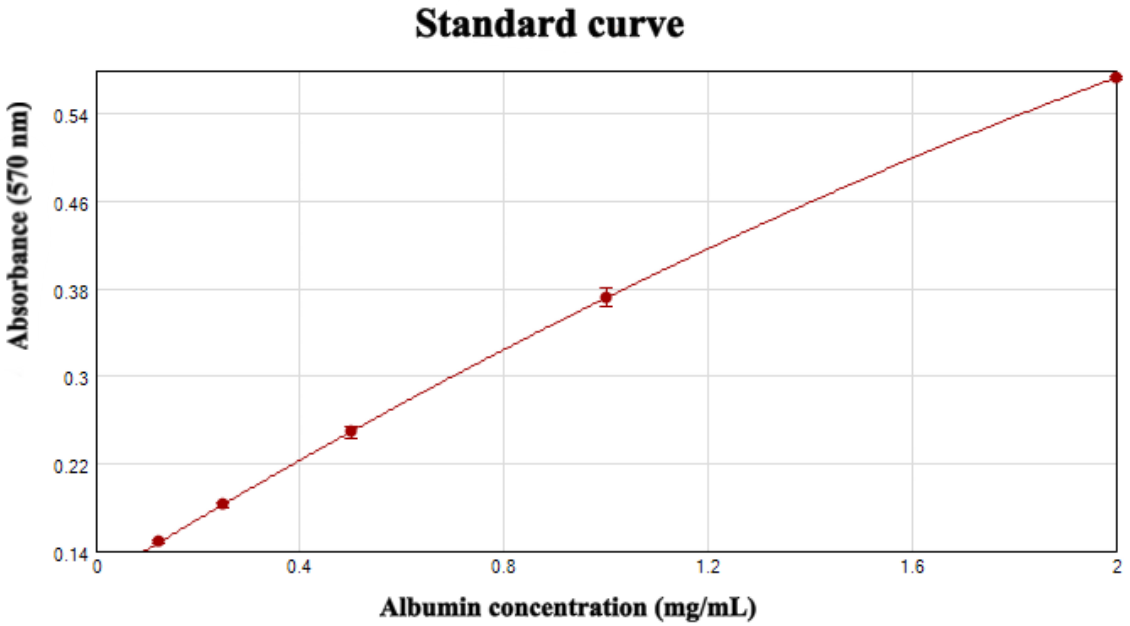


**Figure B1. Standard curve of the albumin concentrations (mg/mL) at 570 nm absorbance.** The standard curve was used for measuring the total protein levels in cell lysate from MDA-MB-231 and MCF-7 cells.

## B.2 Standard curve of FV protein concentrations

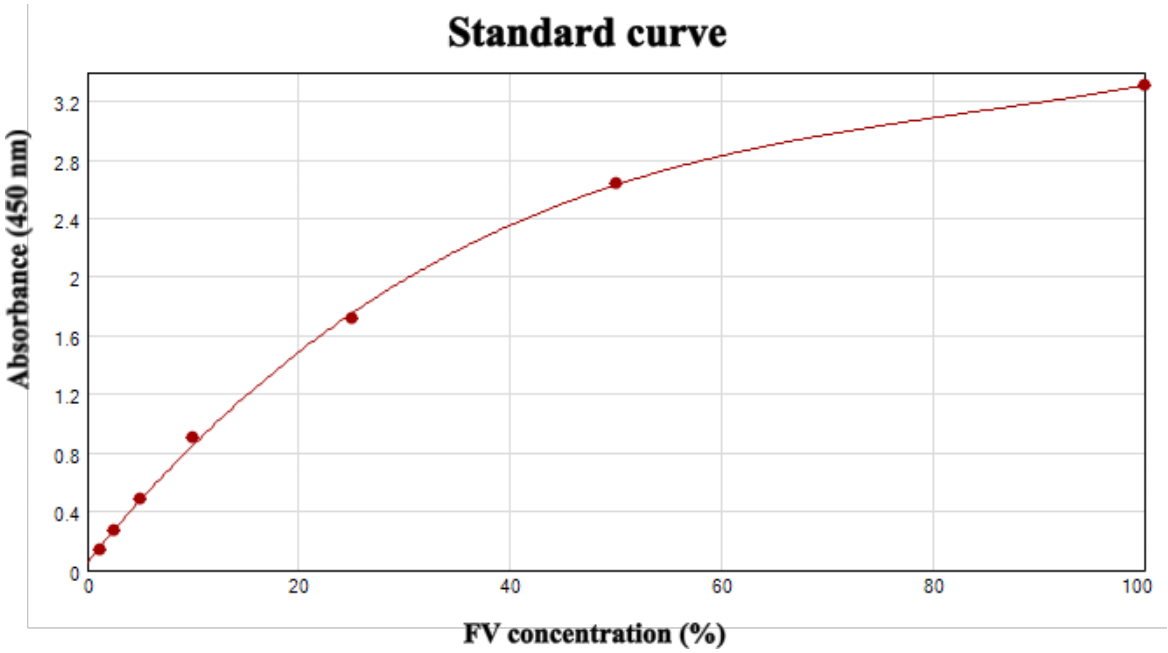


**Figure B2. Standard curve of the FV protein concentrations (%) at 450 nm absorbance.** The standard curve was used for measuring the FV protein levels in cell lysate from MDA-MB-231 and MCF-7 cells.

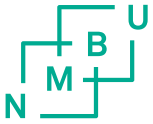


**Norges miljø- og biovitenskapelige universitet**
Noregs miljø- og biovitskapelege universitet
Norwegian University of Life Sciences

Postboks 5003
NO-1432 Ås
Norway